Met komplimente aan die Geologie Departement U.O.V.S

Stony Stromberg

THE SOURCE MATERIAL OF THE BIG PEBBLE MARKER AND ROSEDALE REEFS IN THE WELKOM GOLDFIELD

by

JOHANNES MARTHINUS ANDRIES STEENEKAMP

THESIS

submitted in fulfillment of the degree

MAGISTER SCIENTIAE

in the

FACULTY OF SCIENCE

DEPARTMENT OF GEOLOGY

at the

UNIVERSITY OF THE ORANGE FREE STATE

JUNE 1990

STUDY LEADER: PROFESSOR N.J. GROBLER

ABSTRACT

In this study the clasts of the Big Pebble Marker (BPM) in the Aandenk Formation and the basal conglomerate of the Rosedale Member (RDM) in the Eldorado Formation, in the Welkom Goldfield, were investigated. The aim of this study was to employ a different approach to acquire an insight into the nature of the provenance of the gold-bearing conglomerates in the Welkom Goldfield. To achieve this, the quantitative and qualitative compositions of two coarse and polymictic reefs were studied.

Observations were made at six underground localities per reef. At each locality a clean, reasonably flat surface, of three to four square metres, with sufficient conglomerate exposure, was investigated. A modal count of the different types of clasts present was done at one thousand points per exposure with the aid of two grid frames. The long axes of at least two hundred clasts, falling on preselected lines, were measured. The long axes of the ten largest clasts in the selected area were also measured. Representative samples of the various clast types present were taken for laboratory study. Every exposure studied, was photographed.

All samples were cleaned meticulously to prevent any contamination with matrix material. A total of 126 samples were analyzed for gold, major and trace elements. A selection of samples were also analyzed by means of XRD and microprobe for mineral composition. Petrographic studies were carried out on thin sections of all the samples. A few samples were investigated by means of electron microscope. Fluid inclusion studies were carried out on four quartz samples.

All the field data and analytical results were processed statistically on computer. Petrographic information were plotted on standard ternary diagrams. Average gold concentrations in the different clast types were compared with world wide averages for comparable rock types.

Field data indicate different transport mechanisms for the BPM and RDM. Composite or multiple provenances are also indicated for both reefs. Quartz and chert dominate the clast assemblages of both reefs, but more so in the case of the BPM. Results from the clast assemblage plots on the ternary diagrams indicate thrust belt and recycled orogenic provenances for the BPM and RDM. Clasts, derived from greenstone-type source rocks, occur predominantly in both reefs.

Silica dominates the chemical composition of the majority of the clasts. On average, chert clasts from the BPM contained the highest gold concentrations (143 ppb) of all the clast types. Based on modal composition, the total clast assemblage of the BPM is approximately 6X more auriferous than that of the RDM (76 ppb vs 12 ppb). Respectively, these figures are approximately 30X and 5X higher than the figure of 2,4 ppb, which is generally accepted for a Barberton-type granite-greenstone crust.

CONTENTS PAGE

I

INTRODUCTION

1. PREVIEW

Because the Witwatersrand Basin contains the largest and most productive gold deposit known on earth (Pretorius, 1989), it is therefore probably the most intensively studied and documented gold deposit as well. Although the debate over the origin of the gold started more than a hundred years ago with the discovery of the deposit, the dispute is not resolved yet and perhaps the situation is best summed up in the words of Skinner and Merewether (1986): "We still fight over the origin of the deposit that was found over a century ago on the farm Langlaagte, and it is likely we will still be fighting long after the last grain of gold has been dug from the basin".

Antrobus (1956) pointed out the elemental differences between "reef" conglomerates, normally deposited on discordances, and "normal" conglomerates being polymictic and deposited within sedimentary units (Brink, 1986).

The "reef" conglomerates, apart from containing economic mineralization, is normally highly mature and oligomictic. Due to the economic significance of the "reef" conglomerates, they were studied much more intensely than the "normal" conglomerates. However, due to their mature and oligomictic nature they are for obvious reasons not ideally suited for study to unravel the nature of their provenance.

If the placer or "modified placer" theory in general is accepted, it can be argued that the very fact that the

"normal" conglomerates are immature, explains the scarcity and erratic distribution of economic gold concentrations in them. It then follows that these conglomerates can in fact be "proto"-reefs, which could have become proper "reef" conglomerates, containing more consistent economical concentrations of gold, had they been reworked to "winnow" the gold and become more oligomictic.

In contrast to the "reef" conglomerates, the so-called "normal" conglomerates, being polymictic, offers a wide variety of material for investigation. In addition to this, ongoing underground exploration has proved that the "normal" conglomerates in places do contain economic concentrations of gold, for example the so-called Elsburg stopes on Free State Geduld (FSG) mine.

For these reasons, and bearing the availability of underground exposures in mind, two "normal" conglomerates were selected for investigation. At the same time, however, these two conglomerates lie, to a lesser or larger degree, on unconformities.

2. AIM OF THIS STUDY

From the above considerations stems the decision to study two placers in the Welkom Goldfield, namely the Big Pebble Marker conglomerate in the Aandenk Formation and the basal conglomerate of the Rosedale Member, called the Rosedale Reef, in the Eldorado Formation (hereafter referred to as BPM and RDM, respectively) in an attempt to shed more light on the nature of the provenance of the BPM and RDM. By implication such a study would also provide information on the provenance of the Central Rand Group in general.

In this study the clasts of the above-mentioned conglomerates are investigated mesoscopically, microscopically and chemically in order to determine their provenance. Gold content of the clasts will also be determined to establish which, if any, of the lithologies in the provenance, exhibit enhanced gold values.

The aim of this study is therefore, primarily to employ a different approach to acquire an insight into the nature of the provenance of the gold-bearing conglomerates in the Welkom goldfields.

3. LITHOLOGIES STUDIED

The relative positions of the BPM and RDM are illustrated with a lithostratigraphic column of the Central Rand Group as it occurs in the Welkom Goldfield, *Figure I.1.* (after SACS, 1980).

3.1. BIG PEBBLE MARKER (BPM)

A concise description of the lithology, stratigraphy and depositional framework of the BPM and the Aandenk Formation was done by Jordaan (1986) and is summed up as follows:

The Aandenk Formation consists of finer-grained, immature quartzites and small- to medium-pebble, polymictic conglomerates. Up to three stratabound, oligomictic conglomerate placers are present where the Aandenk Formation shows its maximum development. They occur 40m, 25m and 15m, respectively, below the upper contact with the Eldorado Formation and are classified as the Lower, Middle and Upper "A" Reef placers, respectively.

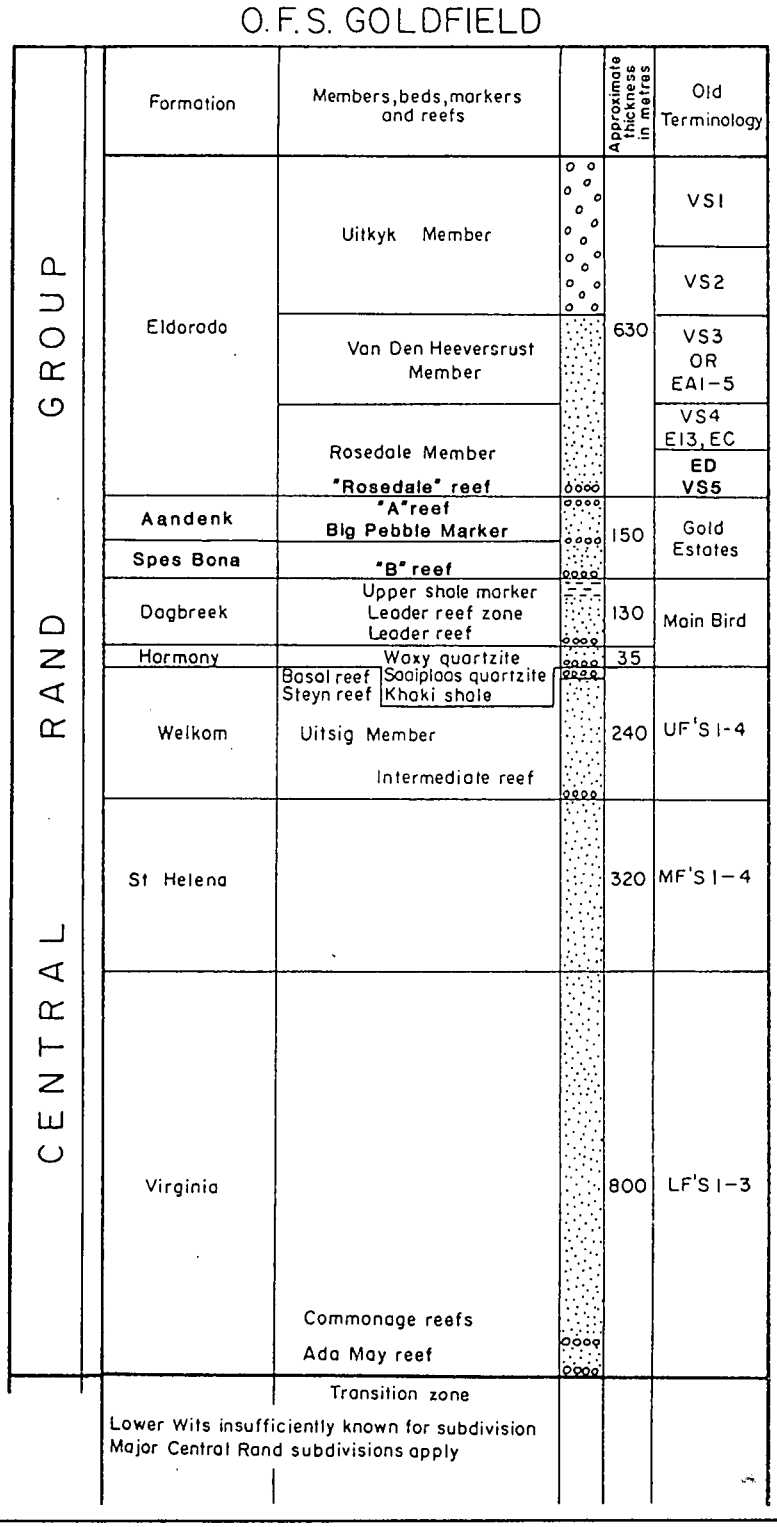

Fig. I.1. Lithostratigraphic column for the OFS goldfield (modified, after SACS).

The BPM is a distinctive conglomeratic unit (at the bottom of the Aandenk Formation) of up to 17m thick, comprising large-pebble, cobble and boulder conglomerates interbedded with coarse- to very coarse-grained quartzites. The BPM shows its maximum development in the central parts of the goldfield and is intertongued with the Spes Bona Formation (below) to the north and south where it forms a poorly defined conglomeratic zone. The BPM conglomerates wedge out in the distal regions, leaving a thin interval of cobble conglomerates at the top of the zone. A plane-bedded, dark coloured, fine-grained quartzite with rare green siltstone intercalations is interbedded with conglomerate in the BPM zone in the southern parts of the goldfield. Where fully developed, the BPM (like the "B" reef) shows thin (< 1m), internal, upwards-fining conglomeratic sequences, and an overall upward decrease in clast sizes.

The BPM have much coarser conglomerates than the rest of the succession. They represent fanhead channel deposits. Paleocurrent directions approximately parallel those in the associated fan deposits which were distributed from west to east. The non-durable clast component in the conglomerates shows an increase upwards in the succession but decreases rapidly where the BPM is well developed.

The BPM conglomerates, mostly cobble conglomerates, were emplaced in response to severe erosion of the orogenic belt. Increased volumes of cobble conglomerate were derived from the source area, but the discharge and extent started decreasing as base level equilibrium was approached. The upward decrease in clast sizes of the BPM in the proximal environment is ascribed to the combined effects of progradation of the fan, aggradation of the basin, and the lowering of source area relief. Occasionally the fanhead drainage was captured by

entrenched distributary channels. Cobble conglomerates was thus diverted into the distal portions of the distributary system, initially by isolated channels but later on by more extensive channel systems. Here they became interbedded with finer-grained sediments in the BPM zone, including reworked fan sediments, to form upwards-coarsening sequences.

3.2. ROSEDALE MEMBER (RDM)

Kingsley (1986) gives a concise description of the lithology, stratigraphic framework and sedimentation model of the RDM and the Eldorado Formation which is summed up as follows:

The Eldorado Formation is a wedge-shaped sequence of fanglomerates and arenites at the top of the Central Rand Group. Broadly speaking, this formation is a coarsening-upward sequence which is subdivided into four smaller fining-upward cycles. Based on these cycles, four members are distinguished which are the following from the bottom upwards: the Rosedale Member, the Van den Heeversrust Member, the EA zone (an informal unit) and the Uitkyk Member.

The Eldorado conglomerates are interpreted as alluvial fanglomerates which interfinger with lithic arenites of the fan, and with braid plain alluvial sands at their toes. Four main pulses of debris influx, which coincide with the four members, can be identified.

The Formation thickens from west to east from 200m to 600m over a distance of 5 km. The rapid decrease in thickness westward is mainly due to basin edge unconformities at the bases of the main conglomerate

units. Concomitant with the thickness change is a major facies change from 100 percent conglomerate in the west to an alternation of conglomerate and arenites in the medial areas and almost 100 percent arenites in the very distal areas some 25 km east of the basin edge. The base of the formation is a sharp unconformity which truncates all the underlying formations of the Central Rand Group.

The Rosedale Member (at the base of the formation) consists of a polymictic conglomerate, the Rosedale Placer, at the base. It is succeeded by an alternation of quartz-arenites, lithic arenites and sub-greywackes. The typical clast assemblage is quartz (25%), chert (30%), yellow silicified siltstone/shale (15%) and minor felsic volcanics, set in a dark grey, gritty and, in some cases argillaceous, matrix.

The shape of the Rosedale Member is well defined by its gravel component. A very consistent and different unimodal southeastward paleoslope is indicated by the more mature Rosedale arenites.

4. SCOPE OF THIS RESEARCH

The area of study lies in the central part of the OFS goldfield (*Figures I.2.* and *I.3.*) and comprises the area belonging to mines of the Anglo American Corporation. This area corresponds with the central part of the gravel distribution plan of the Eldorado Formation conglomerate, as proposed by Kleynhans (1970). He proposed an entry point to the west of number 4 shaft FSG mine, with a fan-like distribution towards the east, which is in general accordance with previous work by Winter (1964a) and Sims (1969). His plan is, however, very generalized and not confined to a specific unit in this formation.

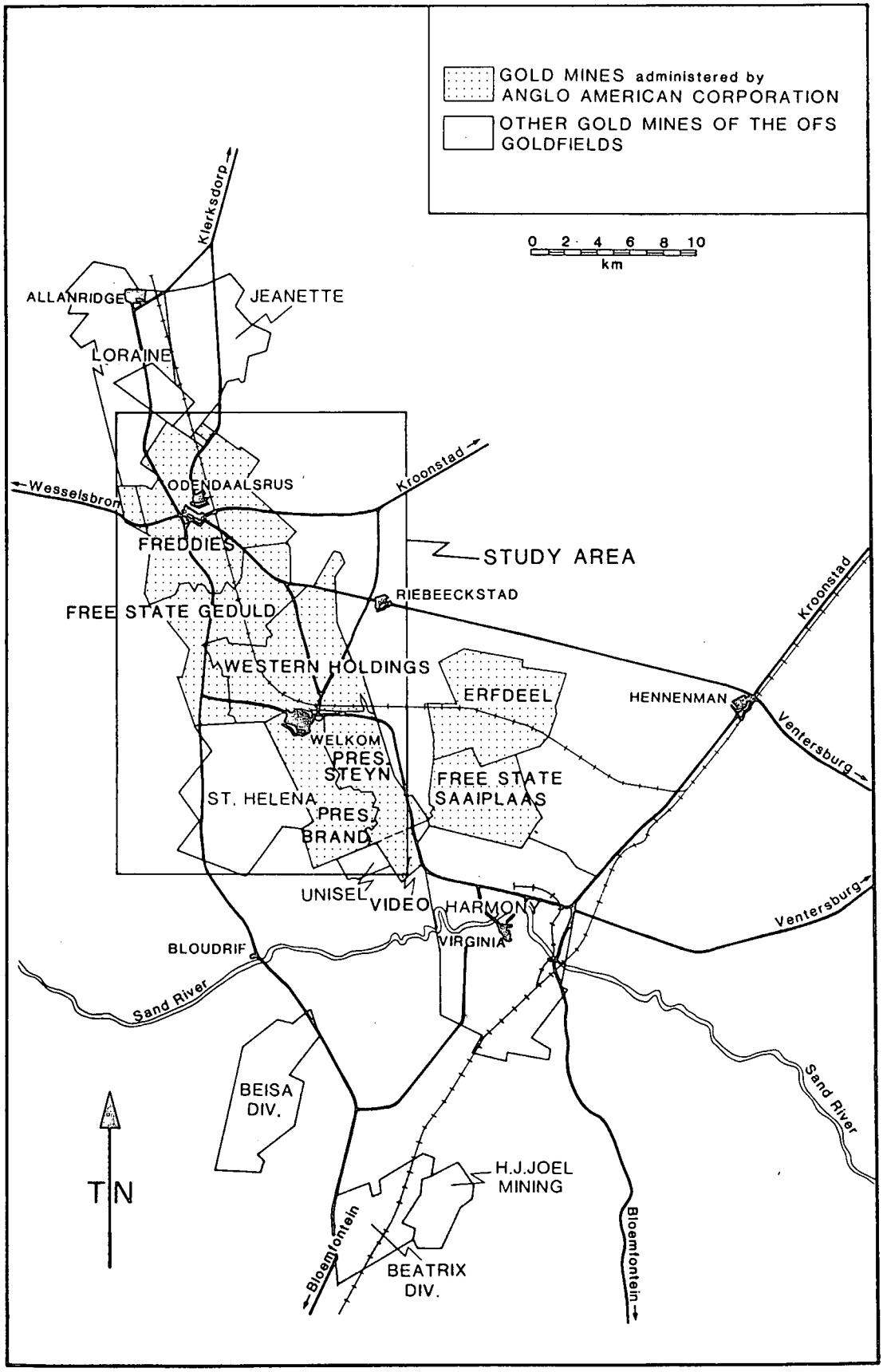

Fig. I.2. Locality plan showing the study area.

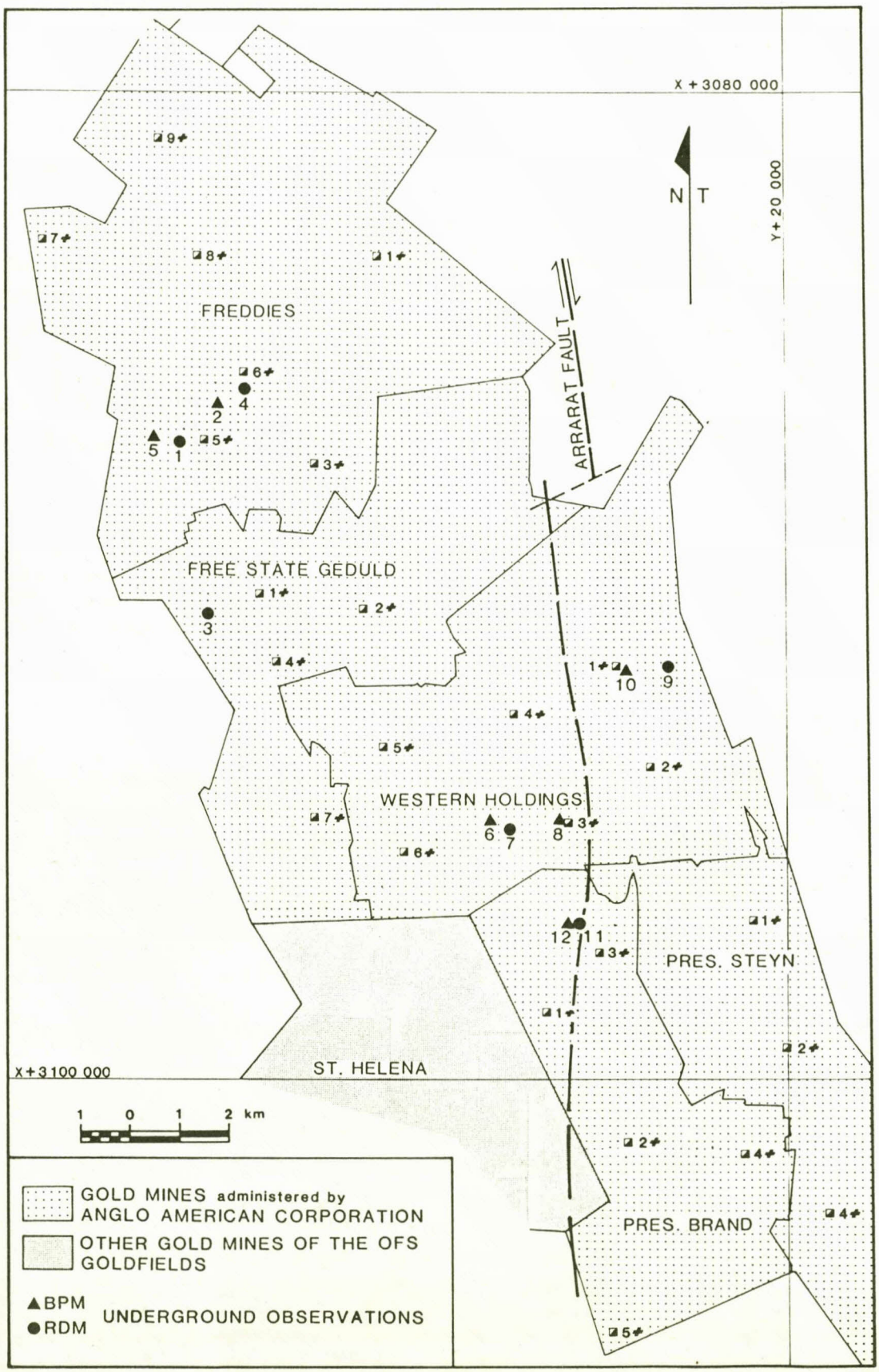

Fig. I.3. The study area, showing the locations of exposures studied.

Twelve underground localities, six for each of the BPM and RDM, were selected for this study. The positions of these localities are given in *Table I.1.* and shown in *Figure I.3.*

Table I.1. Localities of underground exposures studied. Co-ordinates are on the LOI reference system.

No	Locality	Co-ordinates X	Y
1	FREDDIES 5# 45 Hlge W	+3087132	+32287
2	FREDDIES 5# 47A Hlge E	+3086302	+31487
3	FSG 1# 43W2 Line 26	+3090502	+31687
4	FREDDIES 5# 45A 69 XCut	+3086002	+30967
5	FREDDIES 5# 42L W2 65 FWDr N	+3086972	+32767
6	W.HOLDINGS 6# 33E AReef Hlge N	+3094752	+26007
7	W.HOLDINGS 6# 33E AReef Hlge N	+3094862	+25797
8	W.HOLDINGS 3# 37L AReef TW	+3094702	+24547
9	W.HOLDINGS 1# 45L Hlge E	+3091622	+22367
10	W.HOLDINGS 1# 45L Hlge E	+3091662	+23247
11	PRES.BRAND 3# 42L W 22 XCut	+3096796	+24207
12	PRES.BRAND 3# 42L W 22 XCut	+3096782	+24367

On each of these localities:

- a short general description of the exposure was made.
- a photograph of the exposure was taken.
- the long axis of the ten largest quartz clasts were measured.
- a thousand point grid count was done with the aid of two counting frames, resulting in a modal count on the composition of the conglomerate.
- a line count was done, where the long axis of approximately two hundred clasts, falling on a vertical line, was measured and the pebble lithology noted.
- representative samples of the various types of clasts found at the exposure were taken.

A data set, consisting of the information obtained by means of the above procedures, was compiled for each locality.

The samples:

- each clast sample was cleaned of all matrix.
- a thin section was made, and studied, of each sample and submitted for assaying.
- clast samples were submitted for Au assay in p.p.b. and 36-element XRF analysis.
- a representative selection of samples was analyzed by XRD.
- fluid inclusion studies were carried out on a few selected quartz clasts.

The information was then computerized, studied and interpreted before final conclusions were formulated.

5. PRESENTATION

In order to present a report of this study and its results in a logical way, the presentation of this study does not necessarily follows the chronological order in which it was carried out. In **Chapter II** procedures and methods applied during the execution of this study are discussed in detail. **Chapter III** comprises of a detailed description and discussion of the clasts encountered in the two horizons studied and form the basis of this thesis. **Chapter IV**, a discussion of a fluid inclusion study on selected clasts, carried out by the Fluid Inclusion Unit at the UOFS, is an extension of Chapter III. **Chapter V** presents and discusses the wholerock chemistry (major and certain trace elements) of the clasts studied, which were analyzed by Anglo American Research Laboratories, as well as some statistical manipulation of these results. In **Chapter VI** the statistics of the field data are presented and discussed. In the semi-final **Chapter VII**, the results of the study and their implications on provenance synthesis are discussed. **Chapter VIII** contains the final conclusions.

6. PREVIOUS WORK

To date huge volumes of work by numerous researchers have been generated on the Witwatersrand Supergroup. These studies were, however, almost exclusively concentrated on sedimentological aspects, mineralization, or dating, for the formulation of depositional and provenance models. Compared to these aspects, very little research in the tenor of this study, has been done.

A study by Viljoen (1967) is probably the only in which the spectrum of pebbles occurring in a Witwatersrand conglomerate was studied in detail with the aid of thin sections. Although the study was focused more on matrix and detrital minerals rather than on pebble composition, it was nevertheless concluded that the occurrence of chloritoid (which is a function of composition, rather than temperature or stress (Halferdahl, 1961)) can be used tentatively as an indicator of the chemical composition of a probable source (Viljoen, 1967).

Illustrative of the situation, is the apt description by Hallbauer *et al* (1986): "Clay minerals are widely used in sedimentology as indicators of provenance areas and of depositional environments. They have, however, been the stepchild of Witwatersrand mineralogists in spite of their general abundance."

Since approximately 1980 several major models for the provenance of the Witwatersrand appeared in various publications. A few of these models, all of which, in some or other way, took in consideration previous models and available, information, are now briefly mentioned.

Hallbauer (1982 & 1984) proposed a granitic source along the northern and northwestern margin of the Witwatersrand basin,

as provenance for the Witwatersrand Supergroup. His proposals were based on the similarities in Au mineralization and the occurrence of "nodular" carbonaceous material (the so-called fly-speck carbon) in both the auriferous conglomerate reefs of the Witwatersrand, and the adjacent Archaean granites bordering the basin. Subsequent HAGS models for the provenance of the Witwatersrand were based largely on these observations.

Robb and Meyer (1985) proposed the so-called hydrothermally altered granites (HAGS) provenance model for the Witwatersrand Supergroup. They envisage that the earlier granite-greenstone crust was intruded by numerous highly-evolved granitoids, the upper portions of which were characterized by zones of hydrothermal alteration. The HAGS are significantly enriched in Au and U and occur widespread in the Witwatersrand hinterland. A major catastrophic change in the nature of the source region towards the termination of sedimentation of the underlying West Rand Group, evident on a major proportion of the Archaean granitic basement to the north, northwest and west of the Witwatersrand, is indicated. HAGS are considered to represent the principal source rocks for the Witwatersrand Supergroup. The strongest point in favour of the HAGS theory is the fact that, of the currently proposed source rocks for the Witwatersrand, only HAGS are unambiguously enriched in both Au and U.

Although the cratonic foreland, continental back-arc basin model for the development of the Witwatersrand basin, as proposed by Winter (1986), is essentially dealing with plate tectonics, it does however, have definite implications for the probable provenance of the Witwatersrand. The Witwatersrand basin is visualized as a geosyncline, yoked to an active, fold-thrust belt in its hinterland. Such basins are the result of Andean type subduction. Contemporary volcanism in such a situation is rare (Winter, 1986).

Hutchinson and Viljoen (1988) proposed an endogenous source for the gold and a separate extraneous source for the uranium. The former originated in the auriferous pyritic exhalites of the proximal facies of the Dominion and West Rand Groups. The uraninite was derived from the erosion of the granitic terrane surrounding the basin. The exhalatives of the hydrothermal-discharge system along the tectonically active northwestern basin-edge, was a product of shallow marine volcanism and was active at the same time as the formation of the HAGS. This endogenous, primary mineralization was subsequently eroded, detritalized and reworked, by fluvio-deltaic processes along the regressive margin of the basin, to form conglomerate reefs and re-enrich distal algal banks.

The latest model, a magmatic back-arc version of the modified-placer theory, as proposed by Pretorius (1989), is "in fact, a 'white flag' proposition hinting at the possibility that all three schools of thought in the Witwatersrand controversy might be right". This model postulates the occurrence of a magmatic arc, the presence of which is implied if the Witwatersrand Supergroup is accepted as a foreland back-arc basin. It furthermore postulates a rapid succession of:

- emplacement of primary gold at 2800 Ma c.
- uplift of the provenance region by thrusting
- diapiric rising of granite domes
- degradation and erosion of dominantly siliceous material
- fluvial transport of the detritus.

According to Pretorius (1989) repeated regeneration of source material occurred while gold and uranium entered the conglomerates and other sediments as detrital particles, dissolved constituents of fluvial waters and as components of hydrothermal fluids, all more-or-less at the same time.

A constant feature of all these models is that it tries to explain the "abnormal" deposit and mineralization of the Witwatersrand with "normal" source rocks or known environments. This principle also forms the basis of the so-called mass balance arguments. Is it not time to look for an "abnormal" provenance; for a unique deposit certainly requires unique conditions of formation? The most outstanding discrepancy in all these models is, however, the absence of quantitative and/or qualitative clast studies to gain insight into the nature of the provenance(s) of the Witwatersrand.

II

PROCEDURES

1. PRELIMINARY

A reconnaissance underground visit was undertaken to Freddies 5 Shaft 45 RAW North to do an orientation study and decide on certain parameters. Clast (pebble) lithologies were identified and the classes they were to be grouped in, decided upon. Initially the clasts of the RDM were grouped into 18 classes and the clasts of the BPM into 12 classes.

Clasts were classified by means of obvious lithotype (eg. quartz, chert, etc.), colour, texture and hardness. Hardness was determined by scratching with a knife blade (± 5.5 on Mohs' scale). This test served to distinguish some cherts from similar looking, but softer, nondurables. It also served to classify the so-called "yellows" into "soft" and "hard" classes.

After studying the conglomerate and considering the practical implications of the study, it was decided to consider and count all pebbles smaller than 10mm as part of the matrix. The reason for this decision is the fact that the matrix is very coarse-grained and consists largely of very small pebble sized material. Grid densities were arbitrarily decided on, to be 20 x 20 and 40 x 40 millimetres.

To do the grid count of the pebbles two counting frames were constructed. Nineteen milimetre angled aluminium section was used to construct two square frames, the larger one with inside dimensions of 440mm x 440mm and the smaller with

inside dimensions of 220mm x 220mm. Small holes were then drilled into the sides of the frames, 40mm and 20mm apart for the large and small frames, respectively. The frames were then strung, like a tennis racquet, with bright yellow fishing line (*Plate II.1.*). This resulted in 100 intersection points in each frame.

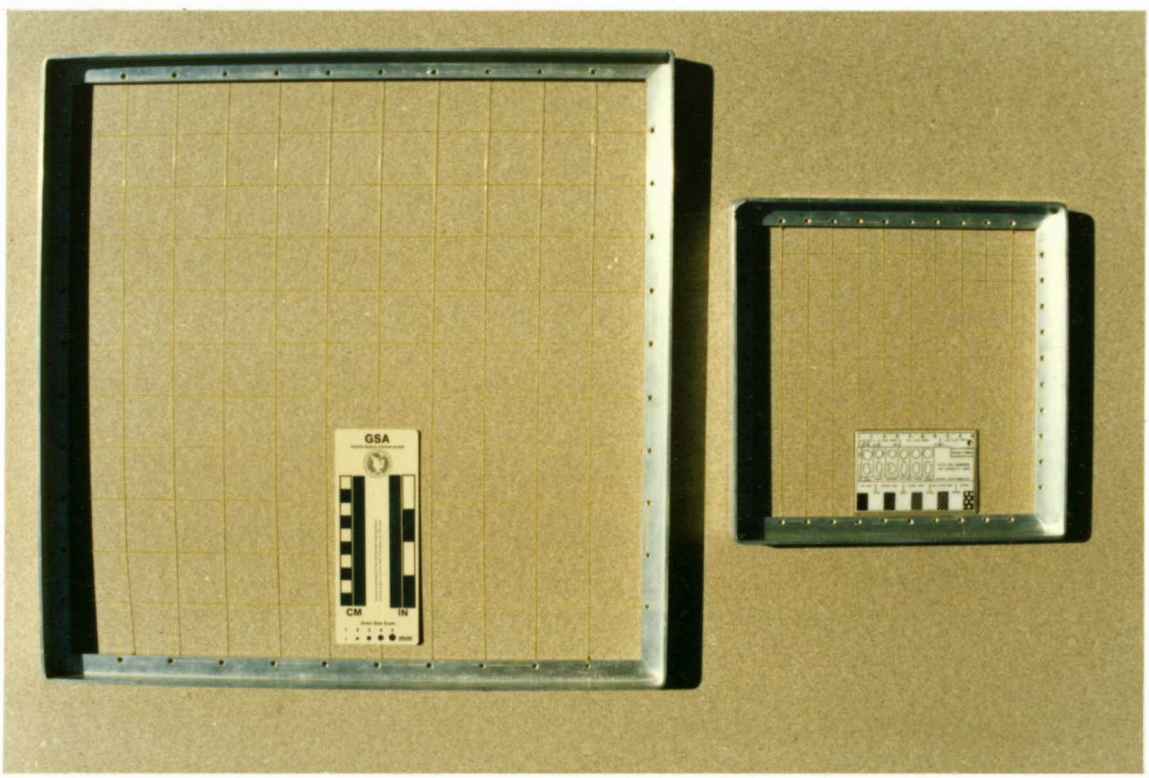

Plate II.1. Photograph of the counting frames used for the study.

2. METHOD APPLIED

2.1. UNDERGROUND

A clean, reasonably flat face, with sufficient conglomerate exposure was selected, as close as practically possible to the bottom contact of the conglomerate to ensure that valid correlations between

exposures could be made. Normally an area of approximately three to four square metres was sufficient.

- The **general setting** of the exposure, eg. part of a channel, gravel bar etc., together with a short description of the conglomerate was noted.
- The **long axis of the ten largest quartz clasts**, in the area investigated, and its immediate proximity, was measured.
- The **grid count** of pebbles was done by holding the frame against the exposure and noting the **clast type** (or matrix) at each intersection point in the counting frame. The outline of each frame was marked with wax crayon on the sidewall to prevent overlapping of areas counted. The use of either the large or small counting frame was arbitrarily decided upon after studying the coarseness of the conglomerate. Ten frames (irrespective of the ratio of small to large frames counted) were counted at each exposure, resulting in a total of 1000 counts per exposure.
- Thereafter one or more vertical lines were drawn through the area where the counting was done. All the clasts falling on this line(s) were then measured along their **long axis**, and their **composition** noted. About 200 readings were taken at each exposure. Again only pebbles larger than 10mm were recorded.
- All counts and measurements taken underground were recorded on a mini tape recorder from which the data were transcribed afterwards.
- A tungsten-tipped chisel and hammer was used to collect **representative samples**, where practical possible, of the clast types occurring at a specific exposure.
- Lastly a **colour photograph**, depicting the general appearance of the conglomerate and its general spatial relation, was taken.

2.2. LABORATORY

The samples taken underground were then prepared for laboratory work. First all the samples were thoroughly cleaned. For this a diamond saw was used to grind off all traces of matrix from the individual pebbles to eliminate any chance of gold contamination from the matrix.

Approximately 100g of material per sample, where possible, was then submitted to Anglo American Research Laboratories (AARL) for 36 element analysis and p.p.b. gold assay. Sample preparation was in the form of pressed powder briquettes. The major and trace elements were determined by X-Ray Fluorescence Spectrometry. Gold values were determined by Atomic Absorption Spectroscopy. A total number of 123 samples were submitted for analysis.

From these samples, 36 representatives of the different clast lithologies were selected for qualitative XRD analysis. The samples were crushed to -325 mesh, while all care was exercised to prevent contamination. Diffractograms were then obtained by irradiating the powdered samples with Cu Kα radiation. A Ni filter was used and the samples were scanned from 5° 2θ to 55° 2θ at a rate of 2°2θ/minute. The diffractograms were measured and qualitatively interpreted for mineral identification and semi-quantitatively for mineral concentration.
Of each sample submitted for assay and analysis a thin section was made for microscopic study. The thin sections were studied under a normal polarizing microscope. It was found that the lower magnifications were the best suited for the study since most of the clasts were originally sedimentary rocks of rather homogeneous composition. Low magnification thus facilitated the study of intergranular relationships.

During the microscopic study of the thin sections no unambiguous differences could be found to distinguish microscopically between dark-tinted quartz (smoky) and white or untinted quartz. It was therefore decided to experiment with the study of the fluid inclusions, which occur in abundance in these quartz pebbles, in an attempt to reveal any information about the genesis and/or later history of the quartz types. Four randomly selected quartz samples (two white and two dark) were chosen for a pilot study.

NOTE: *Due to the thickness of a normal thin section (0,03mm), the fluid inclusions preserved in a thin section will be very small (usually >0,005mm). Normally such small fluid inclusions are not detectable in a standard petrographic investigation, and doubly polished thick sections are therefore used for the purpose. The author, however, devised a technique with which such fluid inclusions can be detected in a normal thin section. Procedures are as follows:*
Firstly, the slide is viewed under maximum magnification with uncrossed polars and perfect focus. Then the substage condenser lens is placed in position, as for conoscopic observations. The focus is then carefully adjusted downwards ("into" the thin section). Any fluid inclusion present, will now become visible, initially as a glowing, pale yellow to orange locus. With careful adjustment of focus, on such a locus, a fluid inclusion can usually be recognized. Because of the minute dimension of such inclusions observations and focus adjustments should be done very carefully. However, once the technique is mastered, it becomes a simple operation.

All the fluid inclusion measurements were made with the aid of two calibrated Chaixmeca instruments. Measurements

represent duplicated melting temperatures and homogenization temperatures. A summary of the microthermometric procedures follows.

Firstly, the doubly polished thick section of quartz is cooled in the thermal cell of the instrument with the aid of liquid nitrogen, while the fluid inclusion is observed under high magnification. By cooling the specimen, the fluid inclusions are frozen, but the nucleation temperature of the ice is usually much lower than the corresponding melting temperature and is not regarded as an equilibrium temperature. Melting data, however, yield information about the composition of the inclusion.

The first reading obtained, during gradual reheating of the frozen inclusion, is the initial melting temperature (Tm_o). Tm_o represents the eutectic equilibrium temperature, which is indicative of the applicable phase system (eg. H_2O - NaCl with T_e at -20,8°C , or H_2O - NaCl - KCl at -23,6°C). However, in fluids of which the composition is somewhat distant from that of eutectic proportions, Tm_e is often impossible to determine.

The second melting event, T_1, represents a cotectic temperature and is actually the first observable reading obtained for many inclusions. The last reading obtained, is the final melting temperature (Tm_f). Tm_f is indicative of the chemical composition of the fluid inclusion, representing the true melting point depression. In instances where all melting events are clearly observable, starting with Tm_o and ending with Tm_f, the amount of intermediate melting events (Tm_1, Tm_2 ...) is indicative of the complexity of the system (number of components).

The same specimen is then heated by an electrical element in the thermal cell while the fluid inclusion is observed as before. By heating the specimen, the homogenization temperature (Th) of the gas and liquid phases in the inclusion is obtained. Th is indicative of density of the inclusion.

Owing to necking down and other secondary processes the measurements obtained from single inclusions may not represent the conditions of entrapment. It is therefore necessary to obtain enough measurements (different inclusions) from a specific specimen to establish the positions of the peaks. In this manner the Tm and Th peak positions are refined to acceptable levels of accuracy.

The composition of the fluid is deduced by reference to the melting point curves of appropriate phase systems eg. H_2O - NaCl. The value of a Th peak represents the characteristic density of the fluid. This value is obtained from calculation by application of the appropriate MRK equation (modified Redlich Kwong equation), or by comparison with isochore maps from the literature. The determined isochore (curve of equal density) now provides a univariate curve on the PT plot, along which the inclusion was trapped.

3. STATISTICAL MANIPULATION

3.1. GEOCHEMICAL DATA

The geochemical data basically consist of a set of 123 samples, comprised of 20 clast types, which were each analyzed for 36 major and trace elements as well as gold content. Average concentrations of all the elements were calculated for each clast type. Out of this "base data

set", smaller populations, consisting of data of related clast types, were taken and submitted to cluster analyses. The cluster analyses were executed with the aid of the SAS release 5.18, statistics programme on an IBM mainframe computer. The method of Ward (Everitt, 1974) was used for the cluster analysis, with certain pre-selected elements as clustering parameters. Spearman correlation coefficients (Conover, 1980) for the elements used as cluster parameters were also calculated with the SAS programme.

The aim of this procedure was to attempt to verify the validity of the macroscopical classification of some of the different clast types. The ideal way to accomplish this would seem to be to use discriminant analyses. In this case it is, however, not appropriate method, since the discriminators (in a geochemical sense) upon which an existing classification (based on physical parameters) is based, are unknown. The primary aim of this exercise was therefore not to find the geochemical parameters which caused the physical differences, but rather to determine, by means of comparison, whether the physical classification is valid in terms of recognized geochemical parameters.

Based on the results of some of the cluster analyses, as well as physical observations (see Chapter III), some of the originally different classes were merged and the averages of element concentrations for the newly formed classes, calculated. The statistical manipulation of the geochemical data is presented in *Chapter V*.

3.1. FIELD DATA

Only basic statistical manipulation of the field data was carried out. Three sets of statistics were compiled for each underground exposure studied. The first one being on the ten largest quartz clasts measured, the second for the grid count performed and the third for the line count done, at each exposure studied. The long axes of the ten largest quartz clasts in each exposure were measured and the respective average values calculated. In the case of the grid count the data were treated as modal analyses. Percentages were calculated for modal composition of the conglomerate, i.e. matrix included, as well as percentages for the clast composition, i.e. matrix excluded. In the case of the line counts the average clast sizes for the different clast types were calculated. The measurements for each different clast type were also counted and the figures used to calculate another set of clast composition averages for comparative purposes. The statistical manipulation of the field data is presented in *Chapter VI*.

III

LITHOLOGICAL DESCRIPTIONS

1. MESOSCOPIC DESCRIPTION

During the underground orientation visit preceding the actual investigation, the clasts of the two conglomerate horizons studied, were classified into different classes, based, firstly on lithology, and then on other physical properties (see *II.1.*). The clasts of the BPM were thus separated into 12 different classes and the clasts of the RDM into 18 classes. This difference in number of classes primarily stems from the fact that the BPM contains less non-durable clasts of smaller variety, dominated by a yellowish type. Although the number of classes may appear to be excessive, it was done in this way to determine if any microscopic and/or chemical evidence exist to justify this classification. If this allocation cannot be verified by means of mineralogy, chemistry and/or thin section study, separate classes will be merged. An extensive cross reference list can be found in *Table III.6.* at the end of this chapter.

An important factor which is seldom taken into account in the study of clasts, is the nature and quality of light available underground, compared to normal daylight. Normally the difference is not observed by the naked eye. Because the intensity and wavelength of light provided by a caplamp is different and much less intense than sunlight, the yellow light from a caplamp enhances yellowish colours underground. Due to this, clasts which appeared to be yellow underground, might in fact be of a much paler hue. The colour descriptions were therefore done in natural light on wet

samples with the aid of the *Standard Soil Color Charts*, which is based on the *Revised Munsell System* (Takehara, 1970). The colours given in *Tables III.1.* and *III.2.*, are the apparent colours as observed underground by the light of a cap lamp. Since it is basically only the description of the "yellows" which is critically influenced by this phenomenon, the true colours of these clasts will be discussed under *III.1.3.*.

1.1. RDM CLAST TYPES

The classification system used for the different clast types from the RDM is given in a summarized form in *Table III.1.*.

1.2. BPM CLAST TYPES

The classification system used for the different clast types from the BPM is given in summarized form in *Table III.2.*.

1.3. DESCRIPTION

QUARTZ

The quartz clasts from the RDM and BPM are very similar in appearance and composition as determined in hand specimens. Based on colour, the quartz clasts were arbitrarily classified into two groups, white and dark quartz. **White** quartz clasts varies from clear, almost transparent, quartz to white milky quartz. Only a very few opalescent quartz clasts, which were classed as white quartz, were encountered. **Dark** quartz clasts varies from translucent smoky quartz, to quartz, which is dark and

Table III.1. The classification system for the RDM clast types.

CLAST TYPE	DESCRIPTION
WHITE QUARTZ	milky, translucent & clear quartz
DARK QUARTZ	smoky & dark-coloured quartz
LIGHT QUARTZITE	white & light-coloured quartzite
DARK QUARTZITE	all dark-coloured quartzite
LIGHT CHERT	all light-coloured chert
DARK CHERT	all dark-coloured chert
BANDED CHERT	all banded varieties, irrespective of colour
IGNEOUS	all igneous rocks, porphyries & lavas
YELLOW-1	hard, non-laminated, fine-grained, yellow-coloured, shaley texture
YELLOW-2	soft, non-laminated, fine-grained, yellow-coloured, shaley texture
YELLOW-3	hard, non-laminated, coarse-grained, yellow-coloured, shaley texture
YELLOW-4	soft, non-laminated, coarse-grained, yellow-coloured, shaley texture
GREY-1	hard, non-laminated, fine-grained, shaley texture, not yellow or black
GREY-2	soft, non-laminated, fine-grained, shaley texture, not yellow or black
GREY-3	hard, non-laminated, coarse-grained, shaley texture, not yellow or black
GREY-4	hard, non-laminated, coarse-grained, shaley texture, not yellow or black
BLACK	black, fine-grained, non-laminated, shaley composition, shaley texture
DARK SILTSTONE	dark-coloured, silty texture

Table III.2. The classification system for the BPM clast types.

CLAST TYPE	DESCRIPTION
WHITE QUARTZ	milky, translucent & clear quartz
DARK QUARTZ	smoky & dark-coloured quartz
LIGHT QUARTZITE	white & light-coloured quartzite
DARK QUARTZITE	all dark-coloured quartzite
LIGHT CHERT	all light-coloured chert
DARK CHERT	all dark-coloured chert
BANDED CHERT	all banded varieties, irrespective of colour
IGNEOUS	all igneous rocks, porphyries & lavas
YELLOW-1	hard, non-laminated, fine-grained, light-coloured, shaley texture
YELLOW-2	soft, non-laminated, fine-grained, light-coloured, shaley texture
BLACK	black, fine-grained, non-laminated, shaley composition, shaley texture
DARK SILTSTONE	dark-coloured, silty texture

opaque, due to alteration and/or the presence of inclusions of diverse nature. Inclusions normally consist of primary and/or secondary pyrite, while a few other unidentifiable substances also occur as inclusions. Secondary, *in situ* alteration, in various stages of progress, converting white quartz to smoky or dark quartz, can occasionally be observed underground. This process normally starts in fractures and along the outer rim of light-coloured clasts. In general the quartz clasts are rather brittle.

QUARTZITE

NOTE: *For the purpose of this study, the term "quartzite" is used as a convenient collective name which may include different compositions from litharenite to wacke.*

As in the case of the quartz clasts, the quartzite clasts occurring in the BPM and RDM are virtually identical. Texturally the quartzites vary from very fine-grained to medium-grained and rarely coarse-grained. Colours are predominantly white and various shades of grey, while pale green and pale yellow is not uncommon. The grey quartzites vary from light grey to almost black. The appearance of some of the grey quartzites is reminiscent of that of quartzite from the Basal Quartzite Member in the Welkom Formation. Again the quartzites were also classified arbitrarily into a **dark**- and a **light**-coloured class. All these quartzites are very pure and highly siliceous, to the extent that it become difficult to distinguish in hand specimens between some of the very fine-grained quartzite and quartz clasts. Correctly classified, they probably are quartzarenites (see *III.2.1.*).

CHERT

Chert clasts of virtually any colour occurs in both the BPM and the RDM. Black is the dominant single colour, however. In general chert clasts from the BPM is macroscopically indistinguishable from chert clasts from the RDM. Amorphous as well as banded chert occur in both the BPM and RDM. Again, the amorphous chert is also divided arbitrarily into a light-coloured class and a dark-coloured class. Occasionally clasts of re-cemented, brecciated chert were encountered. In all cases the cementation agent was silica. The incidence of this

'breccia chert' is the highest in the banded chert, followed by the dark chert.

In general the **banded chert** is more abundant in the BPM (4,4% of total clasts) than in the RDM (1,3% of total clasts). The banded chert displays a wider variety of colours than the more drab, amorphous chert. The banding varies from indistinct to prominent and from very fine to coarse. In some cases the banding appears wavy, while in others the banding is absolutely straight and parallel.

The predominant colour variation displayed by the **light chert** ranges from pale yellow, through white, to a pale, blueish-grey colour. In hand specimen some of the light-coloured chert clasts, especially the yellowish to white clasts, appear to be relatively coarse-grained. Generally the light-coloured chert is tough and tenacious. The **dark chert** consists predominantly of dark-grey to black clasts. Unlike the other chert pebbles which are normally well rounded, black chert often occurs as angular clasts.

Sulphide minerals (predominantly iron pyrite) occur virtually exclusively in the dark chert, as opposed to the low incidence of pyrite in the light chert. The pyrite is predominantly amorphous and probably secondary in origin. It is, however, not easy to determine at what stage the secondary pyrite was introduced into the chert, i.e. before or after deposition of the chert clasts in the conglomerate. In some clasts both "pre- and post-burial" pyrite can be seen. The post-burial secondary pyrite can be recognized by its penetrating habit across layering and pebble boundaries (see *Plate III.1.*). All these observations concerning the occurrence of pyrite also apply to the banded chert. Preferential pyrite replacement along laminae can be seen in some banded chert clasts.

Plate III.1. Photograph of a polished section of a banded chert clast illustrating "pre-burial" and penetrative "post-burial" pyrite (units of scale is 1 mm).

IGNEOUS

The igneous clast class contains all clasts which could be identified with reasonable certainty, from a hand specimen, as to be of igneous origin. All the igneous clasts identified as such, were of a nondescript grey colour and had a porphyritic character. It is not possible, however, to determine whether the clasts are of intrusive or extrusive origin, therefore the 'igneous' designation. Because of secondary alteration and silicification it is extremely difficult to identify the phenocrysts positively. Quartz phenocrysts were identified in some samples, while the outlines of feldspar phenocrysts can occasionally be recognized in others. Due to the mottled appearance of the igneous

clasts, it is virtually impossible to classify their colours by means of the *Standard Soil Color Charts* (Takehara, 1970). The general colour can, however, be described as *gray* (5y 5/1).

"YELLOWS"

Because the first physical parameter upon which the classification of the "yellows" were based, was colour, it was decided to qualify the colour of these clasts with the aid of the *Standard Soil Color Charts* (Takehara, 1970). Due to the phenomenon described and discussed under *III.1.*, vast differences in actual colour, as seen in natural daylight, compared to "apparent" colour as observed underground, is experienced when the colour of the clasts are compared to the *Standard Colour Charts.* Therefore, the true colours of a representative selection of samples from the different "Yellows" clasts are given in *Table III.3.*.

A conspicious feature of the RDM, in particular, and to a lesser extent the BPM, is the occurrence of relatively soft, light-coloured clasts of shaley composition, the so-called "yellows", together with other much more durable clasts. Texture of the clasts vary from very fine-grained to an apparently medium grain size. Hardness varies from very soft to quite hard, which again probably is the result of silicification. The majority of these "yellows" clasts, especially the softer ones, has a slight soapy feeling and are reminiscent of some tuffaceous sediments. Lamination is virtually absent in these clasts, but secondary reaction rims can be observed along the borders of some.

Due to the notable abundance of these clasts in the RDM, they can be classified into eight different classes in

the case of the RDM. These eight classes consist essentially of two basic groups, designated yellow and grey, which are again divided into four subgroups each. This subdivision, which is described above in *III.1.1.*, is based on hardness and apparent texture, as described in *II.1.*. Upon closer investigation, however, it appears that hardness and apparent texture might be a function of post-burial silicification, as much as it is a function of mineralogy. In the case of the RDM, the **yellow** group only consists of clasts with a distinctive greenish- to brownish-yellow colour. The **grey** group contains all the other relatively light- coloured clasts of similar composition, which do not conform to the colour description for the yellow class and are essentially of a grey colour.

Although the non-durable clasts from the BPM is virtually identical to those of the RDM, the BPM conglomerate is more mature than the RDM conglomerate, resulting in a lower percentage nondurables in the BPM (7,3% of all clasts in the BPM and 27% of all clasts in the RDM). Therefore the nondurables in the BPM were classified into two classes only. The yellow and grey class were put together and classified into two groups only, a hard and a soft class. Because the yellow clasts are dominant and only a few grey clasts occur, "**yellow**" was designated as the class name.

BLACK

Black designates a class of clasts of singular appearance, which occurs with a low incidence in the RDM. The clasts are relative soft, very fine-grained (<1/256 mm) and have a jet black colour. No obvious lamination is discernable in the clasts. In general, the clasts are

Table III.3. True colours of "yellows" clasts, viewed in natural light, according to *Standard Soil Color Charts* (Takehara, 1970).

SAMPLE No	ROCK TYPE	MUNSELL NOTATION	COLOUR
FWS-039	1	5Y 6/2	GRAYISH OLIVE
FWS-072	1	2.5Y 5/6	YELLOWISH BROWN
FWS-099	1	10Y 5/1	GRAY
FWS-040	20	2.5Y 5/3	YELLOWISH BROWN
FWS-065	20	2.5Y 5/3	YELLOWISH BROWN
FWS-080	20	7.5Y 5/2	GRAYISH OLIVE
FWS-019	10	5Y 5/3	GRAYISH OLIVE
FWS-042	10	2.5Y 4/3	OLIVE BROWN
FWS-056	10	5Y 6/3	OLIVE YELLOW
FWS-089	10	7.5Y 5/2	GRAYISH OLIVE
FWS-137	10	5Y 6/4	OLIVE YELLOW
FWS-017	11	5Y 5/3	GRAYISH OLIVE
FWS-054	11	2.5Y 6/4	DULL YELLOW
FWS-083	11	7.5Y 4/3	DARK OLIVE
	11	5Y 6/4	OLIVE YELLOW
	11	2.5Y 7/6	BRIGHT YELLOWISH BROWN
FWS-130	11	5Y 5/3	GRAYISH OLIVE
FWS-016	12	5Y 5/3	GRAYISH OLIVE
FWS-023	13	5Y 5/3	GRAYISH OLIVE
FWS-131	13	5Y 4/2	GRAYISH OLIVE
FWS-020	14	10Y 4/1	GRAY
FWS-045	14	5Y 5/2	GRAYISH OLIVE
FWS-085	14	10Y 3/1	OLIVE BLACK
	14	10Y 6/2	OLIVE GRAY
	14	7.5Y 5/2	GRAYISH OLIVE
FWS-132	14	7.5Y 5/2	GRAYISH OLIVE
FWS-018	15	10Y 5/1	GRAY
FWS-014	16	7.5Y 5/2	GRAYISH OLIVE
FWS-053	16	5Y 5/2	GRAYISH OLIVE
FWS-129	16	10Y 6/2	OLIVE GRAY
FWS-015	17	10Y 5/2	OLIVE GRAY
FWS-043	17	5Y 5/2	GRAYISH OLIVE
FWS-084	17	7.5Y 5/2	GRAYISH OLIVE
FWS-114	17	7.5Y 3/1	OLIVE BLACK
	17	10Y 5/2	OLIVE GRAY
FWS-135	17	5Y 4/1	GRAY

Table III.3. *(continued)* Rock type references.

1 - YELLOW-1 BPM	14 - GREY-1 RDM
10 - YELLOW-1 RDM	15 - GREY-2 RDM
11 - YELLOW-2 RDM	16 - GREY-3 RDM
12 - YELLOW-3 RDM	17 - GREY-4 RDM
13 - YELLOW-4 RDM	20 - YELLOW-2 BPM

small and well rounded. Black clasts are virtually absent from the BPM.

DARK SILTSTONE

Clasts with a dark colour and a silty texture occur sporadically in the RDM and to a lesser extent in the BPM. The colour of these clasts vary from dark grey to almost black. Frequently the clasts display a well developed lamination. Some of the darker coloured specimens are rather hard and have a glittery appearance which can cause them to be mistaken for dark quartzite. Upon closer investigation (in thin section), it became evident that this phenomenon is caused by numerous secondary euhedral chloritoid crystals. No light-coloured siltstone clasts were encountered.

1.4. DISCUSSION

Some of the observations made under *III.1.3.* will now be discussed briefly under corresponding headings.

BLACK CHERT

The angularity of the black chert clasts can probably be explained by the fact that the black chert, although very hard, appears to be rather brittle and thus susceptible to mechanical breakdown. This, in turn, is explained by

the occurrence of minute seams and veinlets, of unknown origin, in the black chert. The overall average size of the black chert clasts, compared to the other chert, is however, not influenced by this phenomenon.

If the dark colour of the dark chert is a reflection of organic content, it might possibly explain the almost exclusive presence of pyrite in the dark chert (also see the microscopic discussion of the chert under *III.2.2.*).

YELLOWS

Upon closer investigation it can, however, be seen that the apparent relative coarse texture displayed by some yellows clasts, is a secondary phenomenon, probably due to silicification, recrystallization and/or the presence of secondary euhedral chloritoid crystals.

The shape of these clasts is predominantly sub-angular to blade-shaped, with some clasts displaying a shape that resembles a flattened teardrop. If these shapes are not coincidental, but a result of post-depositional deformation, it can indicate that the sediment from which the clasts were derived, was probably consolidated but unlithified. If this is not the case, and the sediment was lithified at the time the clasts were derived, the angularity of the softer "yellows" clasts, compared to the well rounded durable clasts, would indicate a much shorter distance of transport for the yellows. Since the fact that clasts derived from unlithified sediments would also indicate a short distance of transport, it is apparent that it does not matter which explanation is accepted, different sources for the yellows and the durable clasts are indicated.

BLACK

The relative small size and high degree of roundness, together with its low incidence, can indicate relative extensive transportation of the "black" clasts.

COLOUR

As is clearly demonstrated by the true colours of the yellows clasts (*Table III.3.*) a cap lamp is an unsuitable light source for qualitative colour studies of clasts. Another problem is during qualitative colour studies, is one of reference, since the human eye is inclined to concentrate on relativity of colour, rather than absolute colour. A standard colour reference is therefore essential for comparison during qualitative colour studies. It thus becomes evident that the yellows actually have a greenish khaki (or *grayish olive*) colour, rather than yellow.

2. MICROSCOPIC DESCRIPTION

A thin section was made of every sample that was submitted for 36 element XRF analysis. These thin sections were each studied carefully under a polarizing microscope in transmitted light. The description of thin sections of the samples will, however, be done collectively for the different classes (described in *III.1.3.*).

Optical mineral identification is to a large extent virtually impossible because of the very fine-grained nature of the clasts, as well as extensive secondary alteration, mainly silicification, present in the clasts. This results in the murky appearance observed in the thin sections of argillaceous samples. Textures in these samples are also indistinct or obliterated. Therefore an XRD study (see

III.3.) was carried out on a selection of samples to determine the main mineral phases present. The more silicic clasts (quartzite, quartz and chert), however, are to a large extent unaffected by these phenomena.

2.1. DESCRIPTION

QUARTZ

The most common and outstanding microscopic feature of the quartz clasts is their diversity. Microscopic discrimination between white and dark-coloured quartz and between clasts from the RDM or the BPM was not possible. This can probably be attributed to the small population (10 samples) studied. If a much larger population is studied, subtle discerning differences between different types of quartz might possibly emerge.

Textures, grain sizes and other features vary greatly within and between samples. The occurrence of small to very large grains in individual samples is not uncommon. Individual grains vary from euhedral crystals to anhedral grains with amoeboidal boundaries.

In general all the samples exhibit no or very little evidence of secondary alteration. In one of the cataclastically deformed samples secondary alteration can be recognized by the presence of distinctive euhedral chloritoid crystals and other unidentified amorphous, light-coloured secondary minerals. Anhedral pyrite and unidentified gangue minerals occur in one sample.

Abundant fluid inclusions occur in the quartz. Therefore it was decided to carry out a pilot study on these fluid inclusions in order to determine if microthermometric differences exist between the different types of quartz

and what the conditions of entrapment of the inclusions were. This study will be discussed in detail in Chapter IV.

NOTE: *A description of the technique used to detect the presence of small fluid inclusions in normal thin sections is described in detail under II.2.2.*

QUARTZITE (Quartz-arenite)

The most outstanding feature of all the quartzite samples is the purity thereof. Accordingly to the modified classification of Dott (1964) (Pettijohn, 1975), all the samples are in fact quartzarenites. However, as in the case of the quartz clasts, it was again not possible to distinguish unequivocally in thin sections between either light- and dark- quartzite or between quartzite clasts from the BPM or the RDM. However, very subtle differences between the different types of quartzite do occur. Of these differences, the most obvious is the relative abundance of very small (≥0,003mm) fluid inclusions in grains of the light quartzite, as opposed to very few, in grains of the dark quartzite (See note under *III.2.1.*)

Other differences include the observation that in general the incidence of straight intergranular boundaries are higher in dark-coloured than in light-coloured quartzite. It also appears that the grains are smaller and more densely packed, with slightly less interstitial material, in the dark-, compared to the light- quartzite. It also appears that in the case of the light quartzite, grains in samples from the RDM contain more fluid inclusions than in the grains of samples from the BPM. The abundance of the fluid inclusions seem to vary inversely with the density of packing of grains. All these differences are, however, too subtle to be conclusive.

The quartzites are totally clast-supported and, as a rule, only a very limited amount (1 -3%) of argillaceous matrix occur in the quartzites in the form of clay clots (a term coined by Carozzi (1960) for these phenomena), located at interstitial voids. Apart from small quantities of amorphous argillaceous matrix and a few isolated chert fragments observed in some of the samples, the quartzites consist almost exclusively of quartz fragments. (Only one of the samples studied, a quartz-wacke (FWS-074), was matrix-supported). No heavy/stable mineral grains were encountered in any of the samples.

All stages of deformation, from totally unaffected to extreme cataclastic deformation, can be observed in different samples. Quartz overgrowth of individual grains and pressure solution of grain boundaries is a common feature in the majority of the samples. Examples of various stages in the process of transition of curved grain boundaries to straight boundaries, together with the migration of the small quantities of argillaceous matrix into interstitial locations to form "clay clots".

Despite the fact that overgrowth on grains, pressure solution of grain boundaries and various degrees of deformation can be observed in the thin sections, it can be seen (by the presence of faintly discernable "dust rims" (Scholle, 1979), along the original grain boundaries, which show up as minute "illuminated" specks when a particular quartz grain is viewed in the position of extinction under crossed polars), that in general, all the grains were well rounded to very well rounded at the time of deposition. Sorting, however, is not good, as grain sizes in individual samples vary up to three phi units on the Wentworth-Udden scale (Greensmith, 1981 ; Whitten & Brooks 1979). Grain sizes encountered, cover

the total range for sand(stone), from very fine (0,06mm) to very coarse (2mm).

Due to the low matrix content of the particular quartzites, grain boundaries are virtually indiscernible in unpolarized light. Because of the low matrix content it is in the case of deformed samples very difficult, even in polarized light, to distinguish between inter- and intra-granular grain boundaries. In extreme cases it is almost impossible to determine whether a sample is highly deformed quartzite, or fine crystalline quartz.

Individual grains are predominantly monocrystalline. Where polycrystalline grains occur, they normally consist of less than four crystals and the intragranular boundaries are straight. The majority of the grains display normal extinction and on average the ratio of "normal" to "undulose" grains is estimated to be 70:30 or higher. In one uncharacteristic sample the majority of the grains displayed undulose extinction.

CHERT

Microscopic study of dark chert samples, showed a definitive difference between clasts from the RDM and the BPM. All the samples from the RDM were fine-grained amorphous chert which contained a few small disseminated, euhedral pyrite crystals. In contrast, all the samples from the BPM exhibit some form of secondary alteration which can be classified into three groups. In the first group it can be seen that the chert is in the process of being recrystallized into quartz. In the second group, hydrothermal alteration is evident. Dissolution vugs which are filled with secondary quartz, as well as small amounts of massive ore minerals (predominantly pyrite) can be distinguished. In another case small fractures and

seams were also filled by massive pyrite. The two samples from this group which were submitted for assay, both yielded in excess of 750 p.p.b. Au. (This will be discussed in more detail in *Chapter V.* and *VII.*) The third group consists of brecciated chert which is cemented by silica. Occasionally the silica cement contains finely disseminated amorphous pyrite.

Microscopically no difference could be seen between **light chert** from the BPM and the RDM. Textures range from very fine amorphous to coarse amorphous chert. Thin quartz veins criss-cross the samples and the occasional small euhedral pyrite crystal is not uncommon.

As in the case of light chert, no unequivocal evidence, upon which can be distinguished between **banded chert** from the BPM or from the RDM, was observed. Microscopically the banding in the chert is normally caused by differences in "grain" size or by a succession of small cycles of grading. In some cases the grading is enhanced by the concentration of finely disseminated pyrite, probably of primary origin, which occur in certain bands. Such samples also display slightly elevated Au contents. Small quartz veinlets and small euhedral pyrite crystals are occasionally present in most of the samples.

IGNEOUS

Of all the clast types studied, the igneous clasts suffered the most severe secondary alteration. Silicification is also evident in most of the samples. In general, all the minerals, except quartz, are either murky and semi-opaque or occur as a very fine amorphous mass. As a result, microscopic identification of any mineral or texture is virtually impossible. The only mineral that can be identified positively, is quartz. Due

to the coarse nature of the samples, a very low magnification (10 X) was found to be the most effective for studying them, especially since the emphasis moves to the study of structures and textures, rather than optical mineral identification.

Virtually no igneous textures were preserved. Spherulitic textures, normally consisting of a mass of radiating elongated quartz crystals, is present in most of the samples. Sometimes these textures were formed around an amorphous core. These textures are reminiscent of similar textures, described by Carozzi (1960), in devitrifying welded tuff. Some of the samples display textures very similar to that of accretionary lapilli in pure vitric tuff, illustrated in Fisher & Schmincke (1984). In one sample, small, round, quartz-filled amygdales could be identified. A few samples exhibit gneissose textures. In general, the microscopic study of the "igneous" clasts was, however, rather inconclusive.

YELLOWS

No verification for the classification used in *III.1.1.* and *III.1.2.*, could be found during the microscopic study of the "Yellows" clasts. Neither could any unequivocal differences between Yellows from the BPM and Yellows from the RDM be found, nor could microscopic evidence be found to distinguish between "yellows" and "greys". Textures vary from totally amorphous to very fine but nevertheless granular. In a few of the samples evidence of a sedimentary origin exists in the form of isolated but well rounded quartz grains occurring in the much finer groundmass. In isolated cases a very fine lamination, which is not visible in hand specimen or under the microscope, can be seen with the naked eye when the particular thin section is viewed against the light.

All the samples are strongly affected by secondary alteration and silicification, to the extent that the majority of the minerals are amorphous and semi-opaque. This, and the very fine grain size of the samples, render it impossible to positively identify any of the primary minerals except quartz. Two secondary minerals have been identified. Very fine (± 5 μ), colourless, needle-like crystals, which occur in most of the samples, were identified by means of electron micro-probe as muscovite/hydromuscovite (see *III.2.4.*). The other mineral is chloritoid, which forms large (up to 1mm), light-green, euhedral crystals displaying characteristic hour-glass structures (Kerr, 1977). Chloritoid is present in approximately 50% of the samples.

Because of the macroscopic resemblances of the yellows with some known tuffaceous rocks (see *III.1.3.*), special care was taken to detect any features diagnostic of volcaniclastic sediments. A few samples were also studied by means of an electron microscope (SEM) (see *III.2.3.*), because some diagnostic features can be very small (Fisher & Schmincke, 1984). Although no conclusive evidence to prove or disprove a volcaniclastic origin for the yellows could be found, they do in general conform to descriptions of altered vitric tuff, given by Pirsson (1915), Carozzi (1960) and Pettijohn (1975).

BLACK

Microscopically the "black" clasts appear as a dense mass of very fine-grained, blackish, semi-opaque minerals, interspersed with very small, colourless, needle-like minerals. Optically it is impossible to identify these minerals because they are either too opaque or too small. XRD analysis subsequently proved the minerals to be quartz and pyrophyllite, respectively. The reason for

the black colour and semi-opaque character of the quartz is unclear. No microscopic differences could be found between "black" samples from the BPM and the RDM.

DARK SILTSTONE

Microscopically, three general types of siltstone could be recognized, the first type being a normal siltstone, conforming to the accepted parameters for siltstones (Pettijohn, 1975). The next type reflects various degrees of alteration. Dissolution and recrystallization textures occur in the samples together with sericitization. Secondary minerals like chloritoid and pyrophyllite are present. In one sample spherulitic structures, similar to the ones in some of the igneous clasts described above, occur. The last group is dominated by the presence of large, secondary, euhedral chloritoid crystals, set in a dark, semi-opaque, finely amorphous matrix. In the laminated samples the concentration of chloritoid crystals increases in the darker zones.

2.2 DISCUSSION

QUARTZ

Normal and undulating extinction, observed in some samples, probably indicates varying degrees of deformation in the source area. In two samples cataclastic deformation is evident. Further evidence for primary deformation is the occurrence of mylonite in one sample. The occurrence of both deformed and undeformed clasts in the same conglomerate indicates that the deformation must have occurred in the source area, before deposition of the clasts.

The abundance of the fluid inclusions in the quartz clasts probably indicates a hydrothermal origin for the quartz.

QUARTZITE (Quartz-arenite)

The abundance of very small fluid inclusions in the light quartzite, relative to the dark quartzite probably indicates different source rocks for the two types of quartzite.

If the other observations concerning the subtle differences concerning intergranular boundaries, grain size, interstitial material and fluid inclusions are valid, it might, however, explain the hitherto unexplained difference between light- and dark-quartzite. It can be argued that impurities and the more unreconciled grain boundaries occurring in the less pure and densely packed, light quartzite, disperse light inside the quartzite to create the effect of light-colouredness, analogous to the way the white colour of milky quartz is caused by dispersion of light by numerous minute fluid inclusions. In contrast, the pure, densely packed, dark quartzite absorbs more light than the light quartzite and appears dark.

First-cycle sands in which all rock fragments and feldspars and nearly all heavy minerals have been destroyed, can, according to Blatt *et al* (1980), be produced by lateritic-like weathering processes in hot, humid climates. Evidence for the occurrence of such weathering in Precambrian times does exist (Van Houten, 1982). However, such pure quartzites normally are the product of recycled sediments (Blatt *et al*, 1980).

The presence of interstitial "clay clots" present further evidence of a pressure history. The fact that quartzite clasts from the same conglomerate display such a wide range of deformational features, however, indicates that the event(s) responsible for the deformation observed in some of the quartzite clasts, must have occurred in the source area before deposition of the clasts in the conglomerate.

The poor sorting encountered in the quartzites may indicate an original fluvial origin. The large amount of monocrystalline, non-undulatory, clear grains in the quartzites indicate that the majority of the grains of the dark-coloured quartzite samples were probably derived from volcanic rocks, while the abundance of fluid inclusions in grains of the light-coloured quartzite, is probably indicative of predominantly hydrothermal source rocks. A granitic source rock is indicated for the one sample in which undulatory grains predominate (Blatt *et al*, 1980).

CHERT

No conclusive evidence concerning the origin of the black cherts could be found. According to Pettijohn (1975), iron, present as pyrite or magnetite, is normally responsible for the black colour in chert. This confirms some observations made in the darker banded chert samples. Pettijohn also proposes that the intimate association of black cherts with black pyritic shales, may indicate a restricted basin with attributes of a starved basin as a prerequisite for the formation of black chert. Dunlop (1981) ascribes the black colour in some cherts to carbonaceous matter and minor pyrite, with the carbonaceous matter being of fossiliferous origin. This view is supported by Mel'nik (1982), who quotes

several references on the occurrence of fossiliferous carbonaceous material in chert, as old as 3000 to 3400my.

The observed difference in pyrite mineralization of chert clasts in the two different reefs (RDM and BPM), is significant. Being stratigraphically close to each other, the RDM and BPM were most probably affected similarly by post-burial metamorphism. Therefore the observed difference in pyrite mineralization of these clasts was inherited from the source rocks.

YELLOWS

Concerning the possible volcanigenic origin of the yellows clasts seen in the light of the absence of unequivocal evidence for volcanigenic origin, it should be noted that Pettijohn (1975) duly pointed out that: "Volcanic debris is especially susceptible to diagenetic alteration and rapidly loses its distinctive character. If the rock is further altered by metamorphism, its original character may be greatly obscured."

DARK SILTSTONE

The increase in concentration of chloritoid crystals in the darker zones of the laminated dark siltstone, may suggest that the dark colour of such zones is effected by the presence of relative high concentrations of iron and possibly magnesia.

According to Hurlbut & Klein (1977), chloritoid is a relatively common constituent of low- to medium-grade regionally metamorphosed, iron-rich pelitic rocks. The fact that these chloritoid crystals occur in both the clasts and the matrix in a penetrative habit, indicates that the metamorphism was a post-depositional event.

2.3. ELECTRON MICROSCOPE (SEM) STUDY

Because of the very fine nature of the yellows, it was decided to inspect a few of these samples under very high magnification with the aid of an electron microscope. After careful microscopic study of the yellows, four samples were selected and prepared for SEM investigation. The primary aim of this investigation was to find textures or structures that are diagnostic of volcaniclastic deposits, which can be very small, as is illustrated in Fisher and Schmincke (1984).

No features diagnostic of volcaniclastic origin could, however, be identified. The investigation did, however, confirm the extremely fine-grained nature of the yellows. The textures observed, indicate that the yellows consist largely of clay minerals. A conchoidal fracture texture observed on a quartz grain (Scholle, 1979) indicates that cataclastic processes were active during the formation of the sediment. A selection of photographs taken during the investigation is included in this text (*Plates III.1.* and *III.2.*).

2.4. ELECTRON MICROPROBE STUDY

Due to the very fine-grained nature of the yellows, the fine secondary minerals are too small to be identified optically. Since all these small secondary minerals appear to be identical, it was decided to identify them with the aid of an electron microprobe. Two samples, in which these minerals were well developed, were selected. A few of the minerals in each of the samples were analyzed. The major element compositions which were determined, indicate that the minerals are muscovite/hydromuscovite. An analysis was also done on a

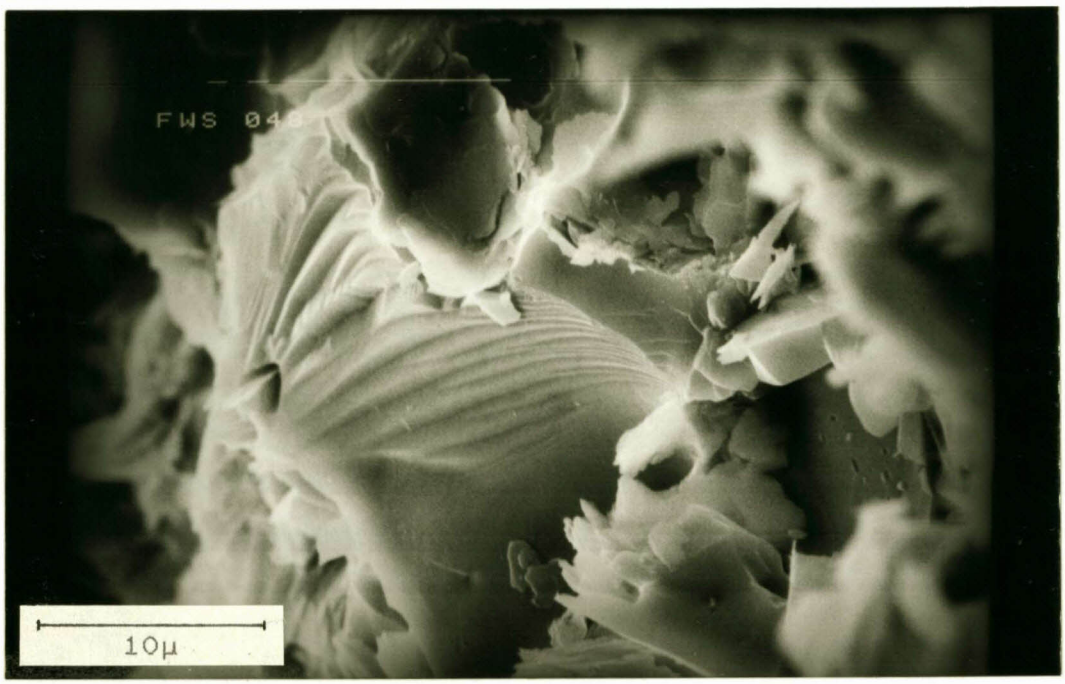

Plate III.1. Scanning Electron micrograph of conchoidal fracture of a mineral grain in a yellows clast, illustrating the clastic nature of the fine-grained sediment.

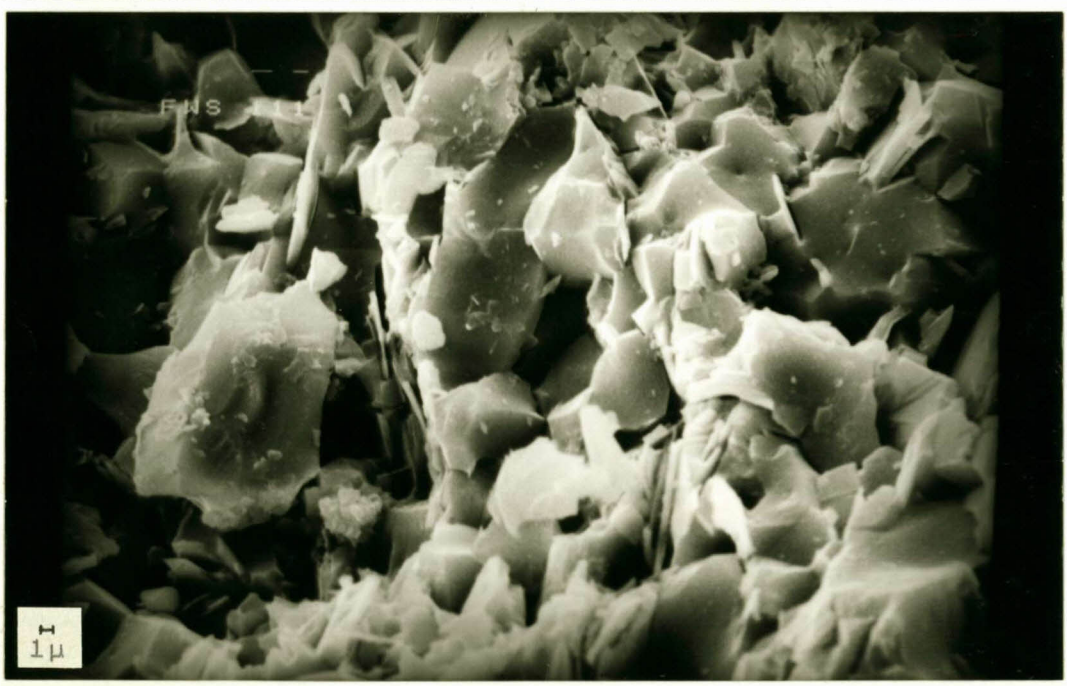

Plate III.2. Scanning Electron micrograph illustrating the typical, very fine-grained nature of "yellows".

chloritoid crystal to determine major element composition. Results are given below in *Table III.4.*.

Table III.4. Chemical analyses of secondary minerals.

	A	B	C	D	E
Na	0.75	1.04	1.25	0.64	0.04
K	7.36	7.59	8.72	10.08	0.00
Cl	0.00	0.02	0.01	*	0.02
F	0.00	0.01	0.00	0.91	0.00
P	0.00	0.00	0.00	*	0.00
Si	47.96	47.09	44.43	45.24	25.09
Al	38.11	38.22	31.71	36.85	41.61
Ca	0.08	0.10	0.02	0.00	0.00
Mg	0.85	0.13	0.57	0.08	1.33
Ti	0.04	0.03	0.23	0.01	0.00
Fe	0.12	0.34	0.75	≈0.08	29.01
Cr	0.26	0.17	0.17	*	0.30
Mn	0.06	0.00	0.01	0.12	2.54
Ni	0.00	0.01	0.00	*	0.01
H_2O	4.69	4.58	4.19	4.12	_
TOT	102.29	99.33	92.07	98.13	99.95

A. Muscovite in sample GI-110
B. Muscovite in sample GI-110
C. Muscovite in sample FWS-114
D. Rose-muscovite, pegmatite, New Mexico (Heinrich, E.W. & Levinson, A.A.) *in* Deer, Howie & Zussman (1974).
E. Chloritoid in sample GI-110
* Not determined
≈ FeO + Fe_2O_3 recalculated as Fe.
_ Not calculated

Based on the above results, the mineral was identified as muscovite. For a comparison of these results with XRD results, see *III.3.2.*.

3. MINERALOGICAL (XRD) STUDY

To determine the mineralogy of the clasts sampled, 34 representative samples, 11 from the BPM and 23 from the RDM, were selected for XRD analyses. **The primary aim of this**

investigation was to identify the clay minerals in the non-durable clasts and, if possible, the matrix of the quartzitic clasts. Five clasts of igneous origin were also analyzed. No quartz or chert samples were analyzed.

3.1. DISCUSSION

The analyses were qualitative and only semi-quantitative, with a lower detection limit of, for all practical purposes, approximately 5% (Zussman, 1977). Because of the semi-quantitative nature of the results, it was not attempted to quantify mineral concentrations. Instead, minerals were classified arbitrarily in order of predominance as: *primary*, *subordinate* and *accessory*.

Accessory minerals being all minerals present in concentrations of ±5% or less, *subordinate* minerals being present in concentrations higher than 5% but not constituting the bulk mineral component of the sample, while *primary* mineral(s), in this context, being the mineral(s) constituting the bulk mineral component of the sample (after personal communication with professor G.J. Beukes at the UOFS). The results of this investigation are summarized in *Table III.5.* under section *3.2.*

3.2. DESCRIPTION

QUARTZITE

Apart from **quartz**, a very small quantity of accessory chlorite, found in one sample (FWS-141) only, was the only mineral identified in the quartzite samples during the investigation. This is in concordance with the findings of the thin section study (see *III.2.1.*), which reported a sparseness of matrix in all the quartzites.

YELLOWS

The mineral assemblages of the yellow and grey clasts are dominated by quartz, pyrophyllite and to a lesser extent chloritoid.

The mineral composition of the BPM yellow-1, RDM yellow-3 and RDM yellow-4 clasts are virtually identical, in that their typical mineral assemblages are: *primary* - **quartz**; *subordinate* - **pyrophyllite**; *accessory* - **illite** and **chlorite**, respectively.

The mineral composition of the RDM yellow-1, yellow-2, grey-1 and grey-2 clasts are very similar, although somewhat more diverse, in that **quartz** is dominant as the *primary* mineral and no subordinate minerals are present, except in one sample (FWS-054), where **pyrophyllite** is present in sufficient quantities to warrant it *subordinate* status. The *accessory* minerals are comprised of various combinations of **chlorite, illite, pyrophyllite** and **Na-plagioclase.**

The mineral composition of the RDM grey-3 and grey-4 clasts are comparable in that the *primary* minerals are **quartz** and **chloritoid,** except in one case (FWS-135), where chloritoid occurs in subordinate quantities. Otherwise no mineral is present in subordinate quantities. *Accessory* minerals are **chlorite** and **pyrophyllite.**

In the case of BPM yellow-2 clasts, pyrophyllite is much more dominant. The *primary* minerals are either **pyrophyllite,** or **quartz** and **pyrophyllite.** No minerals occur in subordinate concentrations and *accessory* minerals are combinations of **chlorite, plagioclase/feldspar** and quartz.

Table III.5. Summary of XRD analysis results.

ROCK TYPE	FMTN	SAMPLE No	MINERAL STATUS		
			PRIMARY*	SUBORDINATE	ACCESSORY
L-QTZE	RDM	FWS-067	QTZ	-	-
D-QTZE	BPM	FWS-077	QTZ	-	-
D-QTZE	RDM	FWS-091	QTZ	-	-
D-QTZE	BPM	FWS-144	QTZ	-	-
L-QTZE	BPM	FWS-145	QTZ	-	-
L-QTZE	RDM	FWS-141	QTZ	-	CH
IGNEOUS	RDM	FWS-027	QTZ	-	PY CH IL
IGNEOUS	RDM	FWS-063	QTZ	-	PY CH IL
IGNEOUS	RDM	FWS-025	QTZ	-	PY CH
IGNEOUS	BPM	FWS-125	QTZ	-	PY CH
IGNEOUS	BPM	FWS-121	QTZ	-	PY IL
IGNEOUS	BPM	FWS-075	QTZ	PY	IL
IGNEOUS	RDM	FWS-041	QTZ	PY	CH IL
YELLOW-1	RDM	FWS-019	QTZ	-	CH IL PY
YELLOW-1	RDM	FWS-042	QTZ	-	CH IL
YELLOW-2	RDM	FWS-054	QTZ	PY	CH
YELLOW-2	RDM	FWS-083	QTZ	-	IL CH NP
GREY-1	RDM	FWS-044	QTZ	-	CH PY
GREY-1	RDM	FWS-045	QTZ	-	CH IL
GREY-2	RDM	FWS-092	QTZ	-	CH IL NP
GREY-2	RDM	FWS-111	QTZ	-	PY CH
YELLOW-1	BPM	FWS-039	QTZ	PY	IL CH
YELLOW-1	BPM	FWS-119	QTZ	PY	IL CH
YELLOW-3	RDM	FWS-016	QTZ	PY	CH IL
YELLOW-4	RDM	FWS-023	QTZ	PY	CH PL
GREY-3	RDM	FWS-014	QTZ CD	-	CH
GREY-4	RDM	FWS-015	QTZ CD	-	PY CH
GREY-4	RDM	FWS-135	QTZ	CD	CH
YELLOW-2	BPM	FWS-065	PY	-	FS QTZ CH
YELLOW-2	BPM	FWS-098	QTZ PY	-	CH PL
BLACK	RDM	FWS-021	QTZ	PY	CH IL
BLACK	RDM	FWS-100	QTZ	PY	CH IL
D-SILT	RDM	FWS-029	QTZ CD	-	PY
D-SILT	RDM	FWS-061	QTZ.CD	-	PY
D SILT	RDM	FWS-116	QTZ	-	CH IL

(Legend overleaf)

Table III.V. Continued (**Legend**).

FMTN - Formation

L-QTZE - Light coloured quartzite
D-QTZE - Dark coloured quartzite
D-SILT - Dark siltstone

QTZ - Quartz	CD - Chloritoid
PY - Pyrophyllite	NP - Na-Plagioclase
CH - Chlorite	PL - Plagioclase
IL - Illite	FS - Feldspar

PRIMARY* - Based on bulk mineral component

IGNEOUS

The mineral assemblages of the igneous samples from the BPM and the RDM are dominated by **quartz** as *primary* mineral. Except for two cases (FSW-041 and FWS-075) where **pyrophyllite** is the *subordinate* mineral, no other minerals are present in subordinate concentrations. The *accessory* minerals are various combinations of **pyrophyllite, chlorite** and **illite.**

BLACK

The mineral compositions of the black clasts from the BPM and the RDM are identical: *primary* - **quartz;** *subordinate* - **pyrophyllite** and *accessory* - **chlorite** and **illite.**

DARK SILTSTONE

Two basic mineral assemblages were recognized in the dark siltstone clasts with the difference being the presence or absence of chloritoid. The first assemblage is: *primary* - **quartz** and **chloritoid;** no subordinate minerals and *accessory* - **pyrophyllite.** The second mineral assemblage is: *primary* - **quartz;** no subordinate minerals and *accessory* - **chlorite** and **illite.**

3.3. CONCLUSIONS

The predominance of quartz and the presence of secondary minerals indicates that all the clasts had undergone various degrees of alteration, and silicification in particular.

The general absence of minerals other than quartz in the quartzites is in accordance with the findings of the thin section study (see *III.2.1.*), which reported a sparseness of matrix in all the quartzites.

Based on the mineral assemblages present in the yellows, the different classes can be clustered into four basic groups:

A. RDM yellow-1 + RDM yellow-2 + RDM grey-1 + RDM grey-2.
B. BPM yellow-1 + RDM yellow-3 + RDM yellow-4.
C. RDM grey-3 + RDM grey-4.
D. BPM yellow-2.

The author is nevertheless of the opinion that, based on their global mineral assemblages, the yellows in general represent only one population and could as such be derived from one common, but extensive, source.

A discrepancy appears to exist between the results of analyses on some fine-grained, light-coloured, micaceous minerals in some yellows clasts, obtained with the microprobe (see *III.2.4.*) and by means of XRD analysis, respectively. Based on microprobe results, the mineral was identified as muscovite. The compositions obtained compare very well with that of a rose-muscovite from a pegmatite (see *Table III.4.*), which, according to Deer, *et al* (1974) is very close to the ideal composition for a muscovite. The relative low potassium content possibly indicates replacement by H_3O and constitutes a transition to hydromuscovite. The fractionally higher silica in the

first two samples is further evidence of this transition (Deer, *et al*, 1974).

Since X-ray diffractograms for muscovite and illite are virtually identical and it has been pointed out that hydromuscovite is present, the discrepancy disappears. Deer, *et al*, (1974) suggest the use of the term *sericite* in cases like this.

The igneous clasts display mineral assemblages very similar to those of the yellows clasts in group A. above. If it is accepted that these yellows are of volcaniclastic origin (*III.1.3.* and *III.2.1.*), this similarity in mineral assemblages may support the postulation that some of the "igneous" clasts can be of volcaniclastic origin as well (see *III.2.1.*).

The mineral assemblages of the dark siltstone are comparable with those of the clasts of the group B. yellows, consisting of BPM yellow-1 + RDM yellow-3 + RDM yellow-4.

The mineral assemblages of the dark siltstone are comparable with those of the RDM grey-3 and grey-4 clasts. The two different mineral assemblages identified in the dark siltstone clasts confirm some of the microscopic observations on different types of dark siltstone (see *III.2.1.*).

Table III.6. Cross reference list of sample numbers with locality, formation, rock type, Au content, thin section number and additional mineralogical investigations carried out on respective samples.

SAMPLE No	Au ppb	ROCK TYPE	FORM-ATION	THIN SECTION	LOCAL-ITY	XRD	FLUID INCL.	SEM	MICRO PROBE
GI-0001	2	16	RDM	FWS-014	1	X			
GI-0002	1	17	RDM	FWS-015	1	X			
GI-0003	2	12	RDM	FWS-016	1	X			
GI-0004	2	11	RDM	FWS-017	1				
GI-0005	1	15	RDM	FWS-018	1				
GI-0006	1	10	RDM	FWS-019	1	X			
GI-0007	1	14	RDM	FWS-020	1				
GI-0008	0	18	RDM	FWS-021	1	X			
GI-0009	0	3	RDM	FWS-022	1				
GI-0010	0	13	RDM	FWS-023	1	X			
GI-0011	3	19	RDM	FWS-024	1				
GI-0012	0	9	RDM	FWS-025	1	X			
GI-0013	1	9	RDM	FWS-026	1				
GI-0014	11	9	RDM	FWS-027	1	X			
GI-0015	13	2	RDM	FWS-028	1				
GI-0016	0	2	RDM	FWS-029	1	X			
GI-0017	0	6	BPM	FWS-030	2				
GI-0018	0	6	BPM	FWS-031	2				
GI-0019	3	5	BPM		2		FWS-16/2		
GI-0020	107	8	BPM	FWS-032	2				
GI-0021	2	8	BPM	FWS-033	2				
GI-0022	5	2	BPM	FWS-034	2				
GI-0023	3	4	BPM	FWS-035	2				
GI-0024	1	7	BPM	FWS-036	2				
GI-0025	6	3	BPM	FWS-037	2				
GI-0026	1	9	BPM	FWS-038	2				
GI-0027	0	1	BPM	FWS-039	2	X			
GI-0028	1	20	BPM	FWS-040	2				
GI-0029	34	9	RDM	FWS-041	3	X			
GI-0030	14	10	RDM	FWS-042	3	X			
GI-0031	5	17	RDM	FWS-043	3				
		14	RDM	FWS-044	3	X			
GI-0032	5	14	RDM	FWS-045	3	X			
GI-0033	4	7	RDM	FWS-046	3				
GI-0034	3	3	RDM	FWS-047	3				
GI-0035	17	13	RDM	FWS-048	3			FWS-048	
GI-0036	1	4	RDM	FWS-049	3				
GI-0037	2	2	RDM	FWS-050	3				
GI-0038	61	6	RDM	FWS-051	3				
GI-0039	12	19	RDM	FWS-052	3				
GI-0040	13	16	RDM	FWS-053	3				
GI-0041	3	11	RDM	FWS-054	4	X			
GI-0042	1	14	RDM	FWS-055	4				
GI-0043	1	10	RDM	FWS-056	4				
GI-0044	2	4	RDM	FWS-057	4				
GI-0045	8	8	RDM	FWS-058	4				
GI-0046	12	6	RDM	FWS-059	4				
GI-0047	34	2	RDM	FWS-060	4				
GI-0048	3	19	RDM	FWS-061	4	X			
GI-0049	2	3	RDM	FWS-062	4	X			
GI-0050	3	9	RDM	FWS-063	4	X			
GI-0051	0	7	RDM	FWS-064	4				
GI-0052	4	20	BPM	FWS-065	5	X			

GI-0053	1	3	BPM	FWS-066	5			
GI-0054	309	4	BPM	FWS-067	5		FWS-27/2	
GI-0055	8	9	BPM	FWS-068	5			
GI-0056	183	6	BPM	FWS-069	5			
GI-0057	796	6	BPM	FWS-070	5			
GI-0058	213	8	BPM	FWS-071	5			
GI-0059	8	1	BPM	FWS-072	6			
GI-0060	89	8	BPM	FWS-073	6			
GI-0061	30	2	BPM	FWS-074	6			
GI-0062	750	9	BPM	FWS-075	6	X		
		9	BPM	FWS-076	6			
GI-0063	21	2	BPM	FWS-077	6	X		
GI-0064	8	4	BPM	FWS-078	6		FWS-78	
GI-0065	6	5	BPM	FWS-079	6		FWS-79	
		20	BPM	FWS-080	6			
GI-0066	750	6	BPM	FWS-081	6			
GI-0067	4	12	RDM	FWS-082	7			FWS-082
GI-0068	1	11	RDM	FWS-083	7	X		
GI-0069	1	17	RDM	FWS-084	7			
GI-0070	3	14	RDM	FWS-085	7			
GI-0071	1	7	RDM	FWS-086	7			
			RDM	FWS-087	7			FWS-087
GI-0072	1	3	RDM	FWS-088	7			
GI-0073	1	10	RDM	FWS-089	7			
GI-0074	1	19	RDM	FWS-090	7			
GI-0075	2	2	RDM	FWS-091	7	X		
GI-0076	1	15	RDM	FWS-092	7	X		
GI-0077	1	6	RDM	FWS-093	7			
GI-0078	1	9	RDM	FWS-094	7			
		9	RDM	FWS-095	7			
GI-0079	1	3	RDM	FWS-096	7			
GI-0080	1	3	RDM	FWS-097	7			
GI-0081	0	20	BPM	FWS-098	8	X		
GI-0082	2	1	BPM	FWS-099	8			
		19	BPM	FWS-100	8	X		
GI-0083	38	6	BPM	FWS-101	8			
GI-0084	34	7	BPM	FWS-102	8			
GI-0085	2	4	BPM	FWS-103	8			
GI-0086	151	8	BPM	FWS-104	8			
GI-0087	1	9	BPM	FWS-105	8			
		9	BPM	FWS-106	8			
GI-0088	0	2	BPM	FWS-107	8			
GI-0089	1	6	BPM	FWS-108	8			
GI-0090	1	4	BPM	FWS-109	8			
GI-0091	12	3	RDM	FWS-110	9			
		14	RDM	FWS-111	9	X		FWS-111
GI-0092	1	6	RDM	FWS-112	9			
GI-0093	1	5	RDM		9			
GI-0094	0	2	RDM		9			
GI-0095	49	6	RDM	FWS-113	9			
		17	RDM	FWS-114	9			FWS-114
GI-0096	2	4	RDM	FWS-115	9			
GI-0097	3	19	RDM	FWS-116	9	X		
GI-0098	4	9	RDM	FWS-117	9			
GI-0099	5	3	BPM	FWS-118	10	X		
GI-0100	8	5	BPM		10			
GI-0101	3	3	BPM	FWS-119	10			
GI-0102	7	7	BPM	FWS-120	10			
GI-0103	4	9	BPM	FWS-121	10	X		
GI-0104	0	3	BPM	FWS-122	10			

GI-0105	1	3	BPM	FWS-123	10		
GI-0106	10	9	BPM	FWS-124	10		
		9	BPM	FWS-125	10	X	
		9	BPM	FWS-126	10		
GI-0107	189	6	BPM		10		
GI-0108	8	8	BPM	FWS-127	10		
		19	BPM	FWS-128	10		
GI-0109	1	16	RDM	FWS-129	11		
		11	RDM	FWS-130	11		
		13	RDM	FWS-131	11		
		14	RDM	FWS-132	11		
GI-0110	3	15	RDM	FWS-133	11		GI-110
		7	RDM	FWS-134	11		
GI-0111	8	17	RDM	FWS-135	11	X	
GI-0112	10	19	RDM	FWS-136	11		
		10	RDM	FWS-137	11		
GI-0113	69	4	RDM	FWS-138	11		
GI-0114	16	6	RDM		11		
GI-0115	6	9	RDM	FWS-139	11		
GI-0116	19	9	RDM	FWS-140	11		
GI-0117	131	3	RDM	FWS-141	11	X	
GI-0118	24	2	RDM	FWS-142	11		
GI-0119	9	6	BPM		12		
GI-0120	223	5	BPM	FWS-143	12		
GI-0121	34	2	BPM	FWS-144	12	X	
GI-0122	10	3	BPM	FWS-145	12	X	
GI-0123	2	3	BPM	FWS-146	12		
GI-0124	2	3	BPM	FWS-037	2		
GI-0125	5	4	BPM	FWS-035	2		
GI-0126	8	10	RDM	FWS-019	1		
GI-0127	45	1	BPM	FWS-040	2		
GI-0128	2	9	BPM	FWS-038	2		
GI-0129	3	16	RDM	FWS-014	1		
GI-0130	2	9	RDM	FWS-025	1		

ROCK TYPE		LOCALITY	
1	YELLOW-1 BPM	1	FREDDIES 5# 45 Hlge W
2	DARK QUARTZITE	2	FREDDIES 5# 47A Hlge E
3	LIGHT QUARTZITE	3	FSG 1# 43W2 Line 26
4	WHITE QUARTZ	4	FREDDIES 5# 45A 69 XCut
5	DARK QUARTZ	5	FREDDIES 5# 42L W2 65 FWDr N
6	DARK CHERT	6	W.HOLDINGS 6# 33E AReef Hlge N
7	LIGHT CHERT	7	W.HOLDINGS 6# 33E AReef Hlge N
8	BANDED CHERT	8	W.HOLDINGS 3# 37L AReef TW
9	IGNEOUS	9	W.HOLDINGS 1# 45L Hlge E
10	YELLOW-1	10	W.HOLDINGS 1# 45L Hlge E
11	YELLOW-2	11	PRES.BRAND 3# 42L W 22 XCut
12	YELLOW-3	12	PRES.BRAND 3# 42L W 22 XCut
13	YELLOW-4		
14	GREY-1		
15	GREY-2		
16	GREY-3		
17	GREY-4		
18	BLACK		
19	DARK SILTSTONE		
20	YELLOW-2 BPM		

II V

FLUID INCLUSIONS

1. OBJECTIVES OF THE INVESTIGATION

During the microscopic study of the thin sections (see *II.2.2.*), no unambiguous differences could be distinguished between dark-tinted quartz (smoky) and white (or untinted) quartz. Abundant fluid inclusions were, however, observed in the quartz. Therefore it was decided to carry out a pilot study on these fluid inclusions. **The aims of this study were to determine**, where possible:

- The composition of the fluid inclusions.
- Temperature and pressure conditions at the time of entrapment.
- Microthermometric differences, if any, between the two types of quartz.
- The viability of microthermometry as a tool to discriminate between the two types of quartz.

This pilot study was carried out by the Fluid Inclusion Unit of the Department of Geology, at the University of the OFS. The techniques employed in this study are described in detail under *II.2.2.* The full report on this study appears in ***Appendix 1.***.

Since the study of fluid inclusions is time consuming, only four samples were submitted for study. Two white, and Two dark, quartz sample was randomly selected from both the BPM. (FWS 16/2 - dark quartz; FWS 79 - dark quartz; FWS 27/2 - light quartz; FWS 78 - light quartz.)

Data obtained in this pilot study are not sufficient to derive conditions of formation unequivocally. The ultimate goal of this pilot study, namely to evaluate the viability of microthermometry as a tool in the (re)search for the provenance of the Witwatersrand, was however achieved.

2. RESULTS

Due to the fact that this is only a pilot study, results should be seen in that context. The scope of this field of study warrants an independent investigation. It is concluded that a microthermometric study can yield valuable information to aid the reconstruction of the provenance(s) for the Witwatersrand.

The results and conclusions of the study are discussed briefly in the following sections. For more detail, refer to ***Appendix 1***..

2.1. COMPOSITION OF INCLUSIONS

Compositional variation was determined by recording melting temperatures (T_m), which are indicative of the composition of individual fluid inclusions.

WATER
Rather pure water (containing < 1,5% eNaCl), is the dominant fluid in three samples (FWS 16/2, FWS 78 and FWS 79), but is also present in sample FWS 27/2 in lower concentrations.

CARBON DIOXIDE
Minor quantities of clathrate ($CO_2.5,75H_2O$) were found in all the samples, while major quantities were found in FWS

27/2. Carbon dioxide is therefore present in all the samples. Based on observations made during the study, the CO_2:H_2O ratio in the aqueous inclusions must be between 30:70 and 10:90. Discrete carbon dioxide inclusions were found in one sample (FWS 79).

BRINE

Minor quantities of brine, containing 11% to 13% eNaCl, were found in FWS 79, while major quantities were found in FWS 27/2. The applicable brine system is H_2O-NaCl-CO_2, which contain, according to melting temperature data, very few other mobile components such as CH_4 and N_4.

2.2. PT-CONDITIONS DURING ENTRAPMENT

At constant density, all the variations possible in PT-conditions, produces a characteristic isochore ("curve of equal density") on a PT projection plane. Such characteristic isochores can be derived from homogenization temperatures (T_h) because these temperatures are primarily controlled by the density prevailing at the time of entrapment. It must, however, always be taken into account that density is influenced by composition as well. Homogenization temperatures can thus, in effect, be used to derive the PT-conditions during entrapment.

DENSITY

Densities of 0,88g/cm^3 and 0,92g/cm^3 to 0,95g/cm^3 are proposed for the majority of the **aqueous inclusions**, particularly in samples FWS 16/2, FWS 78 and FWS 27/2. Additional density values of 0,80g/cm^3 and 0,85g/cm^3 were reported in sample FWS 79.

A density of 0,87g/cm^3 is proposed for the discrete **carbon dioxide** inclusions.

Brine (12% eNaCl), for which a density of > 1,0g/cm^3 is proposed, is prominent in one sample only (FWS 27/2).

PRESSURE

Pressure conditions at the time of entrapment cannot be determined directly. They are derived by obtaining the intersection point of isochores, plotted on a PT diagram, of genetically related, co-existing inclusions of different composition.

Due to the large spread of relevant T_h-values, $T_h(H_2O)$ = 120-250°C and $T_h(CO_2)$ = -3°C to +19°C, an analogous spread in pressure values (0,8kb - 3,8kb) was obtained.

TEMPERATURES

The **aqueous inclusions** exhibit a wide and complex spread in the homogenization temperatures, ranging from 110°C to 250°C, with a broad peak zone between 160°C and 180°C and subsidiary peaks at 200°C and 250°C. A minimum temperature of entrapment of 200-270°C is proposed for the pure system H_2O-CO_2.

The discrete **carbon dioxide inclusions** exhibit a wide spread in homogenization temperatures, ranging from -3°C to +19°C with a peak at +13,0±0,7°C. The discrete carbon dioxide inclusions in sample FWS 79 must have been entrapped at conditions below solvus. This implicates a maximum temperature of entrapment of 200-270°C for a NaCl-deficient fluid; or 300-440°C in the case of a fluid containing 12% eNaCl at 2kb.

The **brine inclusions** exhibit a homogenization temperature peak at 150±5°C, while the one sample which contains the

dominant brine inclusions (FWS 27/2), exhibits a second peak at 120±10°C. A minimum temperature of entrapment of 300-410°C is proposed for the brine inclusions.

From the T_h-values obtained from the genetically related H_2O and CO_2 inclusions, a temperature range of 170-500°C, during entrapment, was derived by means of the intersecting isochore method.

2.3. DIFFERENCES

In terms of composition of the inclusions, dark- and light-coloured quartz are indistinguishable. The presence of auxiliary low-density fluids (T_h = 200-210°C, 250°C) in the dark-coloured quartz may prove to be a notable difference. However, enough work to verify this observation has not been done.

2.4. DISCRIMINATION

If the observation that the dark-coloured quartz contains low-density fluid inclusions while these inclusions are absent from light-coloured quartz, can be verified, microthermometric discrimination between the two types of quartz is quite simple. The sample is only heated to a temperature of 200°C and inspected for a large number of as yet unhomogenized fluid inclusions (i.e. vapour bubbles still visible), of which the presence would indicate that the host mineral is a dark-coloured quartz.

2.5. CONCLUSIONS

Based on the derived compositions of the fluids and especially the general homogeneity thereof, it would appear that the majority of the inclusions contain fluids which played major roles during diagenesis and metamorphism of the quartz pebbles, rather than paleo-fluids inherited from the provenance region(s) of the quartz, in which case dissimilar microthermometric properties is expected for different quartz types, unless a homogeneous provenance is proposed. Considering the volumetric prerequisites for a source for the quartz clasts, such a provenance is, however, rather unlikely. The low-density fluids occurring in the dark-coloured quartz (see *II.2.3.*) may, however, represent provenance conditions.

Much more work needs to be done to determine concise entrapment conditions and characterize the low density fluids. In general, however, PT-conditions of entrapment falls within the range 250±100°C and 2,0±1,5kb.

GEOCHEMICAL STUDY

A total number of 123 samples were submitted to Anglo American Research Laboratories (AARL) for 36 element analysis and p.p.b. gold assay. The results of these analyses form the geochemical data set which is presented, statistically manipulated and discussed in this chapter.

1. ANALYTICAL TECHNIQUES

Gold values were determined by Atomic Absorption Spectroscopy in a graphite furnace. The lower detection limit for accurate values was 2 p.p.b. Due to the very low detection calibrations used, the highest accurate determinable value was 750 p.p.b.

The 36 element analyses were done by means of X-Ray Fluorescence Spectrometry. All major elements, excluding Mg and Na, but including trace elements Cr and V were determined with Energy Dispersion Spectrometry. The rest of the trace elements, as well as Mg and Na were determined with Wavelength Dispersion Spectrometry.

2. THE DATA

The analysis results are given uncorrected and in elemental format in *Table V.1.* below. Except for minor changes in format, the data are presented as received from AARL. For the sake of convenience of comparison, the data were grouped in order of rock type. The average values for each rock type

Table V.1. Results of 36 element XRF analyses.

		ppb	ppm																				%											
Sample No	Rock T	Au	U	Th	Bi	Pb	W	Ta	Ba	Te	Sb	Sn	Mo	Nb	Zr	Y	Sr	Rb	Se	As	Zn	Cu	Ni	Co	Fe	Mn	Cr	V	Ti	Ca	K	S	P	Si	Al	Mg	Na
GI-0053	BPM-3	1	4	3	6	80	19	0	150	-71	-76	-37	2	-5	-8	-1	-8	-1	5	13	1	-17	-4	-6	0.4	0.1	0.1	0	0.1	0.2	0.2	0	0.2	36.5	2	0	0
GI-0090	BPM-3	1	10	-5	-7	-4	18	5	555	-29	-2	-6	-5	8	223	80	65	130	-5	-2	1	-14	12	-5	0.8	0.2	0.1	0	0.3	0.4	2.6	0.1	0.3	43.5	6.3	0	0
GI-0099	BPM-3	5	12	-10	-12	-6	17	13	317	-46	-7	-16	-5	7	157	63	13	22	-8	-12	-2	-18	4	-8	0.7	0.1	0.2	0	0.5	0.3	0.6	0	0.2	40.3	8.3	0	0
GI-0101	BPM-3	3	5	-17	-3	-8	11	0	278	-43	-11	-16	-4	-3	38	11	3	21	-4	56	-2	-9	42	8	1	0.2	0.1	0	0.1	0.3	0.6	0	0.4	36.1	3	0.1	0
GI-0104	BPM-3	0	4	-19	-5	-12	10	0	235	-50	-21	-19	-2	-3	-9	4	-3	6	-4	-12	-3	-8	1	-6	0.5	0.2	0.2	0	0.1	0.3	0.3	0	0.1	61.3	2	0	0
GI-0105	BPM-3	1	2	-13	-1	-5	12	-2	196	-52	-35	-20	0	-3	-6	3	-4	1	-2	-9	-3	-20	7	-4	0.7	0.2	0.1	0	0.1	0.3	0.2	0	0.3	61.9	1.8	0.1	0
GI-0122	BPM-3	10	3	-17	-6	-9	6	-2	231	-41	-5	-9	-3	3	135	12	64	19	-5	-11	5	-9	26	-2	1.5	0.3	0.2	0	0.2	0.6	0.6	0.1	0.2	51.1	4.1	0.2	0
GI-0123	BPM-3	2	3	-17	-4	2	8	-4	178	-52	-24	-17	-3	-3	-11	3	-4	3	-4	-13	58	-16	0	-6	1	0.2	0.1	0	0.1	0.3	0.2	0	0.2	61	1.7	0	0
GI-0025	BPM-3	6	1	-17	-2	83	7	0	234	-38	-9	-20	45	-2	12	3	4	7	-4	51	370	85	65	8	0.7	0.2	0.2	0.2	0.1	0.3	0.2	0.1	-1.2	61	2.1	0	0.3
x		3	5	-12	-4	13	12	1	264	-47	-21	-18	3	0	59	20	14	23	-3	7	47	-3	17	-2	0.8	0.2	0.1	0.0	0.2	0.3	0.6	0.0	0.1	54.8	3.5	0.0	0.0
GI-0034	RDM-3	3	3	-17	-3	-3	11	1	177	-48	-13	-18	-4	-3	31	6	2	4	-4	-5	-2	12	0	-5	0.8	0.2	0.1	0	0.1	0.3	0.21	0	0.3	58.4	2.3	0.1	0
GI-0049	RDM-3	2	4	-17	-5	-10	9	-3	253	-34	-3	-4	-3	-2	58	11	5	16	-4	-4	-2	32	25	-4	1.2	0.2	0.1	0	0.1	0.3	0.5	0	0.2	58	2.7	0.1	0
GI-0072	RDM-3	1	2	-16	-4	-8	8	2	306	-36	-4	-14	-4	-3	166	11	11	34	-4	-17	-3	-13	7	-5	1.1	0.2	0.2	0	0.1	0.3	1	0	0.2	55.1	3.3	0.1	0
GI-0079	RDM-3	1	3	-20	-5	13	9	3	223	-45	-14	-16	-1	-3	-10	4	-3	4	-5	-22	-5	-20	-3	-8	0.8	0.2	0.1	0	0.1	0.3	0.2	0	0.3	60.7	2	0.1	0
GI-0080	RDM-3	1	3	-17	-6	-10	10	1	313	-43	-8	-17	5	-2	38	12	12	38	-5	-19	-3	-6	4	-7	0.7	0.2	0.1	0	0.1	0.3	1	0	0.1	56.2	3.3	0.1	0
GI-0091	RDM-3	12	3	-16	-5	-11	12	1	326	-40	-10	-15	2	-3	46	10	3	31	-4	-9	-2	-11	12	-5	1	0.2	0.2	0	0.1	0.3	1.1	0	0.4	54.7	3.2	0.1	0
GI-0117	RDM-3	131	2	-18	-4	-12	12	2	258	-54	-16	-18	1	-2	36	11	18	28	-5	-14	-1	-19	2	-7	0.7	0.2	0.2	0	0.1	0.4	0.8	0	0.1	55.3	3	0.1	0
GI-0009	RDM-3	0	3	-16	-3	-11	10	4	445	-18	8	-11	-3	-2	114	21	18	82	-5	-10	-2	-16	7	-4	0.9	0.2	0.2	0.2	0.1	0.3	2.1	0	-0.7	46.7	5.1	0.1	0.4
x	Th	19	3	-17	-4	-7	10	1	288	-40	-8	-14	-1	-3	60	11	8	30	-5	-13	-3	-5	7	-6	0.9	0.2	0.2	0.0	0.1	0.3	0.9	0.0	0.1	55.6	3.1	0.1	0.1
GI-0061	BPM-2	30	4	-17	-3	-8	9	-4	212	-47	-17	-20	1	-3	-6	4	-1	2	-3	-7	-2	-13	22	-2	1.1	0.2	0.1	0	0.1	0.3	0.2	0	0.4	61.1	2.1	0.1	0
GI-0063	BPM-2	2	3	-17	-3	-10	10	0	234	-42	-14	-16	-3	-3	31	8	6	12	-4	-11	-4	29	16	-4	1	0.2	0.1	0	0.1	0.3	0.4	0	0.3	58.9	2.4	0.1	0
GI-0088	BPM-2	0	4	-19	-4	-8	10	-2	232	-46	-10	-12	4	-2	57	10	26	7	-4	5	2	57	32	0	1.3	0.2	0.1	0	0.1	0.3	0.2	0	0.1	58.4	2.2	0.1	0
GI-0121	BPM-2	2	2	-17	-4	-10	10	-3	234	-52	-14	-17	1	-3	22	6	1	4	-4	-16	-3	7	5	-4	0.9	0.2	0.1	0	0.1	0.3	0.2	0	0.3	62	1.8	0.1	0
GI-0022	BPM-2	5	1	-18	-3	-9	7	-1	267	-29	0	-16	-5	-2	24	6	8	10	-5	-5	-6	85	5	0	0.7	0.2	0.1	0.2	0.1	0.3	0.2	0.1	-0.9	60.8	2.4	0.1	0.3
x		8	3	-18	-3	-9	9	-2	236	-43	-11	-16	0	-3	26	7	8	7	-4	-7	-3	33	16	-2	1.0	0.2	0.1	0.0	0.1	0.3	0.2	0.0	0.0	60.2	2.2	0.1	0.1
GI-0037	RDM-2	2	4	-16	0	-6	8	-2	231	-46	-22	-17	-4	-3	33	8	-1	7	-3	181	1	15	5	-5	0.9	0.2	0.1	0	0.1	0.3	0.3	0	0	60.5	1.9	0.2	0
GI-0047	RDM-2	34	5	-15	-1	-5	5	-10	217	-22	2	-9	-5	3	132	26	3	15	-4	16	12	16	40	5	3.7	0.4	0.2	0	0.2	0.2	0.4	0.2	0.2	47.9	4.3	0.3	0
GI-0075	RDM-2	2	5	-16	2	-5	9	-1	203	-42	-14	-17	9	-2	32	8	9	4	-2	-9	0	137	27	-1	1.5	0.2	0.1	0	0.1	0.3	0.2	0	0.3	59.5	2.1	0.3	0
GI-0094	RDM-2	0	3	-19	-4	-10	9	-2	220	-50	-19	-17	-4	-3	17	7	-3	8	-4	-10	-3	-2	7	-2	0.8	0.2	0.1	0	0.1	0.3	0.3	0	0.2	62.3	1.8	0.1	0
GI-0118	RDM-2	24	5	-16	-5	-8	11	1	334	-42	-10	-16	-2	-3	61	15	32	34	-4	-13	0	-19	2	-6	0.6	0.2	0.2	0	0.1	0.4	1.1	0	0.1	54.2	3.5	0.1	0
GI-0015	RDM-2	13	4	-21	1	-10	6	-5	209	-23	3	-17	-1	-4	-8	6	-2	6	-4	-6	-8	-23	12	2	1.1	0.2	0.1	0.1	0.1	0.4	0.2	0.2	1	63	2.1	0	0.3
GI-0016	RDM-2	0	2	-18	-2	-8	6	-8	235	-15	7	-10	-5	0	37	32	3	24	-5	-5	1	-12	8	-3	2.7	0.5	0.2	0.2	0.2	0.3	0.6	0	0.4	52.4	4.1	0.1	0.3
x		11	4	-17	-1	-7	8	-4	238	-34	-8	-15	-2	-2	43	15	6	14	-4	22	0	16	14	-1	1.6	0.3	0.1	0.0	0.1	0.3	0.4	0.1	0.3	57.1	2.8	0.2	0.1
GI-0054	BPM-4	309	7	-20	5	22	8	-9	123	-26	2	-10	-1	-2	0	12	0	5	0	56	-1	15	86	12	2.1	0.3	0.1	0	0.1	0.3	0.2	1.1	0.8	58	2.1	0	0
GI-0064	BPM-4	8	3	-18	-3	-10	11	-2	215	-52	-14	-17	-3	-3	-9	3	-4	2	-4	-16	-4	-20	1	-6	0.7	0.2	0.2	0	0.1	0.3	0.2	0	0.1	62.5	2	0	0
GI-0083	BPM-4	2	3	-18	-4	-4	7	-4	203	-47	-19	-19	-1	-3	-11	3	-4	3	-3	-16	-4	-17	7	-5	1	0.2	0.1	0	0.1	0.3	0.2	0	0.3	62.4	1.8	0	0
GI-0023	BPM-4	3	2	-21	-1	-12	6	-6	242	-33	2	-20	-5	-4	-9	1	-2	6	-5	-16	-8	-24	1	-3	1.1	0.2	0.1	0.2	0.1	0.3	0.2	0.1	-0.9	63.1	2	0	0.3
x		81	4	-19	-1	-1	8	-5	196	-40	-7	-17	-3	-3	-7	5	-3	4	-3	2	-4	-12	24	-1	1.2	0.2	0.1	0.1	0.1	0.3	0.2	0.3	0.1	61.5	2.0	0.0	0.1
GI-0036	RDM-4	1	2	4	10	35	17	-3	124	-66	-86	-42	2	-6	-5	-1	-7	-7	7	24	1	-12	2	-6	0.8	0.2	0.1	0	0.1	0.3	0.2	0	0.1	55.4	2.2	0.1	0
GI-0044	RDM-4	2	3	-18	-3	-4	9	-3	198	-44	-17	-17	11	-3	-2	6	-3	5	-3	-14	-4	-13	5	-4	1	0.2	0.2	0	0.1	0.4	0.2	0	0.3	61.3	2.1	0.1	0
GI-0096	RDM-4	2	3	-17	-2	-4	9	-3	200	-53	-18	-20	0	-3	-10	3	-4	3	-4	-16	3	-21	-4	-5	0.8	0.2	0.1	0	0.1	0.3	0.2	0	0.1	62.8	1.6	0	0
GI-0113	RDM-4	69	3	-19	-3	-13	8	-6	191	-44	-10	-17	-3	-3	-6	4	-3	7	-4	-14	-1	-12	8	-5	1.5	0.3	0.1	0	0.1	0.4	0.2	0	0.4	59.9	2.2	0.2	0
x		19	3	-13	1	4	11	-4	178	-52	-33	-24	3	-4	-6	3	-4	2	-1	-5	0	-15	3	-5	1.0	0.2	0.1	0.0	0.1	0.4	0.2	0.0	0.2	59.9	2.0	0.1	0.0
GI-0065	BPM-5	6	1	-20	-5	-8	9	-1	221	-59	-20	-21	3	-3	-10	2	-3	3	-5	-19	-5	-22	-3	-7	0.6	0.2	0.2	0	0.1	0.3	0.2	0	0.1	62.5	1.9	0	0
GI-0100	BPM-5	8	3	-17	-2	-8	-13	-2	195	-46	-11	-15	0	-3	0	6	-1	7	-4	39	-4	-8	-46	5	0.9	0.2	0.1	0	0.1	0.3	0.3	0	0.4	60.6	2.5	0.1	0
GI-0120	BPM-5	223	3	-18	-1	-4	9	-4	207	-49	-12	-14	-5	-3	-10	2	-4	2	-3	-10	-4	-11	5	-2	1	0.2	0.1	0	0.1	0.3	0.2	0.1	0	62.4	1.7	0	0
GI-0019	BPM-5	3	1	-19	-1	-11	7	-3	241	-39	-7	-20	0	-4	-8	2	-2	6	-5	-17	-7	-20	-1	-5	0.7	0.2	0.1	0.2	0.1	0.3	0.2	0.1	-1	63.4	2.2	0	0.3
x		60	2	-19	-2	-8	3	-3	216	-48	-13	-18	-1	-3	-7	3	-3	5	-4	-2	-5	-15	-11	-2	0.8	0.2	0.1	0.1	0.1	0.3	0.2	0.1	-0.1	62.2	2.1	0.0	0.1
GI-0093	RDM-5	1	3	-17	-3	-11	10	-3	216	-50	-20	-18	-3	-3	-9	3	-2	3	-3	-16	-5	-17	-1	-5	0.9	0.2	0.1	0	0.1	0.3	0.2	0	0.4	62.2	2.1	0.1	0

Table V.1. Continued

		ppb	ppm																				%											
Sample No	Rock T	Au	U	Th	Bi	Pb	W	Ta	Ba	Te	Sb	Sn	Mo	Nb	Zr	Y	Sr	Rb	Se	As	Zn	Cu	Ni	Co	Fe	Mn	Cr	V	Ti	Ca	K	S	P	Si	Al	Mg	Na
GI-0056	BPM-6	183	5	-15	-3	20	11	-1	206	-47	-16	-15	6	-2	4	7	-3	4	-3	-7	-2	-5	18	-4	0.7	0.2	0.1	0	0.1	0.3	0.2	0.1	0.3	61.8	2	0	0
GI-0057	BPM-6	796	18	-32	32	92	6	-31	-207	5	42	2	1	2	-8	3	3	17	7	679	5	67	378	139	8.9	0.5	0	0	0.1	0.3	0.1	6.8	0.4	41.9	2.5	0.1	0
GI-0066	BPM-6	750	23	-41	49	66	10	-29	-387	4	54	11	4	6	-2	3	5	25	13	1085	-28	47	944	451	12.6	0.6	0	0	0.1	0.2	0.1	9.6	0.3	34.1	2.5	0.1	0
GI-0083	BPM-6	38	3	-19	-4	4	10	1	207	-57	-18	-21	-4	-3	-8	5	-3	5	-4	30	-2	89	17	9	0.6	0.2	0.1	0	0.1	0.3	0.2	0	0.2	62.9	2	0	0
GI-0089	BPM-6	1	3	-14	-3	7	8	-5	193	-43	-20	-20	-1	-2	-6	4	0	3	-3	41	-1	-8	59	3	1.1	0.2	0.1	0	0.1	0.3	0.2	0.1	0.3	60.6	2.1	0.2	0
GI-0107	BPM-6	109	4	-17	0	-2	10	-4	219	-46	-8	-15	6	-3	-7	4	-2	6	-3	37	-4	-11	58	9	1	0.2	0.2	0	0.1	0.3	0.2	0.2	0.3	59.8	2.4	0	0
GI-0119	BPM-6	9	2	-17	-4	37	10	-1	234	-53	-21	-21	-1	-3	-9	3	-3	6	-4	15	170	-6	16	0	0.6	0.2	0.2	0	0.1	0.3	0.3	0	0.4	61.8	2.1	0.1	0
GI-0017	BPM-6	0	0	-14	-11	-3	11	3	247	-27	5	-18	-4	7	115	25	89	9	-7	-4	6	-22	65	-3	3.1	0.3	0.2	0.2	0.4	0.5	0.2	0	-0.3	33.7	7	2.1	0.6
GI-0018	BPM-6	0	3	-19	4	-2	7	-2	223	-27	3	-18	-2	-2	-2	22	0	11	-4	28	-7	14	35	14	1	0.2	0.1	0.2	0.1	0.3	0.3	0.4	-0.7	39.2	2.7	0.1	0.3
X		218	7	-21	7	25	9	-8	104	-32	2	-13	1	0	9	8	10	10	-1	212	15	18	177	69	3.3	0.3	0.1	0.0	0.1	0.3	0.2	1.9	0.2	33.1	2.8	0.3	0.1
GI-0038	RDM-6	61	7	-16	-1	-3	4	-11	209	-23	4	-8	-4	0	13	13	0	7	-3	12	36	-10	24	-4	3.6	0.4	0.1	0	0.1	0.3	0.3	0.2	0.2	49.2	3.5	0.9	0
GI-0046	RDM-6	12	4	-17	-4	-5	5	-7	176	-23	3	-11	-6	0	17	7	-2	8	-4	3	10	-9	38	2	3	0.4	0.1	0	0.2	0.3	0.3	0.1	0.2	50.6	4.4	0.3	0
GI-0077	RDM-6	1	2	-18	-6	-13	-2	-14	232	-25	-2	-18	-2	-1	11	15	0	7	-4	-2	27	-9	136	8	5.1	0.5	0.1	0	0.1	0.3	0.3	0.1	0.1	44.7	4.3	1.5	0
GI-0092	RDM-6	1	3	-20	-5	-12	12	1	208	-51	-12	-15	-3	-2	-6	4	-4	3	-5	-1	-3	-15	18	-2	0.7	0.2	0.1	0	0.1	0.3	0.2	0	0.4	59.1	2.4	0.1	0
GI-0093	RDM-6	49	5	-19	2	4	9	-6	153	-35	-2	-12	-6	-2	-3	4	-2	4	-3	37	-4	-15	134	22	1.5	0.2	0.1	0	0.1	0.3	0.2	0.5	0.1	59.2	2.2	0.1	0
GI-0114	RDM-6	16	3	-18	-3	-8	-1	-16	238	-20	4	-10	-3	0	11	13	4	11	-3	6	52	-13	152	7	5.2	0.7	0.1	0	0.1	0.3	0.3	0	0.1	45.3	4	1.3	0
X		23	4	-18	-3	-6	5	-9	203	-30	-1	-12	-4	-1	7	9	-1	7	-4	9	20	-12	84	6	3.2	0.4	0.1	0.0	0.1	0.3	0.3	0.2	0.2	51.4	3.5	0.7	0.0
GI-0084	BPM-7	34	3	-19	-5	-13	12	1	318	-52	-14	-17	1	-3	23	14	21	33	-5	-14	-3	-13	8	-5	0.6	0.2	0.2	0	0.1	0.3	1	0	0.1	55	3.3	0.1	0
GI-0102	BPM-7	7	4	-18	-4	-8	12	2	251	-57	-19	-19	-4	-3	0	10	1	19	-4	5	-1	38	14	-3	0.5	0.2	0.2	0	0.1	0.3	0.6	0	0.2	58.7	2.5	0.1	0
GI-0024	BPM-7	1	2	-12	4	0	11	-4	218	-15	-27	-19	-1	-2	18	7	0	9	0	33	81	-16	73	9	1.2	0.2	0.2	0.2	0.2	0.3	0.2	0	-0.7	58.7	2.4	0.1	0.3
X		14	3	-16	-2	-7	12	0	262	-41	-20	-18	-1	-3	14	10	7	20	-3	8	26	3	32	0	0.8	0.2	0.2	0.1	0.1	0.3	0.6	0.0	-0.1	57.5	2.7	0.1	0.1
GI-0033	RDM-7	4	7	-13	-2	-10	2	-11	222	-22	1	-9	-5	8	121	29	3	8	-4	-11	27	-9	20	-6	3.6	0.5	0.2	0	0.3	0.3	0.22	0	0	50.4	3.2	0.7	0
GI-0051	RDM-7	0	4	-19	-6	-16	13	2	202	-40	-8	-16	0	-1	13	6	-1	12	-5	-14	0	22	18	-7	1.2	0.2	0.2	0	0.1	0.3	0.4	0	0.1	54	3.9	0.2	0
GI-0071	RDM-7	1	4	-17	-1	-8	6	-7	246	-29	-1	-7	-2	0	37	16	7	24	-4	-9	12	-10	63	0	3	0.4	0.1	0	0.2	0.3	0.6	0.1	0.1	49.3	3.7	0.9	0
X		2	5	-16	-3	-11	7	-5	223	-30	-3	-11	-2	2	57	17	3	15	-4	-11	13	1	34	-4	2.6	0.4	0.2	0.0	0.2	0.3	0.4	0.0	0.1	51.2	3.6	0.6	0
GI-0058	BPM-8	213	10	0	5	342	16	-9	155	-36	-12	-17	-4	-3	-7	1	-2	3	0	50	-3	-3	37	7	1.6	0.2	0.1	0	0.1	0.3	0.1	0.6	0.2	59	2	0.1	0
GI-0060	BPM-8	89	6	-17	6	67	7	-11	164	-27	0	-14	-4	-2	-8	5	0	3	-1	36	-2	9	32	6	2.1	0.3	0.1	0	0.1	0.3	0.2	0.5	0.4	59.3	2.1	0.1	0
GI-0086	BPM-8	151	7	-22	8	13	6	-15	115	-15	5	-4	7	-1	-7	20	1	7	0	212	2	4	159	19	3.1	0.3	0.1	0	0.1	0.4	0.2	1.2	0.5	57	2	0.1	0
GI-0108	BPM-8	8	4	-19	-3	-11	8	-3	217	-56	-19	-17	1	-3	-9	5	-5	1	-4	-16	-5	-21	5	-4	0.8	0.2	0.1	0	0.1	0.3	0.2	0	0.5	61.9	2	0	0
GI-0020	BPM-8	107	19	-48	47	59	5	-27	-201	-13	46	-2	1	0	-5	0	5	30	9	1182	-11	58	1085	305	11.5	0.7	0	0	0.2	0.2	0.2	9.4	-0.2	33.6	3	0.1	0.4
GI-0021	BPM-8	2	2	-14	-6	-6	9	0	281	-13	7	-11	-2	6	189	22	9	45	-6	-5	10	-2	23	-2	2.5	0.4	0.2	0.2	0.3	0.2	0.9	0.1	-0.7	43.7	3.9	0.3	0.3
X		95	8	-20	10	111	9	-11	109	-27	3	-11	0	-1	26	9	1	15	0	243	-2	8	224	55	3.6	0.4	0.1	0.0	0.2	0.3	0.3	2.0	0.1	52.8	2.8	0.1	0.1
GI-0045	RDM-8	8	4	-18	-5	-6	8	-3	211	-34	1	-12	-5	-1	24	6	-3	6	-4	33	2	-7	84	3	1.7	0.3	0.1	0	0.1	0.3	0.2	0.1	0.3	54.6	3.6	0.3	0
GI-0055	BPM-9	8	10	-3	-6	-7	19	8	244	-38	2	-10	-1	14	472	107	20	29	-6	-13	-1	-7	11	-5	0.8	0.2	0.2	0	0.4	0.3	0.7	0	0.2	49.1	5.3	0.1	0
GI-0062	BPM-9	750	27	-3	-3	-3	20	8	263	-42	-7	-15	2	22	616	79	35	5	-4	-9	-3	-12	10	-4	1	0.2	0.2	0	0.3	0.3	0.2	0	0.2	52.3	4.2	0	0
GI-0087	BPM-9	1	4	-20	-4	-13	9	-1	197	-57	-20	-18	-2	-3	-11	3	-4	1	-4	-21	-6	-21	-3	-7	0.5	0.2	0.2	0	0.1	0.3	0.2	0	0.4	63.5	1.8	0	0
GI-0103	BPM-9	4	16	0	-8	-3	18	9	368	-36	-2	-12	-4	17	733	66	38	61	-4	-10	-3	-13	7	-5	0.8	0.2	0.2	0	0.3	0.3	1.5	0	0.4	47	5.8	0	0
GI-0106	BPM-9	10	10	-2	-7	-4	19	10	314	-40	-13	-9	-4	12	424	58	29	42	-5	-5	-1	-13	9	-6	0.5	0.1	0.2	0	0.3	0.3	1	0	0.5	47.9	5.5	0.1	0
GI-0026	BPM-9	1	8	-1	-14	-5	18	20	359	-36	0	-24	-2	27	883	86	24	9	-8	-12	-5	-28	2	-6	0.3	0.1	0.2	0.2	0.4	0.3	0.2	0	-0.4	41.6	7.2	0	0.3
X		129	13	-5	-7	-6	17	9	291	-42	-7	-15	-2	15	520	67	24	25	-5	-12	-3	-16	6	-6	0.7	0.2	0.2	0.0	0.3	0.3	0.6	0.0	0.2	50.2	5.0	0.0	0.1
GI-0050	RDM-9	3	6	-5	-5	-10	10	-1	272	-19	7	-5	-5	15	396	40	21	35	-5	-10	10	-12	35	-5	2.2	0.3	0.1	0	0.3	0.3	0.8	0	0.4	46.4	5.5	0.3	0
GI-0078	RDM-9	1	8	-4	-4	-4	14	2	285	-34	-8	-16	-4	21	569	99	53	23	-4	-10	11	-8	40	-1	2	0.3	0.1	0	0.3	0.4	0.7	0	0.2	47.8	4.3	0.6	0
GI-0098	RDM-9	4	13	-1	-6	-3	10	-1	309	-30	-2	-10	-4	14	533	80	32	42	-4	-9	15	25	56	-2	2.4	0.3	0.1	0	0.3	0.3	1	0	0.3	47.7	4.4	0.6	0
GI-0115	RDM-9	6	13	-4	-4	-6	13	0	249	-36	7	-14	-4	19	678	64	64	10	-5	-15	17	7	42	-2	2.1	0.4	0.1	0	0.3	0.6	0.4	0	0.4	49.3	4.3	0.4	0
GI-0116	RDM-9	19	6	-5	-4	-6	8	-3	222	-24	1	-12	-4	12	364	54	65	17	-4	-8	15	-3	49	-3	2.5	0.4	0.1	0	0.3	0.6	0.4	0	0.2	47.5	4.4	0.4	0
GI-0012	RDM-9	0	8	-5	-5	-6	13	6	269	-16	9	-17	-3	23	752	53	15	10	-6	-13	4	-21	17	-4	1.8	0.3	0.2	0.2	0.3	0.3	0.3	0	-0.7	48.8	4.9	0.2	0.3
GI-0013	RDM-9	1	5	-4	-4	-6	11	4	327	-19	3	-17	-3	17	490	58	30	55	-6	-14	-1	-24	9	-4	1.3	0.2	0.2	0.2	0.3	0.3	1.2	0	-0.6	47.1	5	0.2	0.4
GI-0014	RDM-9	11	5	-3	-5	-9	13	6	319	-16	6	-17	-4	18	480	59	30	57	-6	-8	0	-23	14	-4	1.2	0.2	0.1	0.2	0.3	0.3	1.2	0	-0.7	47.4	5.3	0.2	0.5
X		6	8	-4	-5	-6	12	2	292	-24	3	-14	-4	17	533	63	39	31	-5	-11	9	-7	33	-3	1.9	0.3	0.1	0.1	0.3	0.4	0.8	0.0	-0.1	47.8	4.8	0.4	0.2

Sample No	Rock T	Au	U	Th	Bi	Pb	W	Ta	Ba	Te	Sb	Sn	Mo	Nb	Zr	Y	Sr	Rb	Se	As	Zn	Cu	Ni	Co	Fe	Mn	Cr	V	Ti	Ca	K	S	P	Si	Al	Mg	Na
GI-0059	BPM-1	8	8	-5	-9	-5	17	8	398	-51	-16	-20	-5	11	186	58	67	51	-6	-15	6	-20	6	-8	0.4	0.1	0.2	0	0.5	0.3	1.3	0	0.2	45.5	6.1	0.1	0
GI-0082	BPM-1	2	3	-15	-11	-12	12	9	206	-54	-17	-19	-5	3	108	20	31	7	-7	-6	4	-16	15	-7	0.7	0.2	0.2	0	0.3	0.4	0.2	0	0.2	47.3	5.9	0.1	0
GI-0027	BPM-1	0	1	-14	-10	-10	14	10	277	-27	2	-17	-2	11	168	40	10	13	-8	-12	-3	-20	-1	-6	0.5	0.2	0.2	0.2	0.5	0.3	0.3	0	-0.7	44.4	6.7	0	0.3
X		3	4	-11	-10	-9	14	9	294	-44	-10	-19	-4	8	154	39	36	24	-7	-11	2	-21	7	-7	0.5	0.2	0.2	0.1	0.4	0.3	0.6	0.0	-0.1	45.7	6.2	0.1	0.1
GI-0052	BPM-20	4	12	-11	-10	0	16	17	432	-56	-13	-20	-5	14	333	38	41	13	-9	10	1	-10	14	-4	0.4	0.1	0.2	0	0.8	0.3	0.3	0	0.1	35.5	10.1	0.1	0
GI-0081	BPM-20	0	5	-8	-17	-9	14	15	308	-52	-8	-20	-4	9	244	31	18	15	-8	16	3	-2	20	-5	0.5	0.1	0.3	0	0.6	0.3	0.4	0	-0.1	39.1	8.8	0.1	0
GI-0028	BPM-20	1	4	-11	-12	-4	17	12	473	-27	7	-17	-3	12	215	51	47	48	-9	-4	3	-4	7	-5	0.5	0.1	0.2	0.2	0.7	0.3	1.2	0	0.5	38.4	8.5	0.1	0.5
X		2	7	-10	-16	-4	16	15	404	-45	-5	-19	-4	12	271	40	35	25	-8	7	2	-5	14	-5	0.5	0.1	0.2	0.1	0.7	0.3	0.6	0.0	0.2	37.7	9.1	0.1	0.2
GI-0030	RDM-10	14	8	-9	-6	-1	7	-5	328	-24	4	-6	-5	12	200	41	50	42	-4	-5	33	-8	18	-4	3	0.4	0.2	0	0.5	0.4	1	0	-0.1	42.4	5.3	0.6	0
GI-0043	RDM-10	1	3	-12	-9	-8	11	3	285	-34	-4	-9	-2	9	183	29	8	28	-5	-10	6	-16	21	-7	1.6	0.2	0.2	0	0.4	0.3	0.7	0	0.2	44.9	6.1	0.2	0
GI-0073	RDM-10	1	3	-13	-6	-7	8	-5	296	-31	3	-9	-4	9	192	39	33	44	-5	-9	13	-8	68	-3	2.9	0.4	0.2	0	0.4	0.3	1.1	0	0	42.9	5.6	0.8	0
GI-0006	RDM-10	1	4	-8	-5	-6	9	1	304	-18	4	-15	-4	10	187	17	17	64	-6	-7	7	-12	5	-6	1.6	0.3	0.3	0.2	0.5	0.4	1.3	0	-0.8	47.9	5.1	0.2	0.4
X		4	5	-11	-7	-6	9	-2	303	-27	2	-10	-4	10	191	32	27	45	-5	-8	15	-11	28	-5	2.3	0.3	0.2	0.1	0.5	0.4	1.0	0.0	-0.2	44.5	5.5	0.5	0.1
GI-0041	RDM-11	3	5	-10	-7	-10	10	0	287	-33	-1	-10	-4	11	229	46	10	33	-5	-7	10	-16	22	-6	2.5	0.3	0.2	0	0.5	0.3	0.8	0	0.3	41.7	6.7	0.2	0
GI-0068	RDM-11	1	8	-6	-10	-2	24	9	644	-21	7	-9	-3	15	170	38	89	193	-6	-5	8	-19	22	-7	1.1	0.2	0.2	0	0.6	0.3	4.1	0	0	33.6	9.4	-0.1	0
GI-0004	RDM-11	2	3	-8	-13	-8	17	13	343	-23	2	-18	-2	19	275	51	10	38	-8	-5	0	-12	8	-3	0.8	0.2	0.3	0.2	0.8	0.3	0.8	0	-0.4	38.8	8.4	0.1	0.4
X		2	5	-8	-10	-7	17	7	425	-26	3	-12	-3	15	225	45	36	88	-6	-6	6	-16	17	-5	1.5	0.2	0.2	0.1	0.6	0.3	1.9	0.0	0.0	38.0	8.2	0.1	0.1
GI-0067	RDM-12	4	5	-8	-3	-10	10	-2	304	-21	-3	-8	-4	11	197	48	29	45	-4	0	10	-8	56	4	2.6	0.3	0.2	0	0.4	0.3	1.1	0.2	0.3	43	5.7	0.5	0
GI-0003	RDM-12	2	3	-14	-4	-8	10	1	233	-11	4	-9	-1	7	229	33	7	24	-5	-11	6	-7	16	-5	1.7	0.3	0.2	0.2	0.4	0.2	0.5	0	0.7	46.9	5.1	0.3	0.3
X		3	4	-11	-4	-9	10	-1	269	-16	1	-9	-3	9	213	41	18	35	-5	-6	8	-8	36	-1	2.2	0.3	0.2	0.1	0.4	0.3	0.8	0.1	0.5	45.0	5.4	0.4	0.2
GI-0035	RDM-13	17	10	-9	-4	0	11	-3	302	-22	5	-7	-3	-17	252	66	44	51	-4	-6	23	-12	16	-7	2.3	0.3	0.3	0	0.5	0.4	1.2	0	0.2	45.3	5.3	0.4	0
GI-0010	RDM-13	0	3	-12	-9	-11	11	5	276	-25	4	-17	-2	-10	259	39	8	21	-7	-10	4	-2	15	-5	1.5	0.2	0.3	0.2	0.5	0.3	0.5	0	-0.7	43.6	6.8	0.2	0.3
X		9	7	-11	-7	-6	11	1	327	-24	5	-12	-3	-14	236	53	26	36	-6	-9	14	-7	16	-6	1.9	0.3	0.3	0.1	0.5	0.4	0.9	0.0	-0.3	44.5	6.1	0.3	0.2
X-Y		4	5	-18	-7	-6	12	2	335	-24	2	-11	-3	7	216	41	28	53	-5	-7	11	-11	24	-4	2	0.3	0.3	0.1	0.5	0.3	1.2	0	0	42.8	6.3	0.3	0.1
GI-0032	RDM-14	5	4	-12	-5	-5	6	-7	284	-23	6	-13	-4	7	144	27	11	31	-5	-12	26	13	17	-7	2.9	0.4	0.2	0	0.4	0.3	0.6	0	-0.1	47	4.6	0.6	0
GI-0042	RDM-14	1	1	-14	-8	-13	9	3	249	-40	-7	-16	-9	1	56	19	6	25	-6	-12	2	-3	16	-5	1.4	0.2	0.2	0	0.2	0.2	0.6	0	0.1	48.3	4.9	0.2	0
GI-0070	RDM-14	3	5	-11	-5	-13	7	-5	291	-33	-3	-11	-4	5	164	47	27	37	-4	-10	13	-12	58	-1	2.6	0.3	0.2	0	0.4	0.3	0.9	0	0.1	45.5	4.4	0.8	0
GI-0007	RDM-14	1	7	-17	-4	-8	-2	-21	251	-23	8	-14	-4	7	152	64	3	10	-5	-3	19	-15	18	-7	6.5	0.9	0.2	0.2	0.4	0.3	0.2	0	-0.6	42.2	5.4	0.3	0.3
X		3	4	-14	-6	-10	5	-8	269	-30	1	-14	-5	5	129	39	12	26	-5	-9	15	-4	27	-5	3.4	0.5	0.2	0.1	0.4	0.3	0.6	0.0	-0.1	45.8	4.8	0.5	0.1
GI-0076	RDM-15	1	6	-7	-8	1	14	5	649	-30	-1	-11	-6	9	165	58	76	166	-6	-3	14	-17	54	-4	2	0.3	0.2	0	0.6	0.3	3.7	0	-0.1	31.8	9.2	0	0.1 0
GI-0110	RDM-15	3	7	-12	-4	-8	5	-6	312	-26	4	-10	-2	8	163	72	47	47	-5	-6	39	-14	112	-1	4.2	0.5	0.2	-0	0.5	0.4	1.1	0	0	39.7	6	0.7	0
GI-0005	RDM-15	1	3	-17	-8	-9	15	7	301	-23	3	-19	-5	2	48	50	9	26	-8	-10	-1	-22	5	-4	0.9	0.2	0.2	0.2	0.2	0.3	0.6	0.1	-0.7	47.1	5.7	0.1	0.3
X		2	5	-12	-7	-5	11	2	421	-26	2	-13	-4	6	125	60	44	80	-6	-6	17	-18	57	-3	2.4	0.3	0.2	0.1	0.4	0.3	1.8	0.0	-0.3	39.5	7.0	0.3	0.1
GI-0040	RDM-16	13	6	-13	-7	-8	8	-2	230	-27	1	-7	-5	7	180	35	6	13	-5	-9	22	-1	18	-5	2.5	0.3	0.2	0	0.4	0.3	0.4	0	-0.1	45.8	5	0.5	0
GI-0109	RDM-16	1	6	-11	-4	-2	0	-16	269	-50	2	-11	-5	9	138	30	16	28	-5	0	22	-13	44	-3	4.9	1.4	0.2	0	0.3	0.3	0.6	0	0.2	44.8	5.3	0.3	0
GI-0001	RDM-16	2	7	-8	-2	-3	1	-21	226	-16	5	-18	-5	8	143	27	0	7	-2	3	15	-20	18	0	5.9	0.8	0.2	0.2	0.4	0.3	0.2	0	-0.6	43.2	5	0.2	0.2
X		5	6	-11	-4	-4	3	-13	242	-31	3	-12	-5	8	154	31	7	16	-4	-2	20	-11	27	-3	4.4	0.8	0.2	0.1	0.4	0.3	0.4	0.0	-0.2	44.6	5.1	0.3	0.1
GI-0031	RDM-17	5	5	-12	-9	-8	11	-1	289	-28	-1	-9	-4	13	215	64	32	33	-5	-9	38	-12	12	-6	3.4	0.4	0.2	0	0.6	0.3	0.7	0	0	38.4	7.1	0.7	0
GI-0069	RDM-17	1	5	-12	-7	-8	11	0	350	-28	0	-8	-4	9	178	98	28	58	-6	-11	17	-16	78	-2	3.1	0.4	0.2	0	0.5	0.3	1.3	0	0	33.4	7.8	0.6	0
GI-0111	RDM-17	8	7	-11	-5	-9	4	-11	332	-19	8	-9	-5	10	158	71	37	50	-4	1	39	-13	104	-2	5.1	0.9	0.2	0	0.5	0.4	1.1	0	-0.1	37.7	6.2	0.7	0
GI-0002	RDM-17	1	3	-12	-5	-7	7	-2	253	-12	4	-8	-3	10	178	37	7	26	-6	-5	8	-3	13	-6	2.9	0.4	0.2	0.2	0.5	0.2	0.5	0	-0.6	42.8	6.2	0.2	0.3
X		4	5	-12	-7	-8	8	-4	306	-22	3	-9	-4	11	182	68	26	42	-5	-6	26	-11	52	-4	3.6	0.5	0.2	0.1	0.5	0.3	1.0	0.0	-0.2	38.6	6.8	0.6	0.1
X-G		3	5	-12	-6	-7	7	-6	306	-27	2	-12	-5	8	149	50	22	40	-5	-6	20	-11	41	-4	3.5	0.5	0.2	0.1	0.4	0.3	0.9	0	-0.2	42.1	5.9	0.4	0.1
X-Y+G		4	5	-11	-6	-7	9	-2	319	-26	2	-11	-4	7	178	46	24	46	-5	-6	16	-11	33	-4	2.8	0.4	0.2	0.1	0.5	0.3	1	0	-0.1	42.4	6.1	0.4	0.1
GI-0008	RDM-18	0	4	-17	-3	-9	8	0	238	-22	0	-21	-5	0	27	9	0	19	-5	-2	2	-18	11	-3	1.8	0.3	0.2	0.2	0.2	0.3	0.4	0.1	-0.8	49.9	4.9	0.2	0.2
GI-0039	RDM-19	12	7	-9	-3	-1	8	-3	248	-26	-2	-13	-3	5	158	20	5	24	-3	27	40	5	61	3	4	0.5	0.2	0	0.3	0.3	0.6	0.2	0.1	41.3	6.2	0.7	0
GI-0048	RDM-19	3	4	-14	-5	-6	10	0	224	-28	5	-11	-4	4	140	28	1	21	-5	-8	6	0	24	-3	2.1	0.3	0.2	0	0.2	0.3	0.5	0	0.2	46.6	5.3	0.2	0
GI-0074	RDM-19	1	3	-13	-5	-10	0	-9	322	-31	1	-15	-6	6	163	33	31	49	-4	-6	32	-10	113	7	4.8	0.5	0.2	0	0.3	0.3	1	0	0	38	5.3	1.5	0
GI-0097	RDM-19	3	7	-11	-1	0	6	-7	265	-26	5	-8	-3	7	196	32	14	37	-3	24	33	10	116	7	4.1	0.4	0.2	0	0.3	0.3	0.9	0.1	0.2	41.4	5.3	1.1	0
GI-0112	RDM-19	10	4	-16	-5	-6	1	-13	289	-20	4	-9	-4	4	126	55	32	31	-5	3	44	-5	121	2	5.6	0.9	0.2	0	0.3	0.4	0.7	0	0	39.1	5.7	1	0
GI-0011	RDM-19	3	3	-22	-3	-14	8	-3	207	-27	7	-16	-4	-2	-8	5	-1	8	-5	0	-7	-21	11	0	0.7	0.2	0.2	0.1	0.1	0.3	0.2	0.1	-0.9	61.6	2.2	0	0.3
X		5	5	-14	-4	-6	6	-6	259	-26	3	-12	-4	4	129	29	14	28	-4	7	25	-4	74	3	3.6	0.5	0.2	0.0	0.3	0.3	0.7	0.1	-0.1	44.7	5.0	0.8	0.1

Table V.1. Continued (**Legend**).

Rock T	- Rock Type
BPM	- Big Pebble Marker
RDM	- Rosedale Member
X	- Arithmetic mean
X-Y	- Arithmetic mean for rock types 10 + 11 + 12 + 13
X-G	- Arithmetic mean for rock types 14 + 15 + 16 + 17
X-Y+G	- Arithmetic mean for rock types 10 to 17

	ROCK TYPE
1	YELLOW-1 BPM
2	DARK QUARTZITE
3	LIGHT QUARTZITE
4	WHITE QUARTZ
5	DARK QUARTZ
6	DARK CHERT
7	LIGHT CHERT
8	BANDED CHERT
9	IGNEOUS
10	YELLOW-1 RDM
11	YELLOW-2 RDM
12	YELLOW-3 RDM
13	YELLOW-4 RDM
14	GREY-1
15	GREY-2
16	GREY-3
17	GREY-4
18	BLACK
19	DARK SILTSTONE
20	YELLOW-2 BPM

(and in some cases, groups of rock types) were calculated and given immediately below the values for the samples belonging to the particular rock type. The values for **Gold** are given in **p.p.b.** and the values for the **trace elements** (from U up to and including Co) are given in **p.p.m.** while the values for the **major elements** (Fe to Na) are given as **percentage.**

The data are not corrected for matrix or inter-element effects, or other mineralogical effects, which can vary from sample to sample. Thus the data consist of relative or comparative values. This unfortunately limits the use and

applications of the data. Although the data are not accurate, they are precise. Therefore the data can be used for fingerprinting and comparative studies such as cluster analyses and correlation matrices or coefficients. These type of studies are, however, limited to results within the AARL database.

A limited amount of correction can be done in some cases to get more acceptable results. In the case of negative values, the data must firstly be inspected for outlier values which must be ignored because such values are normally caused by unknown matrix or inter-mineral effects. After elimination of such values the lowest value can be taken as the zero value to correct the other values accordingly to achieve acceptable results. The correction of results reported as positive values is a much more complicated task which should not be attempted freely.

NOTE: *The gold values reported are accurate and precise, since they were determined by means of Atomic Absorption (AA) and not XRF like the other elements. Therefore the above two paragraphs are not applicable to the reported gold values.*

Emerging from *Table V.1.*, the following observations can be highlighted:

1. Si values are high in all the samples.
2. Three quartzite samples from the RDM, GI-0117, GI-0047 and GI-0118, yielded high Au values.
3. One quartz sample (GI-0054) from the BPM, which contains an elevated Au content, also contains enhanced Cu, Ni and Co values.
4. Anomalous high values of Au occur in the majority of BPM chert samples, such as GI-0056, GI-0057, GI-0066, GI-0083, GI-0107, GI-0054, GI-0058, GI-0060, GI-0086 and GI-

0020 as well as in one igneous sample, GI-0062 originating from the BPM.

5. These high Au values are normally accompanied by similarly enhanced values of some other elements like Pb, As, Cu, Ni, and Co.
6. Two dark chert samples from the RDM, GI-0038 and GI-0095, also yielded relatively high Au values, but in lower concentrations than the chert clasts from the BPM.
7. Some sediment clasts yielded a Na/K ratio of ≥1, indicative of a possible volcanic origin or possibly "contamination" by volcaniclastic derived material. (see *Table V.3.*).
8. In general, clasts from the RDM appears to be relatively enriched in incompatible trace elements, such as Rb, Sr, Ba and Zr.

2.1. DISCUSSION

When the data are studied and some of the rock types are compared on the basis of average values, some differences come to light. Where differences between rock types occur, they are normally small and subtle. Some interesting observations can, however, be made. The only way to quantify these differences are to depict the values of one rock type in a relative sense against the values of the other rock type(s) it is being compared to. The more noticeable differences between some combinations of the different rock types are summarized in *Table V.2.*.

The most outstanding feature concerning all the data, which is not reflected in *Table V.2.*, is the singularly high Si values reported in all the samples, while all the other elements occur in very low concentrations. This can only reflect extensive post-depositional silicification of the clasts. Due to the nature of the AARL data, it is

not possible to determine the exact extent of the alteration that took place.

Table V.2. Main geochemical differences between rock types. (Although enhancement is arbitrary and difficult to quantify due to the uncorrected nature of the data, it is normally at least 2X, but can be as high as 20X.)

ROCK TYPE	ENHANCED ELEMENTS
DARK CHERT BPM	Au Pb As Cu Ni Co
DARK CHERT RDM	Ba Al Mg
LIGHT CHERT BPM	Au Zn As
LIGHT CHERT RDM	Zr Fe Al Mg
BANDED CHERT BPM	Au Pb Bi Sb As Cu Ni Co
BANDED CHERT RDM	Ba Fe Al Mg
ALL CHERT BPM	Au
ALL CHERT RDM	Al Ba
ALL DARK CHERT	Au Pb As Ni Co Fe S
ALL LIGHT CHERT	Ba Zr K
IGNEOUS BPM	Au
IGNEOUS RDM	Fe
YELLOW-1 BPM	Si
YELLOW-2 BPM	Ba Zr As Al
YELLOW-1 RDM	Si
YELLOW-2 RDM	Ba
YELLOW-3 RDM	Si
YELLOW-4 RDM	Si
GREY-1 RDM	Si
GREY-2 RDM	Ba Sr Rb Al
GREY-3 RDM	Si
GREY-4 RDM	Ba Al
ALL YELLOWS RDM	Zr
ALL GREYS RDM	Ni
ALL YELLOWS BPM	Ta Ba
ALL YELLOWS + GREYS RDM	Rb Ni Fe Mn
ALL YELLOWS + GREYS RDM	
ALL IGNEOUS	Au Zr Si

A noticeable feature of the durable clasts in general, is that it appears that the durables from the RDM are enriched in incompatible trace elements (Rb, Sr, Ba, Zr), relative to the durables from the BPM.

NOTE: *For the purpose of this study, the igneous clasts are considered as "durables", since all available evidence suggest that their durability in this particular environment is comparable with the other "durable" clasts such as quartzite, chert and quartz.*

QUARTZITE

No distinctive geochemical differences, except for a few sporadic high Au values (GI-0117 131p.p.b., GI-0061 30p.p.b., GI-0047 34p.p.b., GI-0018 24p.p.b.), exist between the dark- and light-coloured quartzite clasts of either the BPM or the RDM, or between the quartzite clasts from the BPM and the RDM. This confirms the general trend of the conclusions reached in Chapter III. Therefore both types of quartzite will be treated as one population, here and in the underground data.

QUARTZ

In the case of the quartz clasts, a similar situation as in the case of the quartzite clasts exists. This also confirms conclusions reached in Chapter III. Although the fluid inclusion study (*Chapter IV*) concluded that it is possible to distinguish thermodynamically between dark- and light-coloured quartz, it is nevertheless proposed that the two types of quartz clasts be treated as one population since the distinction between the two types is rather arbitrary because of the fact that it appears that some white quartz clasts is in the process of being

converted *in-situ* into dark coloured-quartz (see *III.1.3.*).

CHERT

An interesting feature of the majority of the chert samples, is the strong, to anomalous, enhancement of the average gold values in the clasts from the BPM. This is accompanied by a similar phenomenon in the concentrations of a few other elements which are often used as pathfinder elements in geochemical exploration for gold in greenstone terranes. Four of these elements (Mn, Co, Ni, Cu) are included in a list of elements which, according to Hallbauer and Kable (1982), can be used to distinguish between secondary quartz and quartz genetically related to a primary (mineralized) deposit. (Although As forms part of the above association, it is not included in the list of Hallbauer and Kable.) Although the applicability of this approach on chert and igneous clasts is not verified as yet, it will nevertheless be attempted.

The enhanced gold, as well as compatible trace element concentrations in all three types of BPM chert, relative to the concentrations in RDM chert clasts, strongly suggest a different source for the two units. Based on the enhanced nature of some compatible trace element contents of the BPM clasts (chert and others), a more mafic source is proposed for the BPM, compared to that of the RDM.

IGNEOUS

As in the case of the chert clasts, the anomalous gold content of the igneous clasts from the BPM indicates, in

addition, that the source for the BPM was in comparison, more auriferous than that of the RDM. Therefore it can be said without doubt that gold was present in igneous source rocks. Apart from slightly enhanced iron values in the igneous clasts from the RDM, the compositions of the igneous clasts from the two units are otherwise virtually identical.

YELLOWS

The main difference between the respective nondurable types manifests itself in the Si content, which coincides with the hardness classification as described in *Chapter III*. Normally, a decrease in Si is accompanied by an increase in Al and a consequential decrease in hardness. This trend can be observed in all the nondurables. Other differences between the various "yellow" and "grey" clast types are insignificant and form no obvious pattern or trend. This indicates that the clustering of the RDM yellows and greys in one group and the BPM yellows in another similar group, is appropriate. The only difference between the BPM and RDM yellow classes, would be a slight enhancement of Fe in the RDM yellows. This latter observation probably explains the higher incidence of chloritoid in RDM yellows, compared to BPM yellows.

DARK SILTSTONE

If the RDM dark siltstone chemistry is compared to that of the yellows, the latter are relatively enhanced in Zr, Sr and Rb, while the dark siltstones are enhanced in Fe and Mg. This enhancement in Fe and Mg is probably reflected by the relative abundance of chloritoid in the dark siltstone.

SEDIMENTARY ROCKS

When the Na/K ratio for the sedimentary clasts are calculated, several samples yield a ratio of ≥1 which, according to Pettijohn (1975), suggests volcanic origin or contamination, in the case of sedimentary rocks. This supports observations previously made (see *III.1.3.* and *III.2.1.*). Samples which meet this criteria are given in Table V.3.

Table V.3. List of sedimentary samples, displaying a Na/K ratio of ≥1.

SAMPLE No	ROCK TYPE	FORMATION
GI-0001	YELLOW	RDM
GI-0007	YELLOW	RDM
GI-0015	QUARTZITE	RDM
GI-0017	DARK CHERT	BPM
GI-0018	DARK CHERT	BPM
GI-0020	LIGHT CHERT	BPM
GI-0022	QUARTZITE	BPM
GI-0024	LIGHT CHERT	BPM
GI-0025	QUARTZITE	BPM
GI-0027	YELLOW	BPM

2.2 CONCLUSIONS

During the study of the geochemical data, the following number of conclusions were derived:

1. No significant geochemical differences exist between the light- and dark-coloured quartzite clasts from either the BPM or the RDM.

2. Enhanced Au values occur in all three types of BPM chert clasts.
3. Dark chert samples from the RDM also exhibit enhanced Au values, albeit at lower concentrations, compared to those from the BPM.
4. Au was present in the igneous source rocks of the BPM.
5. The source rocks of the BPM were more auriferous than those of the RDM.
6. Compared to the RDM the source rocks of the BPM were of a more mafic nature.
7. The chemistry of some sediment clasts exhibit a volcaniclastic association.

3. STATISTICAL MANIPULATION

The calculation of average geochemical values for different rock types was performed statistically by computer. These values are given in *Table V.1.* and were used in the comparative study of the different rock types as described above in *V.2.1.* and *V.2.2.*.

3.1. CLUSTER ANALYSIS

In an attempt to statistically verify the rock type classification system (see *III.1.1.* and *III.1.2.*), used to classify the different clasts underground, cluster analyses (Everitt, 1974) (see *II.3.1.*) were performed on some of the data. The classifications which were to be verified were quartz and chert, as well as the global yellows system.

According to Hallbauer and Kable (1982), the concentration levels of nine elements, Cl, Na, Ca, K, Au, Mn, Co, Ni and Cu can be used to distinguish secondary

quartz clasts from quartz clasts genetically related to a primary deposit. Therefore the seven elements among these, for which values were available (Na, K, Ca, Mn, Co, Ni, Cu) were used as discriminators, while all the quartz samples from both the BPM and RDM served as a data base for the first cluster analysis. The programme was set up to create three clusters, which theoretically would cluster the data into a mineralized and an unmineralized class. The third cluster is to accommodate any outlier samples that might occur. A similar cluster analysis was performed on a chert data base consisting of all the chert samples.

Pettijohn (1975) pointed out some chemical criteria which can be used to identify certain sediments. These criteria include the elements Na, K, Mg, Ca and Al. Therefore these elements were used as discriminators in the cluster analyses performed on the sedimentary yellows and greys clasts. The programme was set up to create five clusters. Three data bases were used. The first consisted of all the yellows from the BPM and all the yellows and greys from the RDM. The second database consisted of all the igneous samples. For the third data base, all the igneous samples were added to the first data base.

In ***Appendix 2.*** an example of the **SAS** programme used to perform the cluster analyses and calculate the Spearman correlation coefficients, are given. The results of the cluster analyses as well as simple statistics of the different clusters are also given in ***Appendix 2.***.

3.2. CORRELATION COEFFICIENTS

The SAS programme was set up in such a way that Spearman correlation coefficients (Conover, 1980) were calculated automatically in each cluster formed, for all elements used in the particular cluster analysis, after the analysis was performed. The results of the correlation coefficient analyses will be discussed together with the cluster analysis results. The results of the calculated Spearman correlation coefficients are summarized in *Table V.4.*.

Table V.4. Summarized results of Spearman correlations.

CLUSTER	ELEMENT PAIRS & CORRELATION COEFFICIENTS						
	Ca:Mg	Mg:K	Mg:Al	Na:K	Al:K	Na:Al	Co:Ni
C1-01/1	0,67						
C1-02/1							0,64
C1-03/1		0,73					
C1-03/2			-0,64				
C1-04/1				-0,75	-0,67	0,68	
C1-04/2		-0,81					
C1-04/3		0,65					
C1-04/4		0,70	-0,70		-0,90		
C1-05/1						0,73	
C1-05/3		0,71	-0,71		-0,90		

C1-01 - indicates the cluster analysis performed.
/3 - indicates the cluster number in the particular analysis.

Only significant correlations (coefficients of >.60) are given in *Table V.4.*. The Spearman correlation coefficients of all the clusters, which contained enough samples to allow for the calculation of correlation coefficients, are given with the cluster analyses in ***Appendix 2.***.

3.3. DISCUSSION

QUARTZ (C1-01)

The quartz samples were clustered into three clusters of which the first contained all the samples but two, which were contained in the other two clusters. These two samples (GI-0054 and GI-0100), contain enhanced Cu, Ni and Co values. With the given elements as discriminators, the cluster analysis was unsuccessful in clustering mineralized samples together. The best and only viable correlation was between Ca and Mn, with a coefficient of 0,67.

CHERT (C1-02)

The chert samples, especially those from the BPM, yielded the highest Au values as well as the highest average Au values of all the rock types studied. While Boyle (1979) gives the average Au value for chert internationally as 16 p.p.b., the average for the total chert population studied, is 100 p.p.b. The average gold value for all the dark chert samples from the BPM is an anomalous 218 p.p.b. Therefore it was decided to perform a cluster analysis on the chert population, similar to the one performed on the quartz samples. Three clusters were formed, of which one contained all the samples but three. The other two clusters can, for all practical purposes, be considered as one cluster (see *Appendix 2. C1-02*) In

this case the analysis was more successful in that this combined cluster contained the two chert samples (GI-0066 and GI-0057) which yielded the highest Au values. The best and only viable correlation was between Ni and Co, with a coefficient of 0,64.

IGNEOUS (C1-03)

The igneous samples were submitted to the same cluster analysis as were the yellows, but the programme was set to create only three clusters. Except for one outlier, all the samples clustered into two distinct clusters. The first cluster consisted almost exclusively of RDM samples, while the second cluster contained almost equal amounts of RDM and BPM samples. The best and only viable correlation in the first cluster was between Mg and K, with a coefficient of 0,72, while a negative correlation coefficient of 0,64 between Mg and Al occurs in the second cluster.

YELLOWS (C1-04)

In the case of the yellows, the programme was set to create five clusters. This was done because the classification for both the yellows and the greys consist of four classes. The fifth cluster is again to cater for outliers. Four of the clusters formed are comparable, while the fifth cluster contains two samples (GI-0068 and GI-0076) with relatively anomalously high K values. For the purpose of this discussion this cluster will be excluded.

Upon studying the clusters created, it can be seen that the basis for the formation of the different clusters is formed by the differences in K and Al concentrations. Some good correlations, of which some are negative, occur

in the different clusters. These correlations, however, do not form any discernable pattern or trend.

As was previously concluded, the physical classification correlated well with Si content (which was not included in the cluster analyses) of the samples (see *V.2.2.*). The Si content, however, does not differ sufficiently to justify the different classifications on such a basis alone.

IGNEOUS + YELLOWS (C1-05)

In the last cluster analysis performed, the igneous samples were grouped with the yellows and greys to form the data base for the analysis. Again five clusters were formed. The results of this analysis only served to confirm the results of the previous two analyses. This time the majority of the samples clustered in two large clusters, which basically differ only slightly in K and Al content. The igneous samples from the BPM and the RDM, respectively, fall in these two larger clusters.

3.4. CONCLUSIONS

QUARTZ

In the case of the quartz samples, the cluster analysis was unsuccessful in distinguishing secondary quartz from quartz related to primary mineralization. Alternately, the elements used as discriminators are not applicable in this case. It also comes to light that Au mineralization is not always associated with this particular (Na, K, Ca, Mn, Co, Ni, Cu) association of elements. This is probably the main reason why the analysis was unsuccessful. From inspection of the raw data it is, however, obvious that

two populations (mineralized and unmineralized) are nevertheless present.

CHERT

Based on gold values alone it can be seen that light and dark chert form two distinct populations. It is also obvious that the chert from the BPM is more enriched in gold than that from the RDM. The most important conclusion is, however, that the same elemental association (As, Pb, Cu, Ni, Co) with Au mineralization, which occurs in some quartz samples, also occurs in the better mineralized chert samples.

IGNEOUS

The two distinct populations occurring in the igneous data base are indicative of two provenances. This conclusion is supported by the different correlation matrices which reflect different character and not a mere difference in composition. The RDM contains igneous material from both sources, while the BPM contains igneous material from virtually one source only.

YELLOWS

Because a poor correlation exists between the physical classification (*III.1.1.* and *III.1.2.*) and the cluster analysis (*V.3.1.*) which is based on chemical composition, which does not vary significantly between the different yellows clast types or between individual yellows samples, it is proposed that all the yellows and greys are in fact one population. This is in accordance with similar conclusions previously made (see *III.3.3.* and *V.2.2.*).

YELLOWS + IGNEOUS

The results of the last cluster analysis support the conclusion that the yellows and greys form one population only and that the igneous samples from the BPM and RDM form two slightly different, but nevertheless, distinct populations. The most important fact to emerge from this last analysis is that the igneous samples are very similar in composition to the yellows as far as the discriminator elements are concerned.

VI

FIELD DATA

Despite the fact that the field data were compiled before any other work was done, it was decided for the sake of logical interpretation, to discuss it now, only after the lithological study (*Chapter III*), fluid inclusion study (*Chapter IV*) and the assessment of the analytical data (*Chapter V*) is completed. It was done in this way because the classifications for the statistical data and field measurements, which were compiled in the initial stage of this study, were based on mesoscopic physical parameters like rock type, colour and hardness (see *II.1*). Before these statistics could, however, be presented, the classifications had to be verified by means of the above-mentioned studies (*Chapters III, IV & V*).

Based on observations made, and conclusions reached in *Chapters III* and *V*, it was decided to treat dark and light quartzite as one population. Dark and white quartz will also be treated as a single population. For the same reasons the yellows and greys are treated as one population. Although enough evidence exist to verify the existence of three different chert populations (dark, light and banded), it was decided to treat all the chert as one population for the presentation of the statistics. This was done because the discrimination between light and dark chert is rather arbitrary, as well as the fact that the banded chert consists of both dark and light chert. The relative distribution of the different chert types is given in *Table VI.1.*.

Table VI.1. Relative composition of chert clast assemblages of the BPM and RDM.

FMN	PERCENTAGE OF TOTAL CHERT POPULATION		
	DARK CHERT	LIGHT CHERT	BANDED CHERT
BPM	68,5	8,6	22,9
RDM	62,0	30,9	7,1

For the purpose of this study, all quartzite, quartz, chert and igneous clasts are considered to be "durables", while all the yellows (greys included), black and dark siltstone clasts are considered to be "non-durables" (also see V.2.1).

1. CLAST ASSEMBLAGE STATISTICS

The statistics on the incidence of the various clast types are presented in *Tables VI.1.* and *VI.2.* Statistics for the incidence of durable clasts versus non-durable clasts are also given. Figures obtained, are for all practical purposes equivalent to volume percentage, since they were calculated by means of the grid count (see *Chapter II*). The statistics given for matrix were calculated as percentage of total conglomerate volume. The percentages given for the different clast types were calculated as percentages of total clast volume (matrix excluded). This approach facilitates the final analysis of the clast assemblage and its significance.

1.1. DISCUSSION

BPM

From *Table VI.2.* it is obvious that quartz clasts, with an average incidence of 61,5%, dominate the clast assemblage of the BPM. Second to quartz, is the chert

Table VI.2. Statistical results of grid counts for the BPM.

BPM	% OF TCV	PERCENTAGE OF TOTAL CLAST VOLUME									
LOC	MA	QE	QZ	CH	IG	YE	BL	DS		DU	ND
2	46,3	20,1	46,7	14,5	4,5	13,2		0,9		85,9	14,1
5	34,0	5,5	63,5	24,8	1,7	4,5		0,3		95,2	4,8
6	27,5	3,9	67,3	20,0	3,0	4,0		1,8		94,2	5,8
8	33,4	5,1	67,0	17.6	3,0	6,0		1,4		92,6	7,4
10	25,5	7,1	58,5	20,8	5,6	6,4		1,7		91,9	8,1
12	33,3	7,2	66,7	22,2	0,3	2,8		0,7		96,5	3,5
X	**33,3**	**8,2**	**61,5**	**20,2**	**3,0**	**6,3**		**1,0**		**92,7**	**7,3**

Legend for *Tables VI.2.* and *VI.3.*

LOC - LOCALITY
TCV - TOTAL CONGLOMERATE VOLUME
MA - MATRIX
QE - QUARTZITE
QZ - QUARTZ
CH - CHERT
IG - IGNEOUS
YE - YELLOW
BL - BLACK
DS - DARK SILTSTONE
DU - DURABLES
ND - NON-DURABLES

For locality reference numbers see *Fig. I.3.* and *Table I.1.*

Table VI.3. Statistical results of grid counts for the RPM.

RDM	% OF TCV	PERCENTAGE OF TOTAL CLAST VOLUME									
LOC	MA	QE	QZ	CH	IG	YE	BL	DS		DU	ND
1	41,4	31,2	5,3	24,9	2,7	20,5	2,9	12,5		64,1	35,9
3	37,8	30,1	23,8	13,3	7,4	11,9	2,1	8,2		77,8	22,2
4	38,8	28,1	18,8	15,8	6,0	18,6	1,1	9,8		70,5	29,5
7	28,9	26,3	15,0	30,4	3,9	21,5	0,3	5,3		72,9	27,1
9	41,4	18,6	44,7	23,0	3,8	7,7	0	2,2		90,1	9,9
11	36,6	16,6	19,6	21,6	6,8	21,1	0	14,4		65,5	35,5
X	**37,5**	**25,2**	**21,2**	**21,5**	**5,1**	**16,9**	**1,1**	**8,7**		**73,3**	**26,7**

clasts at an average incidence of 20,0%. The relative abundances of the different types of chert in the total chert population of the BPM are given in Table VI.1. The rest of the clast types (quartzite, igneous, yellows and dark siltstone) are totally subordinate to the quartz and chert clasts, comprising in total only 18,4% of the total clast volume. The igneous component of the total clast assemblage is very small (3,0%). In total the average clast assemblage of the BPM consists of 92,7% durable and 7,3% non-durable clasts.

RDM

From *Table VI.3.* it can be seen that the clast assemblage of the RDM is comprised of virtually equal amounts of quartz, chert, arenaceous sediments (quartzite) and argillaceous sediments (yellows, blacks and dark siltstone). Only a small (5%) igneous component is present. The relative abundances of the different types of chert in the total chert population of the RDM are given in *Table VI.3.* In total the average clast assemblage of the RDM consists of 73,3% durable and 26,7% non-durable clasts.

GENETIC CRITERIA

The durable/non-durable criteria is subject to many factors influencing the relative ratio between the two types of clasts and although these criteria might be valuable in studies of a sedimentological nature, it is of limited use in genetic studies. Because this study is primarily concerned with the provenance, or source rocks, of the conglomerates, a "genetic" approach is proposed and used in this study. In *Table VI.4.* the composition of the BPM and the RDM is compared in terms of genetic association. The figures for durables and nondurables are included in *Table VI.4* for comparison.

All the quartz clasts studied, displayed characteristics typical of primary/hydrothermal quartz deposits and are therefore classified as of hydrothermal origin. Although the quartzites are "durables", while the yellows, blacks and dark siltstone clasts are "non-durables", they are grouped together as sediments (including volcaniclastic sediments) for genetic purposes (designated TOTAL SEDIMENTS in *Table VI.4*). The chert samples are, however, not included in this designation, because their genesis are too different from the clastic sediments (TOTAL SEDIMENTS) and they are therefore kept in a separate class, designated CHEMICAL SEDIMENTS.

Table VI.4. Mean composition of the clast assemblages of the BPM and RDM in terms of genetic association.

FMN	IGNEO	HYDRO	CHSED	ARSED	AGSED	T-SED	DURABL	NONDUR
BPM	3,0%	61,6%	20,0%	8,2%	7,3%	15,5%	92,7%	7,3%
RDM	5,1%	21,2%	21,5%	25,2%	26,7%	51,9%	73,3%	26,7%

FMN - FORMATION
IGNEO - IGNEOUS
HYDRO - HYDROTHERMAL (quartz)
CHSED - CHEMICAL SEDIMENT (chert)
ARSED - ARENACEOUS SEDIMENT (quartzite)
AGSED - ARGILLACEOUS SEDIMENT (yellow, black & siltstone)
T-SED - TOTAL SEDIMENT (ARSED + AGSED)
DURABL - DURABLES (quartzite, quartz, chert & igneous)
NONDUR - NON-DURABLES (yellow, black & dark siltstone)

1.2. CONCLUSIONS

From the preceding work the following few important conclusions emerge:

1. Although the vast majority of the clasts are virtually the same, the compositions of the provenance(s) for the BPM and the RDM were different.
2. The provenance(s) of the BPM contained a large hydrothermal component, almost 3 times that of the RDM.
3. The provenance(s) of the RDM contained a large sedimentary component, 3,3. that of the BPM.
4. The provenance(s) of the BPM contained a rather small argillaceous sedimentary component **or** the argillaceous component was largely destroyed during relatively extensive transport and/or reworking.
5. Chemical sediments (chert) constituted a significant (≥21%) component of the provenances of both the BPM and RDM. However, banded chert is 3 times higher in the BPM than in the RDM, to the expense of the light chert.
6. The igneous component in the provenances of both the BPM and the RDM was relatively small.

2. SIZE DISTRIBUTION STATISTICS

The statistics on the size distribution of the various clast types are presented in *Tables VI.5.* and *VI.6.* The measurements were made according to the "line count" method, which is described under *II.2.2.*

Table VI.5. Size distribution of BPM clasts.

BPM	MEAN CLAST SIZE in mm										
LOC	QE	QZ	CH	IG	YE	BL	DS		DU	ND	LQC
2	105	75	71	60	49		58		78	50	169
5	74	74	59	98	66		59		68	63	171
6	87	74	53	44	29		65		65	33	188
8	76	59	47	43	47		30		56	46	178
10	71	53	42	54	49		61		50	51	152
12	129	67	56	48	37		72		66	46	200
X	**90**	**67**	**55**	**58**	**46**		**58**		**64**	**48**	**176**

LOC - LOCALITY
QE - QUARTZITE
QZ - QUARTZ
CH - CHERT
IG - IGNEOUS
CH - CHERT
YE - YELLOW
BL - BLACK
DS - DARK SILTSTONE
DU - DURABLES
ND - NON-DURABLES
ND - NON-DURABLES
LQC - MEAN SIZE OF TEN LARGEST QUARTZ CLASTS IN EXPOSURE
For locality reference numbers see *Fig. I.3.* and *Table I.1.*

Table VI.6. Size distribution of RDM clasts.

RDM	MEAN CLAST SIZE in mm										
LOC	QE	QZ	CH	IG	YE	BL	DS		DU	ND	LQC
1	66	44	46	62	39	41	94		51	43	145
3	59	47	44	50	39	33	80		50	45	186
4	71	39	41	45	34		55		48	37	148
7	68	71	53	63	57	24	73		62	57	130
9	26	24	23	22	19		26		24	20	78
11	45	43	39	42	41		43		42	41	101
X	**56**	**45**	**41**	**47**	**38**	**16**	**62**		**46**	**41**	**131**

2.1. DISCUSSION

BPM

From *Table VI.5.* it can be seen that the average durable clast size (64mm) lies on the border between the pebble and cobble size classification of the Wentworth-Udden scale (Whitten & Brooks, 1979). The average sizes of the quartzite and quartz clasts are, however, larger at 90mm and 67mm, respectively. Scattered large cobbles and even boulder- sized quartz clasts occur frequently in the BPM. The non-durable clasts are smaller and are on average 75% of the durable clasts' size.

RDM

From *Table VI.6.* it emerges that, on average, all the clasts of the RDM can be classified as pebbles. As in the case of the BPM, the quartzite clasts of the RDM are larger than the rest of the clasts, and scattered quartz cobbles also occur. In contrast with the BPM, the durable clasts from the RDM are only marginally larger than the non-durables from the RDM (46mm *vs* 41mm).

GENETIC IMPLICATIONS

Despite the fact that the size of the components in a gravel is a function of several factors, some useful generalized conclusions may nevertheless be drawn from these data. The size of gravel in a stream is mainly a function of three factors:

1. The size of clasts derived from the source.
2. The decline in size due to abrasion (distance of transport).
3. The competence of a stream at any given point.

Although the average size of the RDM clasts is smaller than the average size of the BPM clasts, they are not as

well rounded as those from the BPM. This indicates that clast size is not always primarily dependant on distance of transport and/or reworking, but rather on other physical conditions, apart from clast composition, which control the initial fragmentation of the host rock.

If the quartz clasts, in both the RDM and BPM, were derived from the same source rock types, only stream competence, could have caused this observed difference in roundness, since bedrock type and abrasion were, for all practical purposes, the same for both reefs. Therefore, a difference in competence of the transport medium, is indicated for the RDM and the BPM by this comparative study.

The clast sizes measured on the various localities for the RDM fit well with Kingsley's (1986) measurements made on Western Holdings and President Brand Mines, but deviate from the measurements made on FSG and Freddies Mines. The present size study is, however, quantitative and more accurate. The various localities and their corresponding size values, can be related to specific positions on the fan (*Figure VI.1.*). Although the shape of the BPM deposit is less well known than that of the RDM, relative proximality between the localities can be drawn in broad terms (*Figure VI. 2.*).

When the average size of the ten largest quartz clasts measured at each locality (see LQC, *Tables VI.5.* and *VI.6.* for values), is plotted against downslope distance, two completely different graphs emerge (*Figure VI.3.*). Extrapolation of the RDM graph towards the source suggests a fan apex only 3 to 4 kilometres west of the St Helena Mine.

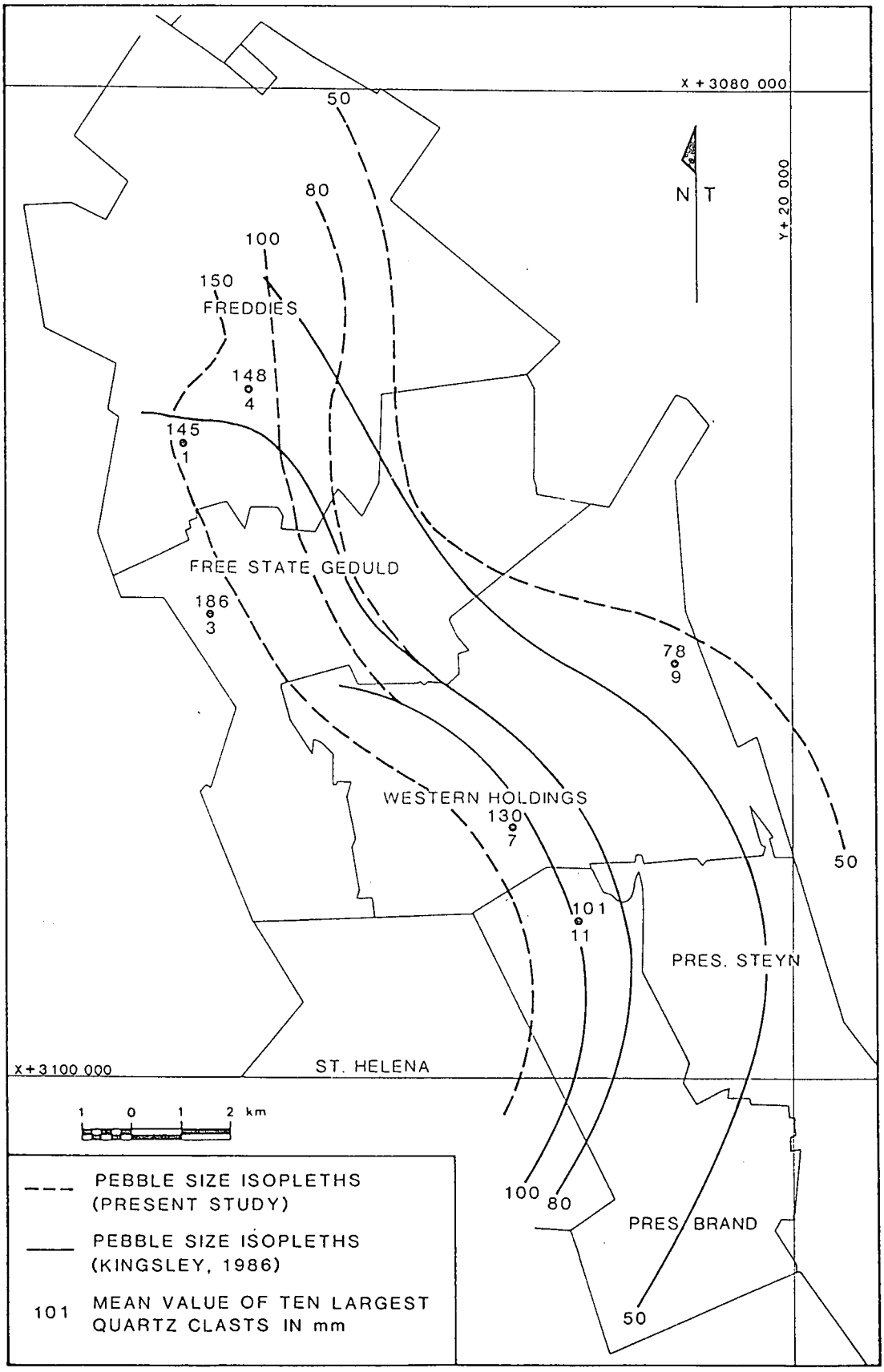

Fig. VI.1. Pebble size isopleth map for the basal conglomerate of the RDM.

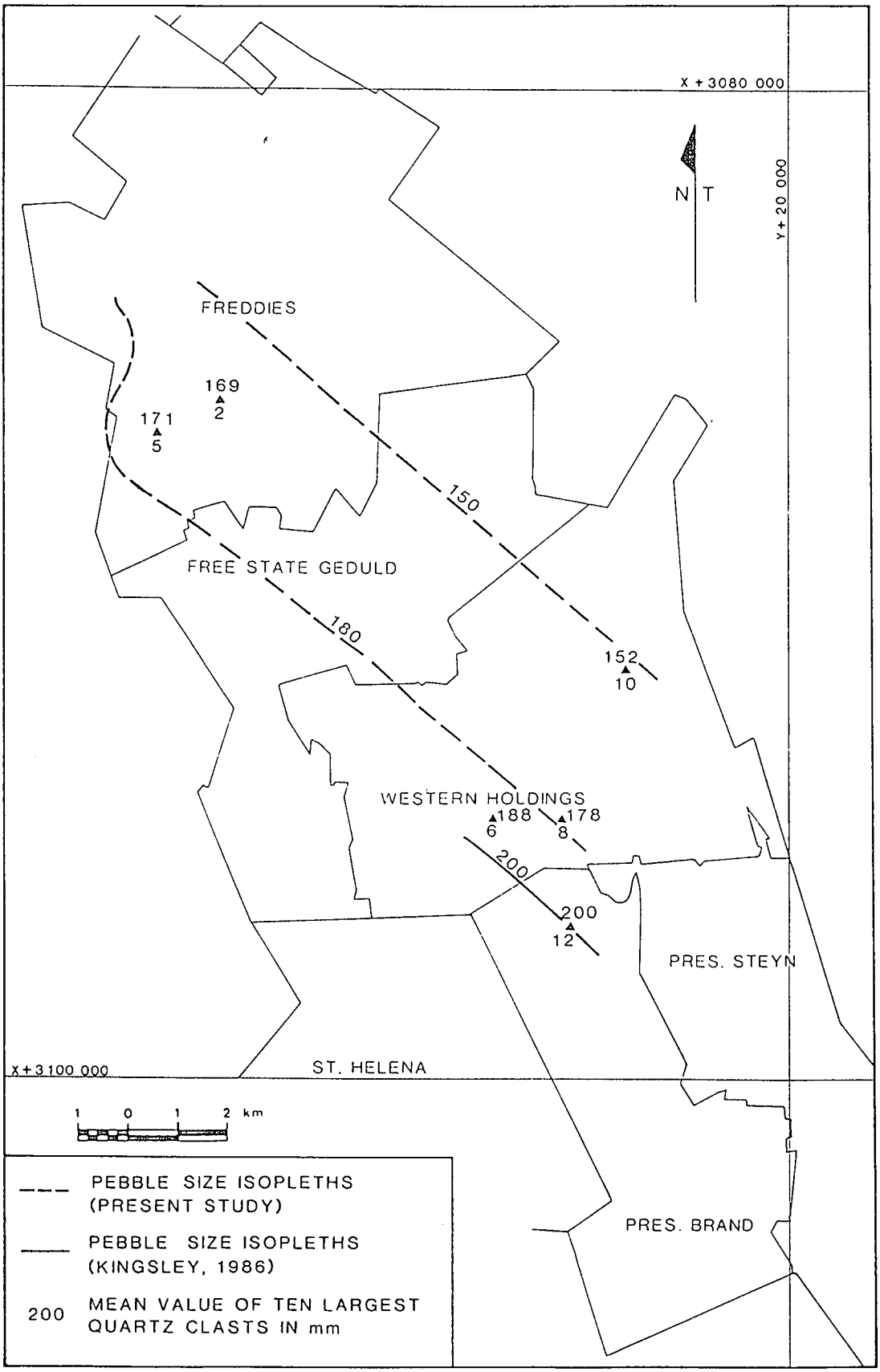

Fig. VI.2. Pebble size isopleth map for the BPM.

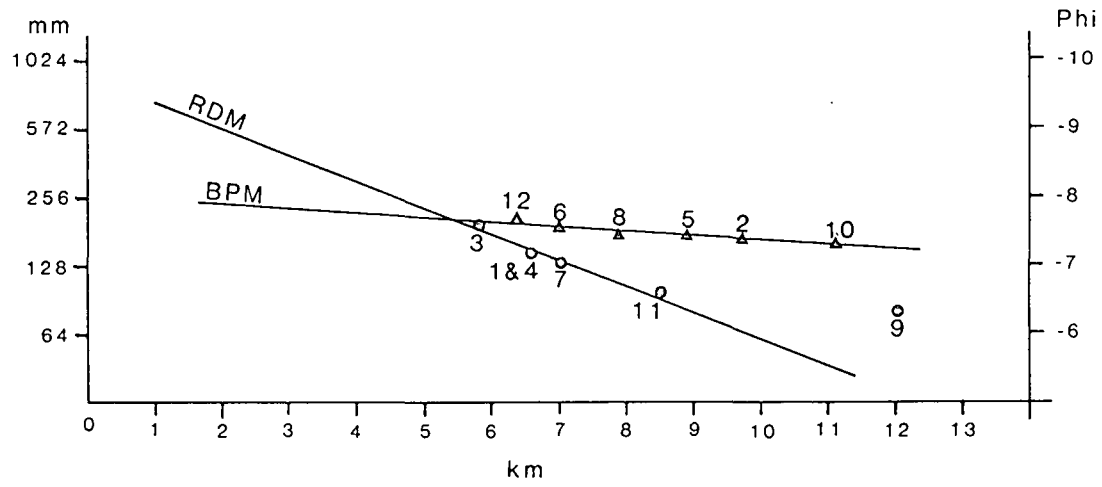

Fig. VI.3. Average size of the ten largest quartz clasts measured at each locality, plotted against downslope distance. The symbols with the figures refer to the exposure locality where the measurements were taken (see *Figure I.3.*). **Note:** The distances given in km are relative and do not confine the distance to the provenance.

The completely different slopes obtained from the distance / clast size graph (*Figure VI.3.*) for the BPM and the RDM suggests different transport mechanisms. The slow decrease in clast size of the BPM suggests a much more competent transport medium, originating further back into the hinterland.

This difference in source area of the RDM and BPM is also shown by the difference in size of the yellows in the two units. In section *III.1.4.* it was concluded that the yellows in both conglomerates originated from provenances different (and more proximal) to those from which the durable clasts originated. This is confirmed by the size distribution of the yellows when the average size and the size ratio of durables versus yellows of the RDM are compared with that of the BPM. The size ratio of durables versus yellows in the RDM is 1:0,89, compared to 1:0,75

in the BPM, which illustrates the fast decline of yellows with increased transport/reworking.

The virtual absence of black clasts from the BPM and their small and well rounded dimensions may indicate extensive transport. The dark siltstone is the only clast type of which the clasts are on average larger in the RDM than in the BPM, which shows conclusively the more local derivation of the siltstone clasts in the RDM. In both conglomerates the dark siltstone clasts are notably larger than the other durable clasts. This, in conjunction with the fact that the hardness and composition of these clasts are roughly comparable with that of some of the yellows clasts, can in both cases, only indicate a provenance different from those, which the durables and yellows were derived from. It is, therefore, quite conceivable that these siltstone clasts could have been derived from the subcrop belt of the West Rand Group.

2.2. CONCLUSIONS

From the above discussion four important conclusions emerge:

1. Different physical conditions, which controlled the initial clast size, prevailed in the provenances of the BPM and the RDM, at the time of their derivation.
2. Different transport conditions/mechanisms prevailed during the deposition of the BPM and the RDM.
3. The material deposited in the BPM was probably transported over a longer distance than the material deposited in the RDM.
4. Different provenances are indicated for durables, yellows and dark siltstone clasts, in order of distal to proximal.

3. COLOUR PHOTOGRAPHS

At each underground exposure studied, a few colour photographs were taken to illustrate the general appearance of the exposure. An attempt was made, where possible, to take one photograph depicting the global features of the outcrop and another, more close-up photograph, exhibiting more detail. A selection of these photographs are presented below (*Plates VI.1.* to *VI.22.*).

Plates VI.1. to *VI.10.* illustrate the BPM exposures and *Plates VI.11.* to *VI.22.* illustrate the RDM exposures. From these photographs the difference in character between the two conglomerates is clearly evident (also see *III.1.3.* as well as *Tables VI.2.* and *VI.3.*). All locality numbers refer to *Table I.1.* and *Figure I.3.*.

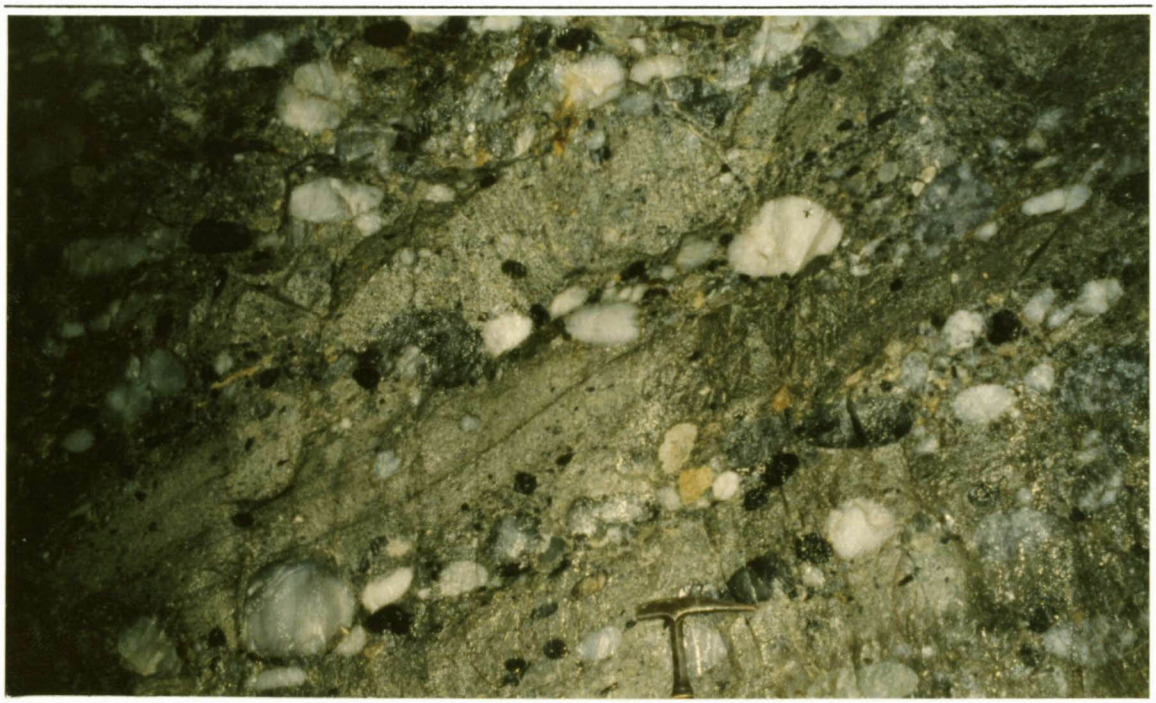

Plate VI.1. Locality 2, BPM : Global features of the exposure; note the scour surfaces and individual conglomerate bands.

Plate VI.2. Locality 2, BPM : In general the individual conglomerate bands are largely clast supported.

Plate VI.3. Locality 5, BPM : Global features of the exposure, denoted by the large, well-rounded clasts.

Plate VI.4. Locality 5, BPM : Close-up detail of the exposure reveal the poor sorting of the conglomerate.

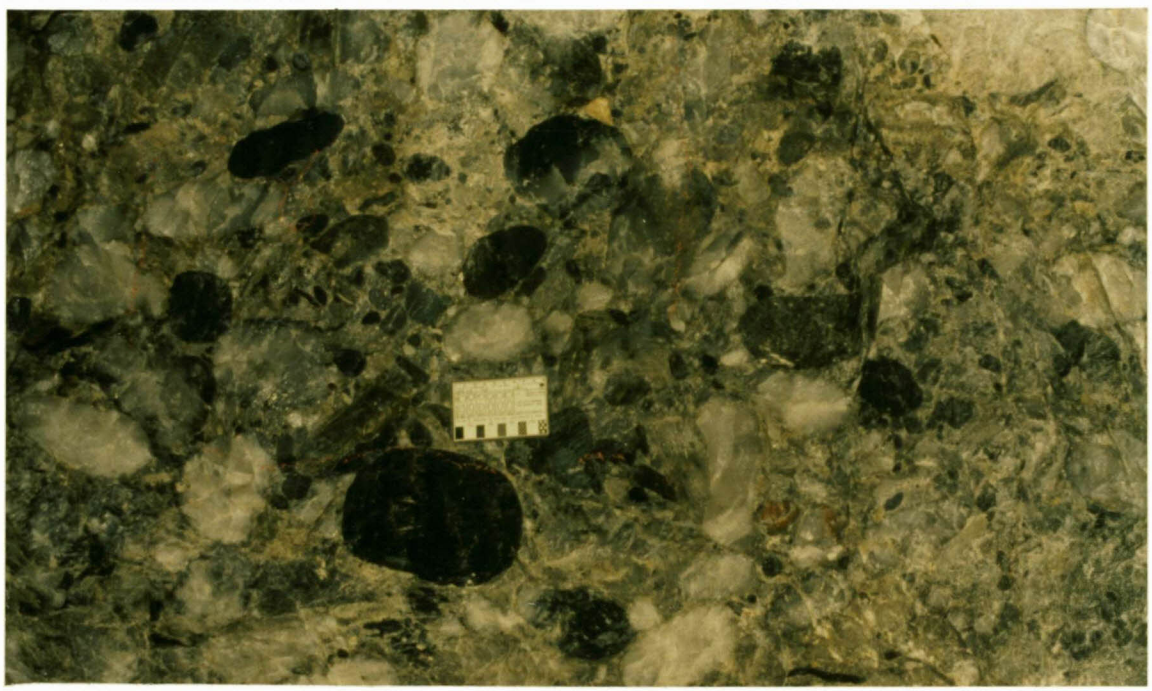

Plate VI.5. Locality 6, BPM : Close-up detail of the exposure; note the large black chert clast below the scale. (Total length of the scale is 9cm)

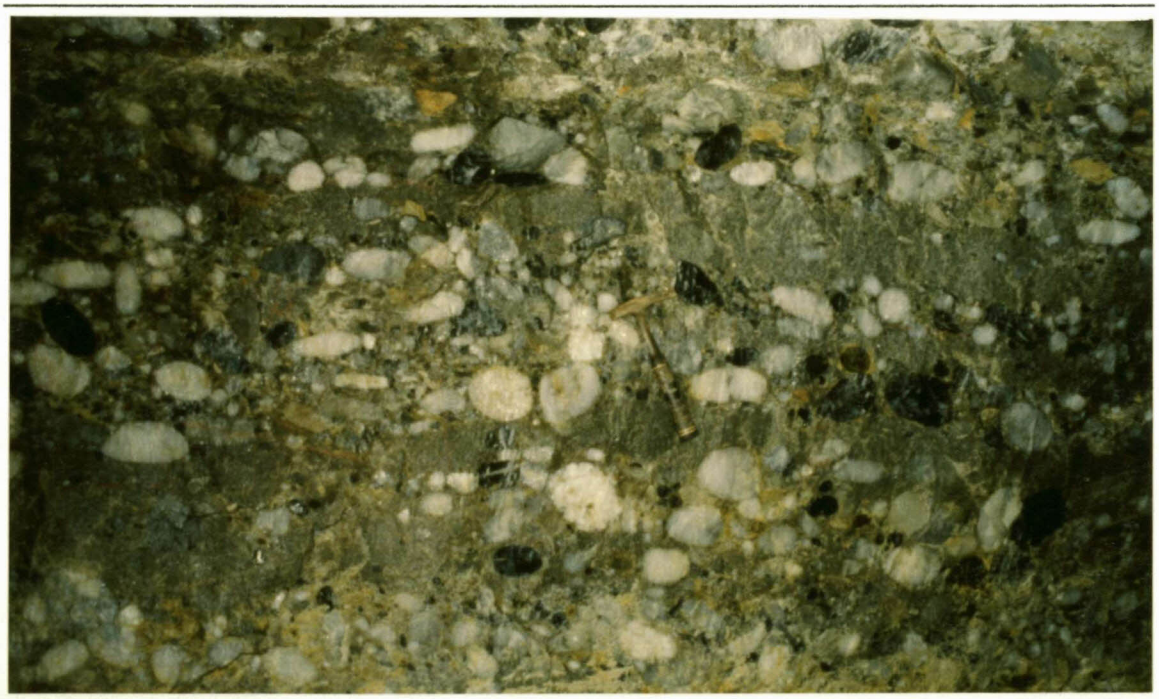

Plate VI.6. Locality 8, BPM : The global impression of this exposure is one of poor sorting and packing.

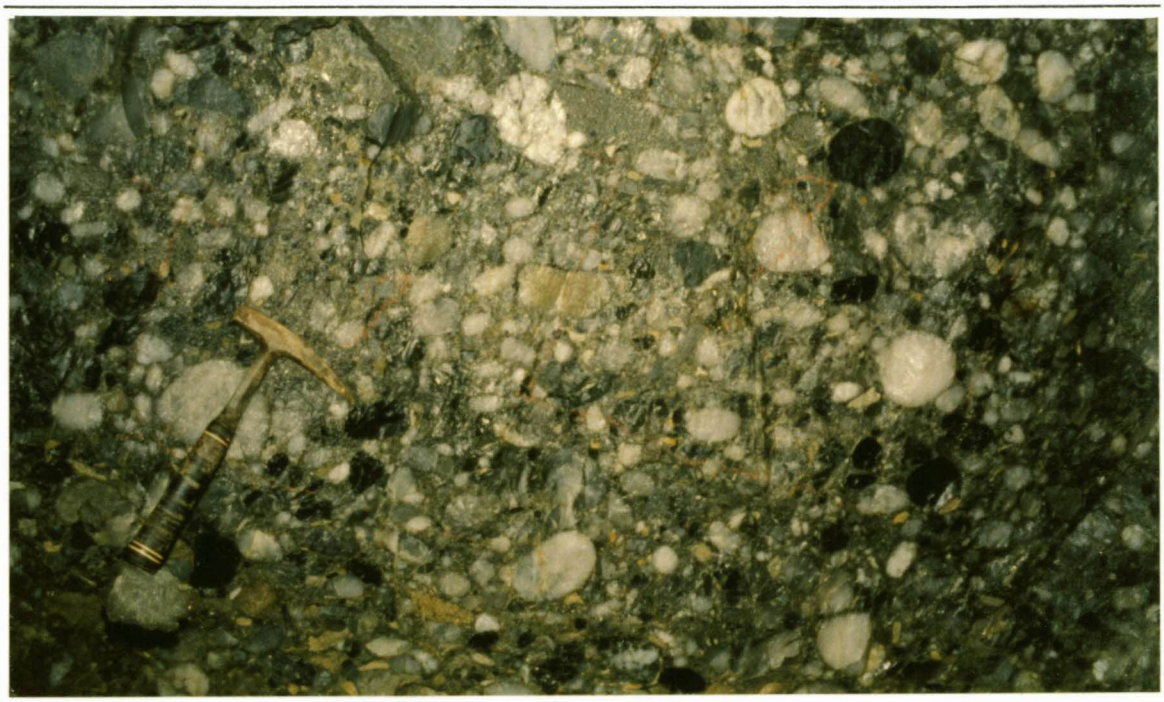

Plate VI.7. Locality 8, BPM : The scattered large clasts in this exposure suggests a highly competent transport medium.

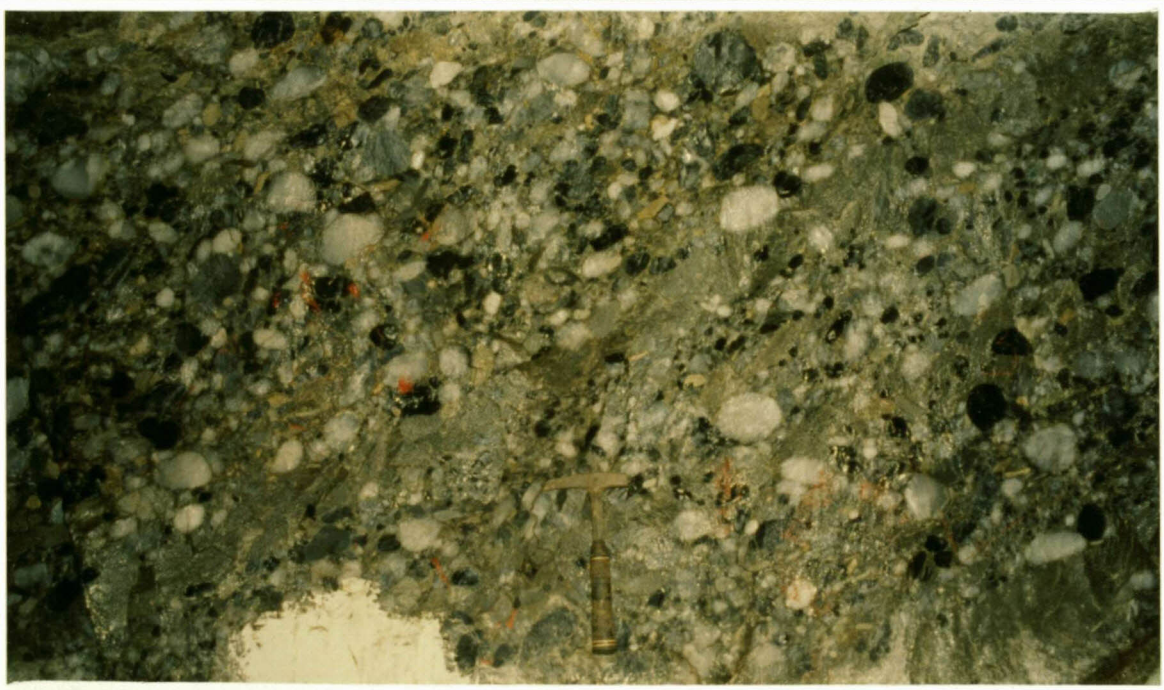

Plate VI.8. Locality 10, BPM : The scour surface (above the hammer) in this exposure clearly indicates two successive depositional events.

Plate VI.9. Locality 12, BPM : Note the different fabrics present in this channel filling, located in a relative proximal position on the fan.

Plate VI.10. Exposure 12, BPM : These well packed, highly rounded clasts is obvious upon close-up investigation.

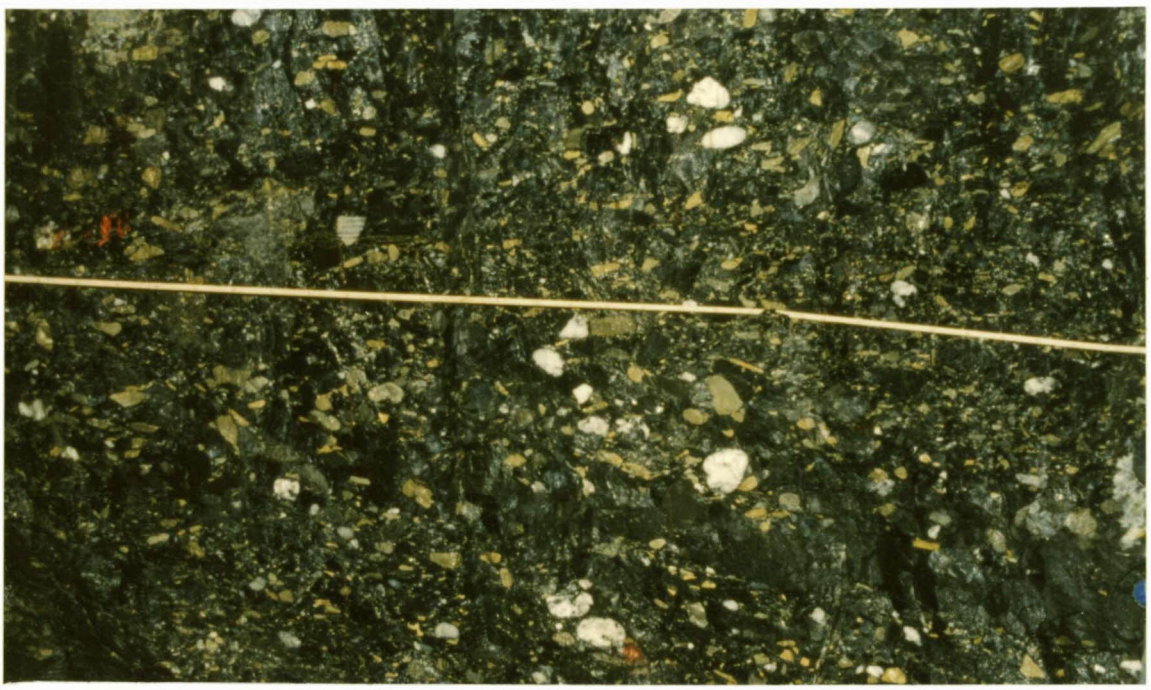

Plate VI.11. Location 1, RDM : Note the abundance of yellows and the angularity of the clasts in this exposure. (Horizontal scale is approximately 3,5m)

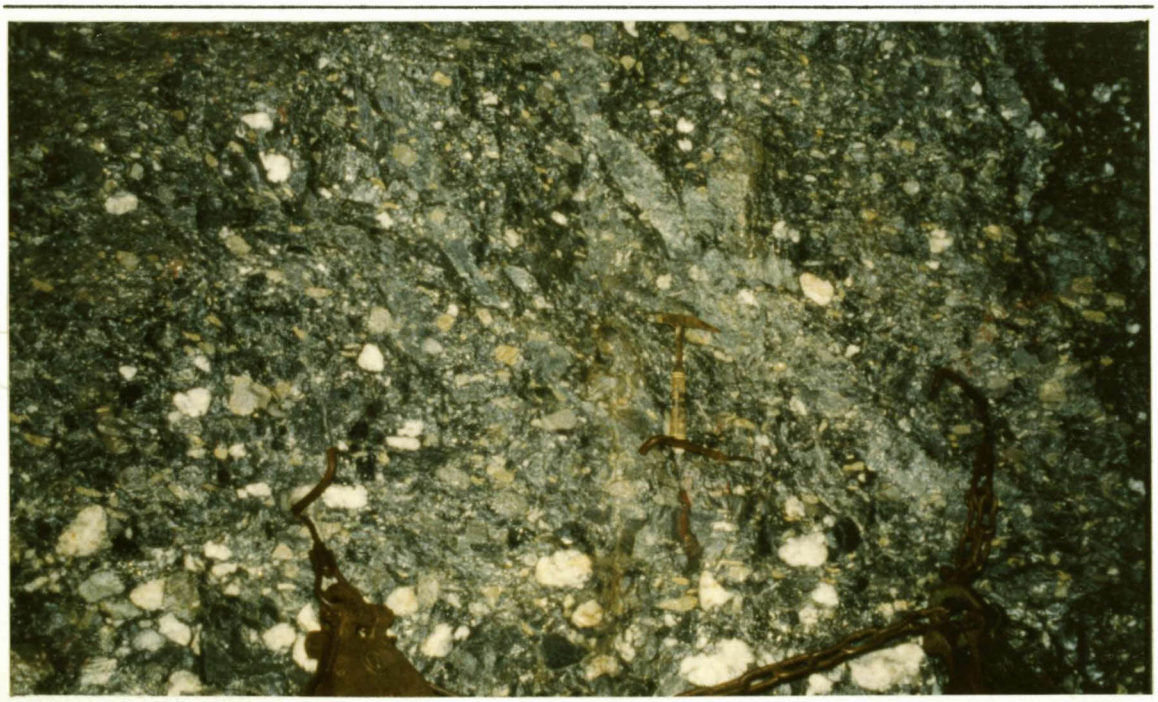

Plate VI.12. Locality 3, RDM : Note the well developed grading visible in this exposure.

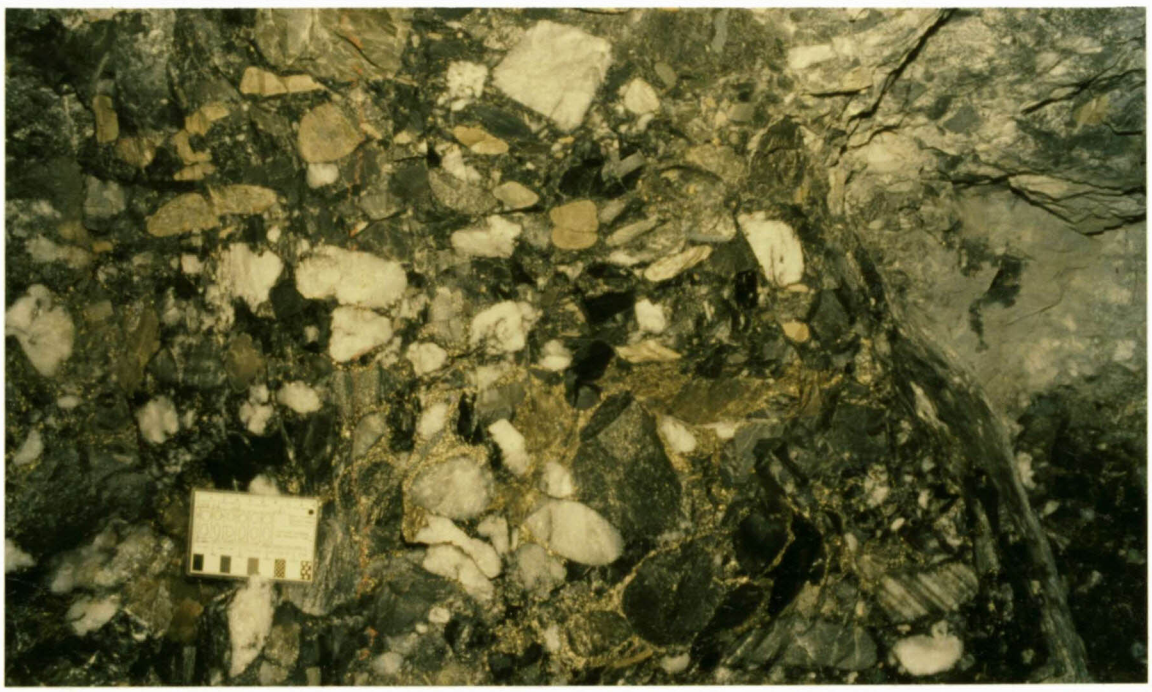

Plate VI.13. Locality 3, RDM : Note the relative angularity of the clasts. (Total length of scale is 9cm)

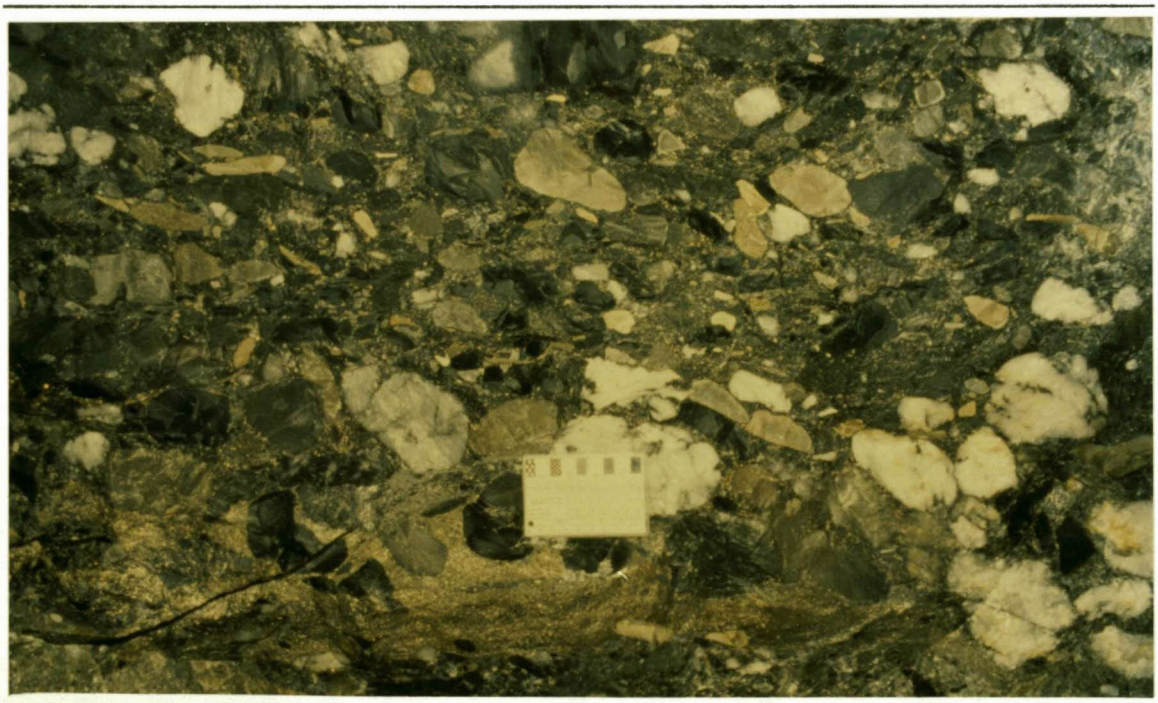

Plate VI.14. Locality 3, RDM : Close-up study of the exposure reveals the concentration of detrital pyrite below the scale. (Total length of scale is 9cm)

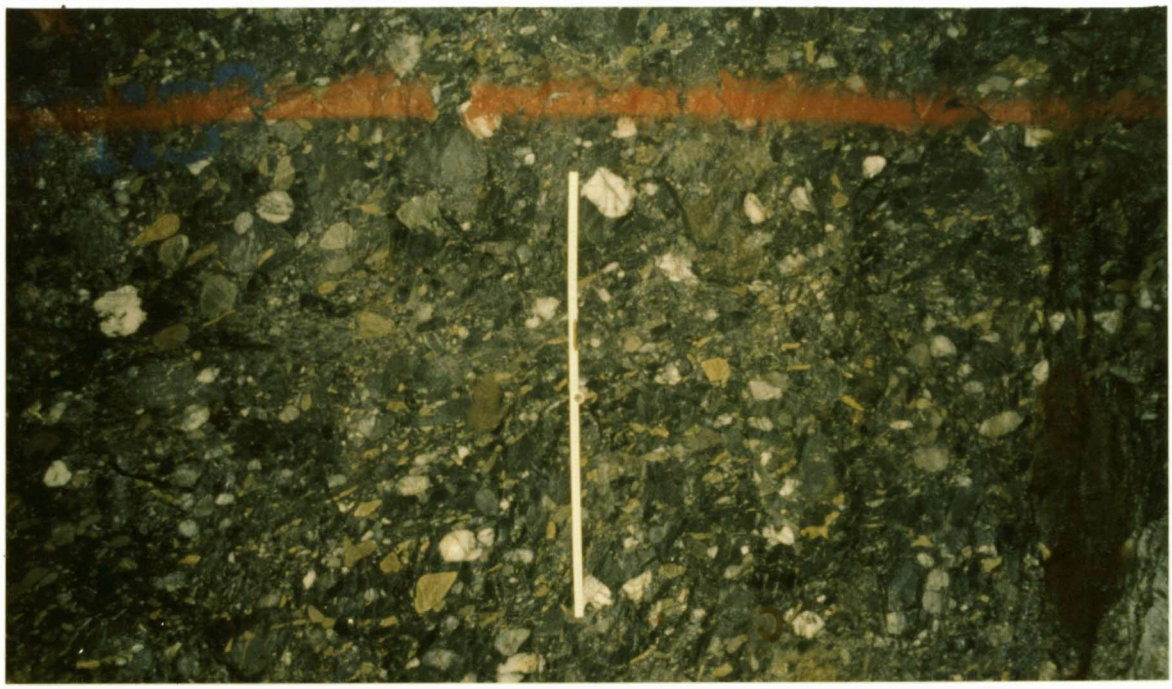

Plate VI.15. Locality 4, RDM : Note the imbrication of the clasts in the centre of the exposure. (Clinorule is 1m long)

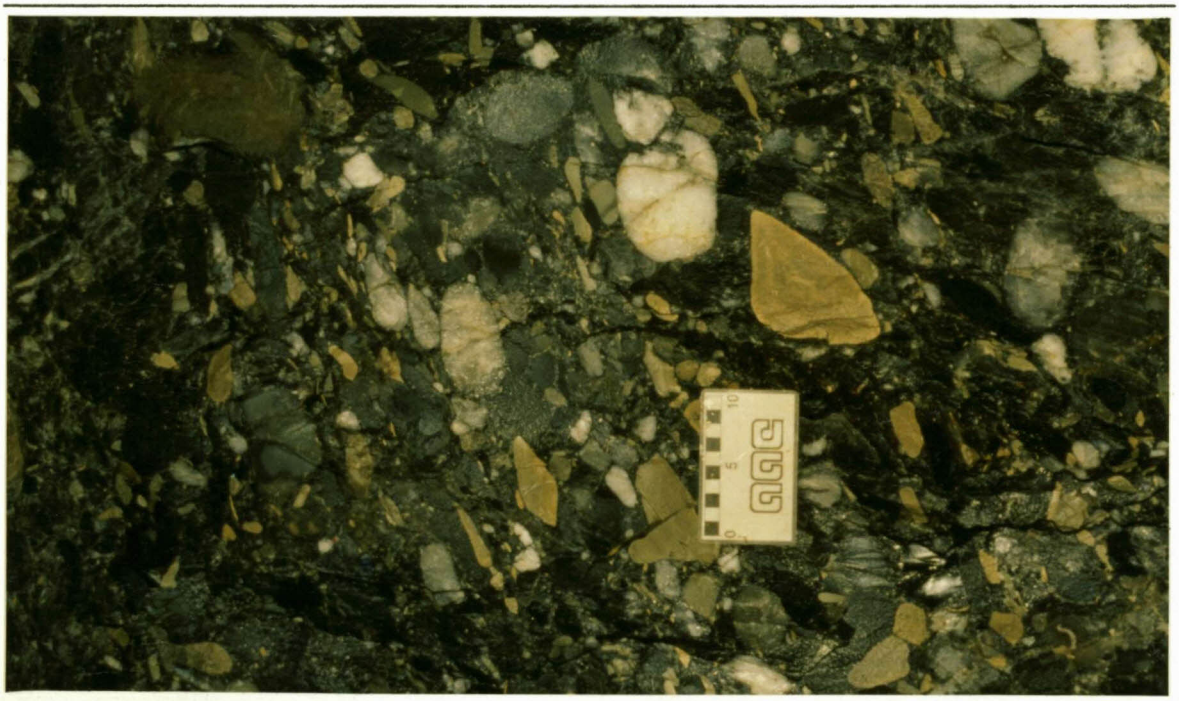

Plate VI.16. Locality 4, RDM : Close-up detail illustrating the angularity of the yellows. (Total length of scale is 10cm, figures on scale indicate right way up)

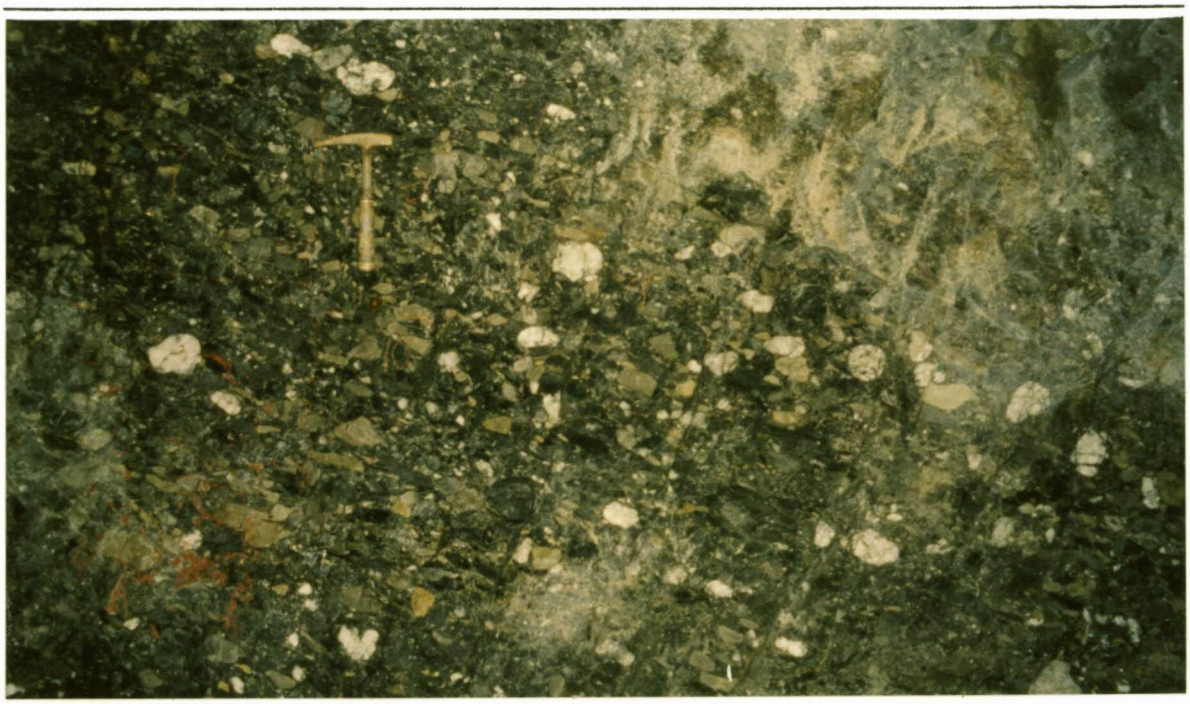

Plate VI.17. Locality 7, RDM : Note the scattered, poorly- to well-rounded white quartz clasts.

Plate VI.18. Locality 7, RDM : Note the "draped" yellow clast in the centre of the photograph.

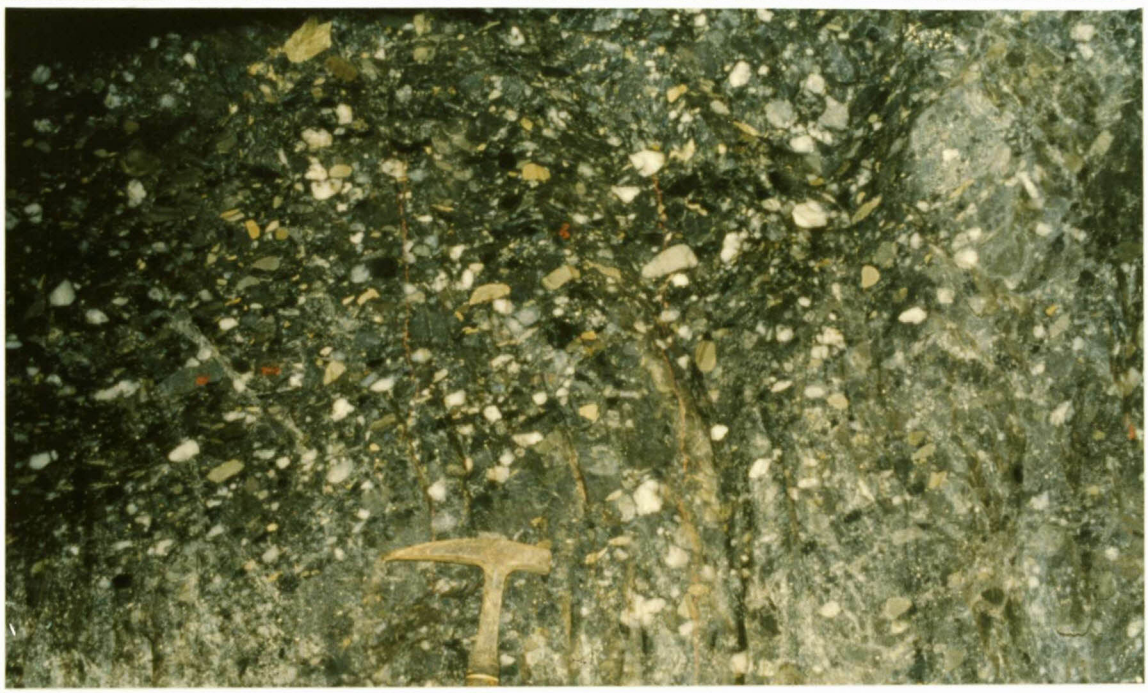

Plate VI.19. Locality 9, RDM : Note the immaturity of the conglomerate at this exposure.

Plate VI.20. Locality 9, RDM : Upon close-up investigation it can be seen that this conglomerate is matrix supported. (Total length of scale is 9cm)

Plate VI.21. Locality 11, RDM : Note the abundance of non-durable clasts in this exposure.

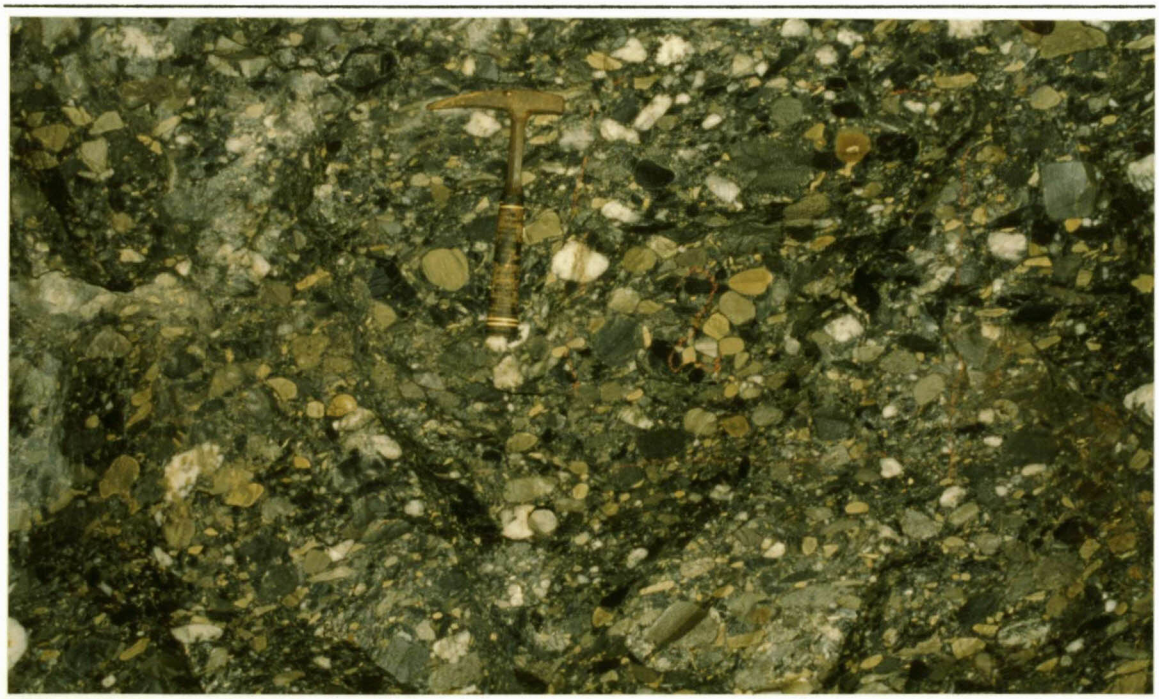

Plate VI.22. Locality 11, RDM : Close-up detail of exposure reveal that a large number of the yellow clasts are relatively well rounded.

VIII

PROVENANCE SYNTHESIS

In this chapter an attempt is made to deduce a probable provenance for the two conglomerate horizons studied, based on observations made and conclusions drawn in the preceding chapters. This postulated provenance model is then compared to existing terranes which probably could have acted as provenance, or represent a model(s) thereof, for the BPM and/or the RDM. The different clasts of rock types will be discussed individually, in context of source rock(s), before the total clast assemblage is viewed in context of provenance.

1. INDIVIDUAL ROCK TYPES

Since the clasts of the same rock type from the BPM and the RDM are normally indistinguishable, they are discussed together. Only where clasts from the BPM and the RDM display significant differences, are they discussed separately.

QUARTZITE

The most outstanding feature of the quartzite samples are their purity. The only other clastic constituent in the quartzites, apart from quartz grains, are a few chert grains occurring in some of the quartzite samples. The quartz grains are predominantly monocrystalline. Chert grain quantities were determined by estimation with the aid of the *Comparison Chart For Visual Percentage Estimation (After Terry and Chilingar, 1955)* (Scholle, 1979) and range from zero to a maximum of approximately 3%. Feldspars and other lithic grains are conspicuous in their total absence.

If these compositions are plotted on standard QtFL and QmFLt diagrams (after Dickinson, 1988), they all fall on the QtL and QmLt lines within three percentage points from the Qt and Qm = 100 points, respectively. From this it is clear that the provenance of the quartzites were continental block quartz-arenite sources on a stable craton (*Figure VII.1.*).

Monocrystalline quartz grains with non-undulatory extinction predominate in the quartzite clasts. According to Blatt *et al* (1980), volcanic rocks, hypabyssal rocks and hydrothermal rocks all yield such grains during weathering. Therefore the very nature of the quartz grains indicates that one or more of the rocks mentioned above, were the most probable source rock(s) for the quartz grains in the quartzite clasts.

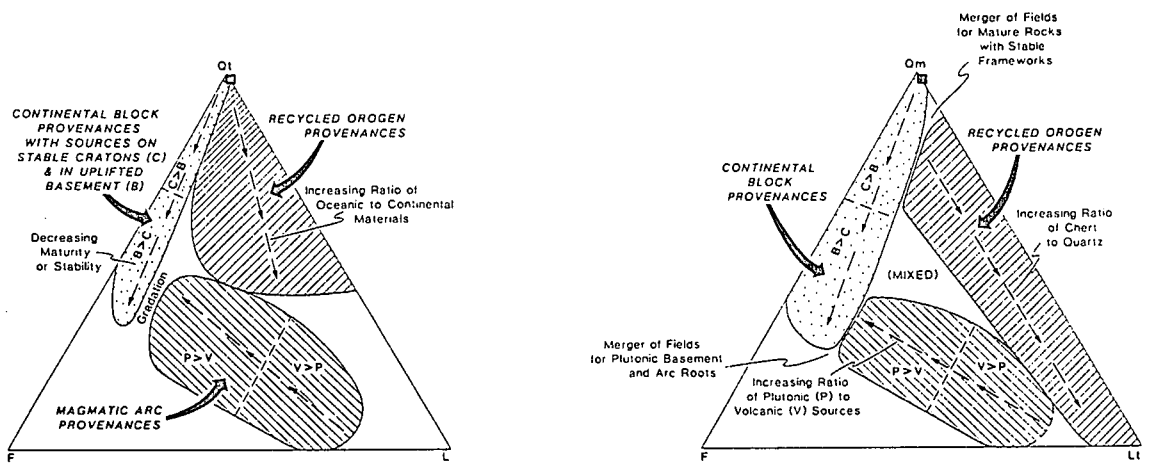

Fig. VII.1. Indicated provenance for the quartzite clasts from the BPM and RDM, as derived from average granular composition plotted on standard ternary diagrams (after Dickinson 1988).

▫ Average quartzite composition for BPM and RDM clasts
Qm Monocrystalline quartz grains
Qt Total quartzose grains
F Total monocrystalline feldspar grains
L Unstable lithic fragments
Lt Total polycrystalline lithic fragments

From *III.2.1.* and *III.2.2.* it is obvious that the quartzites derived from this once stable craton(s) underwent various degrees of deformation before deposition as clasts in the RDM and BPM.

QUARTZ

The origin of the quartz clasts cannot be deduced as unequivocally as that of the quartzite clasts. Despite the durability of the quartz clasts and their resulting relative "concentration" during transport and reworking, a very extensive source is indicated to supply such vast quantities of hydrothermally derived quartz (see *III.2.2.*) clasts, as encountered in the BPM and RDM.

The massive dimensions (up to 350mm in diameter) of quartz clasts occurring in the BPM and RDM (also see *Tables VI.5. and VI.6.*), indicate sizeable quartz deposits in the provenance. To facilitate the formation of such sources (size and volume) of hydrothermal quartz, the provenance must have been active, structurally and tectonically.

In some clasts an enhancement of certain trace elements occur. These particular elements (Bi, Pb, Sb, As, Cu, Ni, Co) are often associated with Au mineralization in greenstone terranes. Together with the well known relative abundance of quartz veins in greenstone terranes, this geochemical character provides strong evidence in favour of a greenstone provenance for the quartz clasts.

Theoretically, the so-called hydrothermally altered granites (HAGS) also qualify as a possible source of quartz clasts. Whether the HAGS are physically capable of supplying such large quartz clasts (as encountered in the BPM), is not documented. The description of the morphology and mineralogy of hydrothermal/quartz veins (Robb & Meyer, 1985

and Klemd & Hallbauer, 1987) encountered in the HAGS also differ substantially from that of the quartz clasts from the BPM and RDM. The quartz clasts from the BPM and RDM virtually consists of pure quartz, which occasionally contains pyrite (euhedral and amorphous). Veinlets and fracture-fill material in the HAGS, described by Robb and Meyer (1985), include carbonate-chlorite, quartz-pyrite, quartz-carbonate, quartz-carbonate-chlorite, quartz-carbonate-hematite-pyrite and fluorite-quartz-chlorite-pyrite-chalcopyrite. Apart from the quartz-pyrite association, none of these mineral associations were observed in the BPM or RDM clasts.

CHERT

Based on the macroscopic physical appearance and morphology of the chert clasts, no primary difference exists between the chert clasts of the BPM and the RDM. The only difference manifests itself in the geochemistry/mineralization of the clasts. Therefore it is accepted that the chert of the BPM and RDM clasts originated under similar conditions, but possibly in different provenances.

The microscopic physical differences between the dark chert from the BPM and the RDM mainly stem from the various forms of secondary and post-depositional alteration imprinted on the dark chert of the BPM, in its provenance (see *III.2.1.*). All these altered cherts from the BPM display enhanced Au values. Whether these alterations were responsible for the enhanced Au and compatible trace element values (see *Table V.2.*), is not clear. Two facts, however, provide evidence in support of the postulation that enhancement of Au concentrations in the chert did occur during alteration:

1. Secondary altered chert contains more secondary pyrite than unaltered chert.

2. Gold concentrations are enhanced in secondary altered dark cherts.

The average gold concentration in the dark chert clasts from the BPM is 218 p.p.b. (*Table V.1.*). The dark cherts from the RDM, which are all unaltered, also exhibit slightly enhanced average Au values (23 p.p.b.) compared to the average for cherts worldwide, which is 16 p.p.b. (Boyle 1979).

Another microscopic feature of the dark- and some of the banded chert clasts of the BPM, is the presence of carbonaceous material. This became evident during a microscopic re-investigation of the chert thin sections under reflected light. The carbonaceous material, which is indistinguishable from secondary pyrite under transmitted light, occur in intimate association with the disseminated secondary amorphous pyrite. The majority of the samples containing carbonaceous material (6 out of 9 samples) exhibit anomalous Au values (GI-0056 183 p.p.b., GI-0083 38 p.p.b., GI-0066 750 p.p.b., GI-0057 796 p.p.b., GI-0058 213 p.p.b., GI-0020 105 p.p.b.).

Although some of the brecciated chert clasts (see *III.2.1.*) contain disseminated secondary chert and/or carbonaceous material, they contain virtually no Au (GI-0018 0 p.p.b., GI-0019 0 p.p.b., GI-0089 1 p.p.b.). From this it appears that a definite correlation exists between Au mineralization, the presence of carbonaceous material, and secondary alteration.

Regarding the source and origin of the chert clasts, a microscopic study of them was inconclusive. It is, however, clear that the difference in pyrite and gold mineralization of the RDM and BPM clasts was inherited from their source rocks (see *III.2.2.*). Therefore different sources are indicated for the BPM and RDM chert clasts. This is

confirmed by the almost exclusive occurrence of carbonaceous material in the BPM chert clasts.

Although most Archaean chert (of the Swaziland Supergroup) was apparently derived from glassy volcanic detritus (Lowe & Knauth, 1977), the purity of the chert and the lack of included sericite, iron oxides, or coarse carbonate, suggest that the original sediment was not composed of volcanic detritus. The overall appearance of the chert clasts and the absence of current structures and textures suggests that they represent either very fine-grained, silicified deep-water suspension sediment or possibly primary silica accumulates. The banded cherts show several features in common with evaporites.

Available evidence indicates a greenstone terrane provenance for the chert clasts. Eriksson *et al*, (1988) described the occurrence of comparable black, white and banded chert clasts in the Gorge Creek Group of the Pilbara greenstone belt in Western Australia, as well as in the Fig Tree and Moodies Groups of the Barberton greenstone belt. According to them the provenance for the latter two groups was the underlying Onverwacht Group. Massive black chert units (up to 400m thick) occur in the Swartkoppie Formation of the Onverwacht Group. Brecciated chert clasts were recorded in the Moodies Group by Eriksson, (1978). Brecciated and banded chert deposits in the Hooggenoeg Formation of the Onverwacht Group (comparable to the BPM and RDM chert clasts), are described by Lowe & Knauth (1977).

According to these authors, evidence points to the deposition of these cherts in a variety of shallow-water and possibly evaporitic environments. They also concluded that the region was volcanically active but otherwise anorogenic. From the discussion above it is clear that the cherts of the BPM and RDM clasts were most probably derived from a

greenstone source, similar to those of the Onverwacht, Figtree and Moodies Groups, with the only exception being the absence of hydrothermal alteration in cherts of these latter groups.

IGNEOUS

The origin of the igneous clasts are enigmatic. All these clasts are highly siliceous, which is ascribed to secondary silicification. Consequently the study of these clasts are seriously impeded (see *III.2.1.*).

Gold is present in some of these clasts and one clast from the BPM yielded an anomalous concentration (GI-0062 750+ p.p.b.). If this single occurrence of an igneous clast, containing anomalous Au, can be ascribed to the well known "nugget effect" of gold, it would be valid to include this sample in the calculation of the mean gold value of the igneous clasts. This calculation yielded a mean value of 129 p.p.b. for the BPM igneous clasts, which is well above the mean value (12 p.p.b.) for igneous rocks (Boyle, 1979).

Cluster analysis distinguished two geochemical populations of igneous clasts, which may indicate two different source rock types. Clasts from both populations occur in the RDM, while the BPM contains clasts from one source only. It appears that the source for the BPM igneous clasts was relatively enriched in gold, compared to clasts from the RDM.

The general physical appearance of the igneous clasts compares very well with a description of lavas from the Renosterhoek Andesite Formation and especially the Syferfontein Porphyry Formation in the Dominion Group (Watchorn, 1980; Strydom, 1986). Both these authors also

point out that these lavas have undergone extensive *in situ* secondary silicification.

YELLOWS

From the preceding study of the yellow clasts no unequivocal conclusion concerning their origin or source could be reached. The mineral assemblages of the yellow and grey clasts are dominated by quartz, pyrophyllite and to a lesser extent chloritoid. Gold concentrations in these clasts are consistently low (average for all yellow clasts is 4 p.p.b.). From these studies it could, however, be concluded that the yellows in general represent only one population and could as such have been derived from one common, but extensive, source (see *III.2.1.* and *V.2.1.*).

Definite evidence of a sedimentary origin exists in some of these clasts and the general appearance of some of them are strongly reminiscent of some tuffaceous sediments. Although no concrete evidence to support this could be found (see *III.2.1.* and *III.2.3.*), some of these clasts yielded a Na/K ratio of ≥1 (see *Table V.3.*), which can be indicative of volcanic origin or contamination (Pettijohn, 1975). Pettijohn also concluded that if the particular rocks are altered by metamorphism, their original character may be greatly obscured.

All the yellows samples are strongly affected by secondary alteration and silicification. This could have obscured any possible evidence of volcanic origin. Hardness and apparent texture of these clasts probably are a function of this post-burial silicification, recrystallization and/or the presence of secondary euhedral chloritoid crystals present in some of the samples. Physical evidence (see *III.1.4.*) indicates a much shorter distance of transport for the yellows compared to the durable clasts. This implies different sources for the yellows and the durable clasts.

Virtually no reference of any material similar to the yellows clasts could be found in literature. Lowe & Knauth (1977) described the occurrence of brownish hematitic shale in the Swartkoppie Formation of the Onverwacht Group. This description is, however, too vague for comparison with the yellows clasts.

BLACK

No specific reference of any material comparable to the black clasts could be found in literature. The general paucity, relatively small dimensions and high degree of roundness of the black clasts (see *III.1.3.* and *III.1.4.*) all indicate extensive transport. The very fine-grained, homogeneous and non-laminated nature of these clasts indicate that they originated under very calm, stable and low-energy conditions.

Several authors (Pettijohn, 1975; Blatt, *et al*, 1980; Greensmith, 1981; etc.) noted the occurrence of black shales together with black cherts. Seen in the light of the above information and the lack of evidence indicating otherwise, it is proposed that the black clasts were derived from the same provenance as the dark cherts.

DARK SILTSTONE

From the literature, microscopic and geochemical studies on the dark siltstone clasts, no specific clues regarding their origin, source or provenance, could be found. In the clast size distribution study (*VI.2.1.*) evidence for the postulation of a different and more proximal source/provenance for the dark siltstone clasts, compared to both the yellows and durable clasts, can be found.

2. TOTAL CLAST ASSEMBLAGE

In an attempt to derive the provenance type from the total clast assemblage, the clast assemblage data (from *Table VI.4.*) were plotted on standard ternary QtFL, QpLvLs and QmFLt diagrams (after Dickinson, 1988). These diagrams are normally used to derive provenance from sandstone compositions. Therefore the definitions of the "end-members" of the diagrams had to be adapted for application of clast types, instead of grain types.

To delineate the modified system, the definitions for the symbols of the "endmembers" of the original system (Dickinson, 1988) are given (*Table VII.1.*), as well as the modified definitions (*Table VII.2.*).

Table VII.1. The original endmember definitions.

Qm	Monocrystalline quartz
Qp	Polycrystalline quartzose lithic fragments (including chert)
Qt	Total quartzose grains (Qm + Qp)
F	Total monocrystalline feldspar grains
L	Unstable lithic fragments
Lv	Volcanogenic lithic fragments (volcanic, metavolcanic, hypabyssal)
Ls	Sedimentary and metasedimentary lithic fragments (except chert and metachert)
Lt	Total polycrystalline lithic fragments (L + Qp)

Table VII.2. The modified endmember definitions.

Qm	Quartz
Qp	Quartz + Chert
Qt	Quartz + Chert + Quartzite
F	Igneous
L	Nondurables (yellows, blacks, dark siltstones)
Lv	Igneous
Ls	Quartzite + Nondurables
Lt	Quartzite + Nondurables + Chert

Using the data from *Table VI.4.*, the values for the modified endmembers were calculated. These values are given below in *Table VII.3.* The data from *Table V.3.* were used to calculate the percentage of sedimentary clasts of possible volcanigenic origin in the respective clast types. These values were then subtracted from the respective figures for the different clast types and added to the igneous component to yield the QpLvLs(B) values.

The calculated values (*Table VII.3.*) were then plotted on the respective standard ternary diagrams (*Figure VII.2.*).

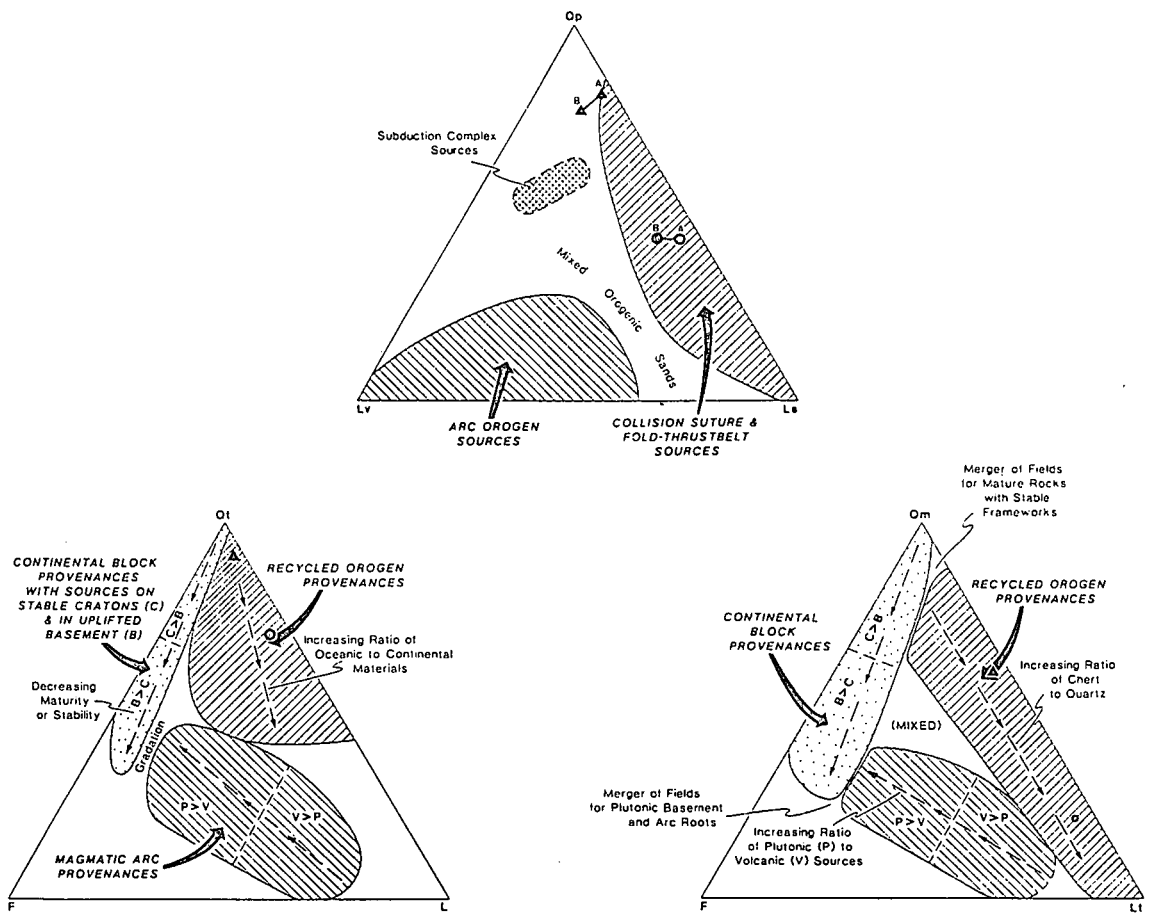

Fig. VII.2. Indicated provenance(s) for the BPM and RDM, as derived from clast assemblage plotted on modified ternary diagrams (after Dickinson 1988). ⚠ = Average BPM clast assemblage; ⏀ = Average RDM clast assemblage.

The QpLvLs plots indicate that the source of the RDM was a collision suture and fold-thrustbelt, while a mixed orogenic/collision suture and fold-thrustbelt source is indicated for the BPM. Both the QtFL and QmFLt plots indicate recycled orogen provenances for the BPM and RDM.

These indicated sources for the BPM and RDM are compatible with a foreland basin model for the Witwatersrand basin, as proposed by Winter (1986a, 1986b, 1987) and Burke, Kidd & Kusky (1986).

Table VII.3. Calculated values for the ternary diagrams.

DIAGRAM	FORMATION					
	BPM			RDM		
QtFL	89,8	3,0	7,2	67,9	5,1	27,0
QpLvLs(A)	81,5	3,0	15,5	42,7	5,1	52,3
(B)	77,2	9,7	13,1	42,7	8,8	48,5
QmFLt	61,5	3,0	35,5	21,2	5,1	73,7

3. PROVENANCES

In this section a few possible sources, which could have acted as a provenance, or represent a model of a probable provenance, are discussed very briefly in terms of similarities or disqualifying discrepancies regarding the BPM and RDM clast assemblage.

DOMINION GROUP

Strydom (1986) and Watchorn (1980) described silicified lavas in the Rhenosterhoek Andesite Formation and the Syferfontein Porphyry Formation, which compare favourable with the general description of the igneous clasts. The

quartzites in the Dominion Group, however, contain too much sericite to compare with the BPM and RDM quartzite clasts.

WEST RAND GROUP

On occasion (Vos, 1975 & Pretorius, 1981, 1989), the West Rand Group was proposed as a provenance for the Central Rand Group. Theoretically the West Rand Group constitutes an ideal source for non-durable, as well as durable clasts. The quartzite clasts from the BPM and RDM are comparable with some quartz-arenites in the West Rand Group, for example the Hospital Hill Quartzites.

KRAAIPAN FORMATION

Investigations of overlying sediments (conglomerates in the Bosch Kop Formation) revealed that Kraaipan detritus were transported to the east (SACS, 1980). However, though cherty sediments are described in the Kraaipan Formation, no general similarities between RDM/BPM clasts and Kraaipan rocks could be found.

HAGS

HAGS featured strongly in recent provenance models for the gold in the Witwatersrand Supergroup. No evidence of HAGS-related clasts could, however be found in the BPM or RDM. Descriptions of hydrothermal veins (Robb & Meyer, 1985 and Klemd & Hallbauer, 1987) in proposed HAGS provenances also differ completely from hydrothermally derived clasts in the BPM and RDM (see *VII.1.*). The capability of HAGS to yield pure quartz clasts as big as those encountered in the BPM (see *Table VI.5*) is perhaps not impossible, but nevertheless, questioned.

ENDOGENOUS GOLD SOURCE

The model, proposed by Hutchinson and Viljoen (1988), according to which the source of the Witwatersrand gold is endogenous within the Witwatersrand Basin, implicates a tensional regime and "basin-edge" faults along the periphery of the basin. Evidence obtained in the present study, however, indicate a compressional regime (orogenic/collision suture and fold-thrustbelt source) in the provenance of the BPM and RDM (see *VII.2.*). It can also be noted that Brink (1986) pointed out that he could find no evidence of peripheral faulting in the western and northwestern parts of the Witwatersrand Basin.

LIMPOPO MOBILE BELT

The composition of the proposed protolith of the Beitbridge Complex, described by Eriksson *et al* (1988), is very compatible with the general clast assemblage of the BPM and RDM. Similarities include: "few, if any, volcanic rocks" and the occurrence of quartz arenite and mudstone. According to interpretations made by Burke *et al* (1986) the Southern Limpopo Province was tectonically in the right position to act as provenance for the Witwatersrand Supergroup. West to east transport directions for the BPM, RDM and other reefs in the Welkom area, as well as extensive transport distances invoked, however, virtually precludes this possibility.

GREENSTONE TERRANES

Substantial evidence exist to support the possibility of a greenstone-type provenance for the BPM and RDM (*V.2.1. and VII.1.*). In this regard the similarities between greenstone derived clasts (Lowe & Knauth, 1977) and the BPM and RDM clasts (see *VII.1.*) are perhaps the most compelling. Elemental associations, particularly in the chert and quartz clasts, also support a greenston-type provenance.

4. GEOCHEMICAL CONSIDERATIONS

If the average Au content of the different rock types (*Table V.1.*) and the modal compositions of the BPM and RDM (*Table VI.4.*) are used to calculate the weighted average Au content for the BPM and RDM provenances (*Table VII.4.*), it can be seen that these provenances were enriched in Au by factors of approximately 30X and 5X respectively, compared to typical Archaean granitoids from the Barberton region (2,5 p.p.b) (Saager & Meyer, 1984), or Barberton-type granite-greenstone crust (2,4 p.p.b.) (Robb & Meyer, 1985). Compared to the value of 6 p.p.b., above which most granites are regarded as being enriched (Meyer *et al*), the respective factors are approximately 13X and 2X.

Table VII.4. Calculation of the proposed average Au contents of the postulated BPM and RDM provenances (Au values - ppb).

FMN		IGNEO	HYDRO	CHSED	ARSED	AGSED	AVE	A-GS	A-GR
BPM	MOD COMP	3,0%	61,6%	20,0%	8,2%	7,3%	**76,4**	2,4	6,0
	AVE Au	129,0	70,3	143,2	4,8	2,5			
RDM	MOD COMP	5,1%	21,2%	21,5%	25,2%	26,7%	**11,8**	2,4	6,0
	AVE Au	5,6	15,0	15,3	15,1	4,6			

FMN - FORMATION
IGNEO - IGNEOUS
HYDRO - HYDROTHERMAL (quartz)
CHSED - CHEMICAL SEDIMENT (chert)
ARSED - ARENACEOUS SEDIMENT (quartzite)
AGSED - ARGILLACEOUS SEDIMENT (yellow, black & siltstone)
AVE - WEIGHTED AVERAGE (Au) FOR PARTICULAR FORMATION
A-GS - AVERAGE Au CONTENT FOR BARBERTON GRANITE-GREENSTONE
A-GR - THRESHOLD VALUE FOR ANOMALOUS Au IN NORMAL GRANITES
MOD COMP - MODAL COMPOSITION
AVE Au - ARITHMETIC MEAN Au CONTENT FOR ROCK TYPE

These figures clearly stress the uniqueness of the gold enriched source rocks of the Witwatersrand in general (also

see the concluding paragraph under *I.6.*). The most significant implication of this fact is, however, the impact the above figures have on existing mass-balance equations and calculations (eg. Reimer, 1984; Robb & Meyer, 1985; De Waal, 1986). Such calculations may, however, not be reliable.

VIII

CONCLUSIONS

In this final chapter, a summary of the most important conclusions drawn during the course of this study, is given.

1. INDIVIDUAL CLAST TYPES

Distinction between dark and white quartz is rather arbitrary, because it appears that some white quartz clasts is in the process of being converted *in-situ* into dark coloured-quartz. A few important facts, nevertheless, emerged from the study of the quartz clasts. The abundance of the fluid inclusions in the quartz clasts probably indicates a hydrothermal origin for the quartz, while all observations suggest that the deformation observed in some quartz clasts, must have occurred in the source area, before deposition of the clasts. Both these facts indicate that the provenance of the quartz clasts must have been active, structurally and tectonically. Finally, strong evidence, indicating a greenstone provenance for the quartz clasts, exist.

No significant geochemical differences exist between the light- and dark-coloured quartzite clasts from either the BPM or the RDM and again, the event(s) responsible for the deformation, observed in some of the quartzite clasts, are indicated to have occurred in the source area, before deposition of the clasts in the conglomerates. The origin of the quartzites were continental block provenances with sources on stable cratons.

The cherts of the BPM and RDM clasts originated under similar conditions, but possibly in different provenances. Pyrite mineralization in the chert clasts was inherited from the provenance. Anomalously high Au values (on average, up to 9X that of the international value for chert) occur in the majority of chert clasts, especially those from the BPM. The chert clasts also yielded the highest average Au values of all the rock types studied. A conspicious feature of the dark (and some of the banded) chert clasts from the BPM, is the occurrence of microscopic carbonaceous material. The majority of these chert clasts exhibit anomalous Au values as well. A definite correlation between Au mineralization and the presence of carbonaceous material, as well as secondary alteration, exists in the chert clasts. Available evidence favour a greenstone-type provenance for the chert clasts.

The igneous component of the total clast assemblage for both the BPM and RDM is very small (3,0% and 5,1% respectively). The igneous clasts have a geochemical composition, very similar to the yellows.

All the "yellows" and "greys" clasts form one population. Evidence, indicating a sedimentary origin for the yellows, can be observed in some of these clasts and in general they conform to descriptions of altered vitric tuff.

2. CLAST DERIVATION AND TRANSPORT

Different physical conditions, which controlled the initial clast size, at the time of their derivation, prevailed in the provenances of the BPM and the RDM, while different transport conditions/mechanisms also prevailed during the deposition of the BPM and the RDM. Evidence suggests that the material deposited in the BPM was probably transported

over a longer distance than the material deposited in the RDM.

Physical evidence indicate a much shorter distance of transport for the yellows, compared to that of the durable clasts. Different sources for the yellows and the durable clasts are therefore indicated. A different and more proximal source/provenance, compared to both the yellows and durable clasts, is proposed for the dark siltstone clasts, while it is proposed that the black clasts were derived from the same provenance as the dark chert clasts.

3. METAMORPHISM

All the clasts had undergone various degrees of alteration, in particular silicification. The main difference between the respective nondurable clast types manifests itself in the Si content. The fact that secondary chloritoid crystals occur in a penetrative habit, in both clasts and matrix, indicates that the metamorphism was a post-depositional event.

The compositions of the fluids in the inclusions, studied in the quartz clasts, and their general homogeneity, indicate that the majority of the inclusions contain fluids which played major roles during diagenesis and metamorphism of the clasts, rather than representing the provenance(s).

4. PROVENANCE COMPOSITION

The compositions of the provenance(s) for the BPM and the RDM were different. Clasts from the RDM appears to be relatively enriched in incompatible trace elements, such as Rb, Sr, Ba and Zr, compared to clasts of the BPM. A more

mafic source is proposed for the BPM, compared to that of the RDM. Strong, to anomalous, enhancement of average gold values is indicated for some of the source rocks of the BPM. Chemical sediments (chert) constituted a significant (±21%) component of the provenances of both the BPM and RDM.

The BPM consists of 92,7% durable and 7,3% non-durable clasts and quartz clasts, with an average incidence of 61,5%, dominate the clast assemblage of the BPM. The provenance(s) of the BPM either contained a large hydrothermal component, but a rather small argillaceous sedimentary component, or the argillaceous component was largely destroyed during relatively extensive transport and/or reworking over a larger distance.

The RDM is comprised of virtually equal amounts of quartz, chert, arenaceous sediments (quartzite) and argillaceous sediments (yellows, blacks and dark siltstone). The provenance(s) of the RDM contained a large sedimentary component, and probably had a more local source, compared to the BPM.

5. PROVENANCES

Some sediment clasts yielded a Na/K ratio of ≥1, indicative of volcanic origin or contamination. No evidence of HAGS-related clasts could be found in either the BPM or RDM. However, evidence in this study support a greenstone-type provenance, probably associated with hydrothermal activity, for the BPM and RDM.

QtFL and QmFLt (for definitions see VII.2) plots indicate thrust belt and recycled orogenic provenances for the BPM and RDM. These indicated sources for the BPM and RDM are

compatible with a foreland basin model for the Witwatersrand basin.

6. MINERALIZATION

Some high Au values encountered in quartz clasts, during this study, were accompanied by similarly enhanced values of some other elements like Pb, As, Cu, Ni, and Co. This elemental association also occurs with Au mineralization in the better mineralized chert samples. Au mineralization in the clasts is, however, not always associated with this particular association of elements.

Although the source rocks of the BPM were far more (± 6X) auriferous than those of the RDM, both these sources were substantially enriched in gold. Compared to typical Archaean granitoids from the Barberton region (2,5 p.p.b.), or Barberton-type granite-greenstone crust (2,4 p.p.b.), the BPM and RDM provenances were enriched in Au by factors of approximately 30X and 5X respectively. Compared to the value of 6 p.p.b., above which most granites are regarded as being enriched, the respective enrichment factors are still approximately 13X and 2X.

The most significant implication of this fact is, however, the impact such figures have on mass-balance equations and calculations, which may imply that many of these calculated figures are significantly miss-calculated and inaccurate.

IX

REFERENCES

Allen, P.A. & Homewood, P. (1986). *Foreland Basins*. Spec. Publn. int. Ass. Sedimentologists, **8**, Blackwell Scientific Publications, Oxford, 453 pp.

Angus, S., Armstrong, B., de Reuck, K.M., Altunin, V.V., Gadetskii, O.G. Chapela, G.A., & Rowlinson, J.S. (1976). *International Thermodynamic Tables of the Fluid State, Vol. 3, Carbon Dioxide*. Pergamon Press, 385 pp.

Antrobus, E.S.A. (1956). The origin of auriferous reefs of the Witwatersrand system. *Trans. geol. Soc. S. Afr.*, **59**, 2 - 22.

Blatt, H., Middleton, G. & Murray, R. (1980). *Origin of Sedimentary Rocks*, 2nd Edn. Prentice-Hall, Inc., New Jersey, 782 pp.

Bowers, T.S. & Helgeson, H.C. (1983). Calculation of the thermodynamic and geochemical consequences of nonideal mixing in the system H_2O-CO_2-NaCl on phase relations in geologic systems: Equation of state for H_2O-CO_2-NaCl fluids at high pressures and temperatures. *Geochim. Cosmochim. Acta*, **47**, 1247 - 1275.

Boyle, R.W. (1979). *The Geochemistry of Gold and its Deposits*. Geological Survey of Canada, Ottawa, 579pp.

Brink, M.C. (1986). *Tektoniese en stratigrafiese ontwikkeling van die Witwatersrand Supergroep en verwante gesteentes in die gebied noord en oos van Klerksdorp.* D.Sc. proefskrif (ongepubl.), Randse Afr. Univ., 317 pp.

Burke, K., Kidd, W.S.F. & Kusky, T.M. (1985). Is the Ventersdorp Rift System of Southern Africa Related to a Continental Collision Between the Kaapvaal and Zimbabwe Cratons at 2,644 Ma ago? *Tectonophysics*, 115, 1 - 24.

Burke, K., Kidd, W.S.F. & Kusky, T.M. (1986). Archean Foreland Basin Tectonics in the Witwatersrand, South Africa. *Tectonics*, 5, 439 - 456.

Carozzi, A.V. (1960). *Microscopic Sedimentary Petrography.* John Wiley & Sons, Inc., New York, 485 pp.

Collins, P.L.F. (1979). Gas hydrates in CO_2-bearing fluid inclusions and the use of freezing data for estimating salinity. *Econ. Geol.*, 74, 1435 - 1444.

Conover, W.J. (1980). *Practical Nonparametric Statistics*, 2nd Edn. John Wiley & Sons, New York, 493 pp.

Crawford, M.L. (1981). Phase equilibria in aqueous fluid inclusions. *In*: Hollister, L.S. & Crawford, M.L., Eds., *Short Course in Fluid Inclusions: Applications to Petrology.* Mineralog. Ass. Can., 6, 75 - 100.

De Waal, S.A. (1986). A Mass-Balance Equation for the Witwatersrand Sediments and an Archaean Provenance. *Ext. Abst. Geocongr. '86, Geol. Soc. S. Afr.*, Johannesburg, 107 - 108.

Deer, W.A., Howie, R.A. & Zussman, J. (1974). *An Introduction to the Rock-forming Minerals.* Longman, London, 528 pp.

Dhamelincourt, P. (1979). *étude et réalisation d'une microsonde moléculaire à effet Raman. Quelques domaines d'application.* Thèse l'Univ. des Sciences et Techniques de Lille.

Dickinson. W.R. (1985). Interpreting Provenanance Relations from Detrital Modes of Sandstones. *In* Zuffa, G.G. Ed. *Provenance of Arenites.* D. Reidel Publishing Company, 333 - 361.

Dickinson, W.R. (1988). Provenance and Sediment Dispersal in Relation to Paleotectonics and Paleogeography of Sedimentary Basins. *In* Kleinspehn, K.L. & Paola, C., Eds. *New Perspectives in Basin Analysis.* Springer-Verlag, New York, 3 -25.

Dunlop, J.S.R. (1981). Shallow-water Sedimentation at North Pole, Pilbara, Western Australia. *In* Glover, J.E. & Groves, D.I. Eds. *Archaean Cherty Metasediments: Their Sedimentology, Micropalaeontology, Biogeochemistry and Significance to Mineralization.* The University of Western Australia, Perth, 88 pp.

Elsmere, D.(1987). *The characteristics of fluid inclusions in the metamorphites and mineralized rocks of the Boksputs region, Upington.* M.Sc. thesis (unpubl.), Univ OFS., 101 pp.

Eriksson, K.A. (1978). Alluvial and Destructive Beach Facies From the Archaean Moodies Group, Barberton Mountain Land, South Africa and Swaziland. *In* Miall, A. D. *Fluvial Sedimentology.* Can. Soc. Petrol. Geol. Mem. 5, 859 pp.

Eriksson, K.A., Kidd, W.S.F. & Krapez, B. (1988). Basin Analysis in Regionally Metemorphosed and Deformed Early Archean Terrains: Examples from Southern Africa and Western Australia. *In* Kleinspehn, K.L. & Paola, C., Eds. New perspectives in Basin Analysis. Springer-Verlag, New York, 371 - 404.

Everitt, B. (1974). *Cluster Analysis.* Heineman Educational Books Ltd., London, 122 pp.

Fisher, J.R. (1976). The volumetric properties of H_2O - a graphical portayal. *J. Res. U.S. Geol. Surv.*, 4, 189 - 193.

Fisher, R.V. & Schmincke, H.-U. (1984). *Pyroclastic Rocks.* Springer-Verlag, Berlin, 472 pp.

Frantz, J.D., Mao, H.K., Zhang, Y., Wu, Y., Thompson, A.C., Underwood, J.H., Giauque, R.D. Jones, K.W. & Rivers, M.L. (1988). Analysis of fluid inclusions by X-ray fluorescence using synchrotron radiation. *Chem. Geol.*, 69, 235 - 244.

Greensmith, J.T. (1981). *Petrology of the Sedimentary Rocks*, 6th Edn. George Allen & Unwin, London, 241 pp.

Halferdahl, L.S. (1961) Chloritoid : Its Composition, X-Ray and Optical Properties, Stability and Occurence. *J. Petrol.*, 2, 49 - 135.

Hall, D.L., Sterner, M.S. & Bodnar, R.J. (1988). Freezing point depression of NaCl-KCl-H_2O solutions. *Econ. Geol.*, **83**, 197 - 202.

Hallbauer, D.K. (1982). A review of some aspects of the geochemistry of the Witwatersrand gold deposits. *In* Glen, H.W., Ed., *Proc., 12th CMMI Congress. S. Afr. Inst. Min. Metall., Johannesburg*, 957 - 964.

Hallbauer, D.K. (1984). Archaean granitic sources for the detrital mineral assemblage in Witwatersrand conglomerates. *Ext. Abstr. Geocongress '84, Potchefstroom, geol. Soc. S. Afr.*, 53 - 56.

Hallbauer, D.K. & Kable, E.J.D. (1982). Fluid Inclusions and Trace Element Content of Quartz and Pyrite Pebbles from Witwatersrand Conglomerates: Their Significance with Respect to the Genesis of Primary Deposits. *In* Amstutz G.C., El Goresy, A., Frenzel, G., Kluth, C., Moh, G., Wauschkuhn, A. & Zimmermann, R.A., Eds. *Ore Genesis.* Springer-Verlag, Berlin, 742 - 752.

Hallbauer, D.K., Von Gehlen, K., Kable, E.J.D., & Bühmann, D. (1986). The geochemistry and mineralogy of some mineral components in Witwatersrand conglomerates and their use in delineating facies and correlating strata. *Ext. Abstr. Geocongress '86, Johannesburg, Geol. Soc. S. Afr.*, 139 - 144.

Hurlbut, C.S. & Klein, C. (1977). *Manual of Mineralogy* (after J.D. Dana), 19th Edn. John Wiley & Sons, New York, 532 pp.

Hutchinson, R.W. & Viljoen, R.P. (1988). Re-evaluation of gold source in Witwatersrand ores. *S. Afr. Journ. Geol.*, **91**, 157 - 173.

Jordaan, M.J. (1986). The depositional framework of the Kimberley Placers in the Welkom Goldfield. *Ext. Abstr. Geocongress '86, Johannesburg, Geol. Soc. S. Afr.*, 456 - 459.

Kerr, P.F. (1977). *Optical Mineralogy*, 4th Edn. McGraw-Hill, New York, 492 pp.

Kingsley, C.S. (1986). Stratigraphic framework and model of sedimentation of the Eldorado sequence in the Welkom Goldfields. *Ext. Abstr. Geocongress '86, Johannesburg, Geol. Soc. S. Afr.*, 461 - 464.

Kingsley, C.S. (1987). Facies changes from fluvial conglomerate to braided sandstone of the early Proterozoic Eldorado Formation, Welkom Goldfield, South Africa. *In* Ethridge, F.G., Flores, R.M. & Harvey, M.D., Eds. *Recent developments in Fluvial Sedimentology.* Soc. econ. Paleont. & Miner. spec. Publn., **39**. 359 - 370.

Klemd, R. & Hallbauer, D.K. (1987). Hydrothermally altered peraluminous Archaean granites as a provenance model for Witwatersrand sediments. *Mineralium Deposita.* **22**, Springer-Verlag, 227 - 235.

Kleynhans, J.J. (1970). *A sedimentological study of the conglomerates in the Elsburg Stage on the Welkom and Western Holdings mines.* M.Sc. thesis (unpubl.), Univ. OFS., 139 pp.

Lowe, D.R. & Knauth, L.P., (1977). Sedimentology of the Onverwacht Group (3.4 Billion Years), Transvaal, South Africa, and its Bearing on the Characteristics and Evolution of the Early Earth. *Journ. Geol.* **85**, 699 - 723.

Mel'nik, Y.P. (1982). *Precambrian Banded Iron-Formations.* Elsevier, Amsterdam, 310 pp.

Meyer, M., Oberthur, Th., Robb, L.J., Saager, R. & Stupp, H.D. (1985). Ni, Co and Au contents of pyrites from Archaean granite-greenstone terranes and early Proterozoic sedimentary deposits in southern Africa. *Inform. Circ. Econ. Geol. Res. Unit, Univ. Witwatersrand, Johannesburg*, **176**, 11 pp.

Pettijohn, F.J. (1975). *Sedimentary Rocks*, 3rd Edn. Harper & Row, New York, 628 pp.

Pettijohn, F.J., Potter, P.E. & Siever, R. (1987). *Sand and Sandstone*, 2nd Edn. Springer-Verlag, New York, 553 pp.

Pirrson, L.V. (1915). The Microscopical Characters of Volcanic Tuffs - a Study for Students. *Am. J. Sc. Ser. 4.*, **40**, 191 - 211.

Pretorius, D.A. (1981). Gold and Uranium in Quartz-Pebble Conglomerates. *75th Anniv. Vol. Economic Geology*, 117 - 138.

Pretorius, D.A. (1989). The sources of Witwatersrand gold and uranium : 'a continued difference of opinion'. *Inform. Circ. Econ. Geol. Res. Unit, Univ. Witwatersrand, Johannesburg*, **206**, 43 pp.

Redlich, O. & Kwong, J.N.S. (1949). On the thermodynamics of solutions, V: An equation of state. Fugacities of gaseous solutions. *Chem. Rev.*, **44**, 233 - 244.

Reimer, T.O. (1984). Alternative model for the derivation of gold in the Witwatersrand Supergroup. *J. geol. Soc. London*, **141**, 263 - 272.

Robb, L.J. & Meyer, M. (1985). The nature of the Witwatersrand hinterland : Conjectures on the source-area problem. *Inform. Circ. Econ. Geol. Res. Unit, Univ. Witwatersrand, Johannesburg*, **178**, 25 pp.

Roeder, E. (1984). *Fluid Inclusions. Reviews in mineralogy, 12.* Mineralog. Soc. Am., 643 pp.

Roeder, E. & Bodnar, R.J. (1980). Geologic pressure determinations from fluid inclusion studies. *Ann. Rev. Earth Planet Sci.*, **8**, 263 - 301.

Saxena, S.K. & Fei, Y. (1987). Fluids at crustal pressures and temperatures. I. Pure species. *Contrib. Miner. Petrol.*, **95**, 370 - 375.

Scholle, P.A. (1979). *Constituents, Textures, Cements, and Porosities of Sandstones and Associated Rocks.* Mem. 28, Am. Ass. Petrol. Geologists, Tulsa, U.S.A., 201 pp.

Sims, J.F.M. (1969). *The stratigraphy and paleocurrent history of the upper division of the Witwatersrand System on the President Steyn mine and adjacent areas in the Orange Free State Goldfield with specific reference to the origin of auriferous reefs, Vol. I & II.* Ph.D. thesis (unpubl.), Univ. Witwatersrand, Johannesburg, 181 pp.

Skinner, B.J. & Merewether, P. (1986). Genesis of the Witwatersrand ores : Evidence versus prejudice. *Ext. Abstr. Geocongress '86, Johannesburg, Geol. Soc. S. Afr.*, 81 - 83.

South African Committee for Stratigraphy (SACS), (1980). Stratigraphy of South Africa. Part 1 (Comp. L.E. Kent). Lithostratigraphy of the republic of South Africa, South West Africa/Namibia, and the Republics of Bophuthatswana Transkei and Venda: *Handb. geol. Surv. S. Afr.*, 8.

Spry, A. (1969). *Metamorphic Textures*. Pergamon Press, Oxford, 350 pp.

Strydom, P.M. (1986). The Rocks of the Witwatersrand Triad in the Klerksdorp Goldfield. *In Field guide, Geocongress '86, Johannesburg, Geol. Soc. S. Afr.*, 15 pp.

Takehara, M.O.H. (1970). *Revised Standard Soil Color Charts*. Research Council for Agriculture, Forestry, and Fisheries, Japan.

Takenouchi, S. & Kennedy, G.C. (1964). The binary system H_2O-CO_2 at high temperatures and pressures. *Am. J. Sci.*, 262, 1055 - 1074.

Tödheide, K. & Franck, E.U. (1963). Das Zweiphasengebied und die Kritische Kurve im System Kohlendioxid-Wasser bis zu Drucken von 3500 bar. *Zeits. Phys. Chem. Neue Folge*, 37, 387 -401.

Van den Kerkhof, A.M. (1988). *The system CO_2-CH_4-N_2 in fluid inclusions: theoretical modeling and geological applications*. Ph.D. thesis, Vrije Univ. te Amsterdam. Free University Press, 206 pp.

Van Houten, F.B. (1982). Ancient Soils and Ancient Climates. *In* Climate in Earth History, *Studies in Geophysics*. National Acadamy Press, Washington, D.C., 112 - 117.

Viljoen, R.P. (1967). The composition of the Main Reef and Main Reef Leader Conglomerate horizons in the northeastern part of the Witwatersrand basin. *Inform. Circ. Econ. Geol. Res. Unit, Univ. Witwatersrand, Johannesburg*, **40**, 54 pp.

Vos, R.G. (1975). An Aluvial Plain and Lacustrine Model for the Precambrian Witwatersrand Deposits of South Africa. *J. Sediment. Petrol.*, **45**, 480 - 493.

Watchorn, M.B. (1980). Continental Sedimentation and Volcanism in the Dominion Group of the Western Transvaal : A Review. *Inform. Circ. Econ. Geol. Res. Unit, Univ. Witwatersrand, Johannesburg*, **146**, 8 pp.

Whitten, D.G.A. & Brooks, J.R.V. (1979). *The Penguin Dictionary of Geology*. Penguin Books Ltd, Middlesex, England, 495 pp.

Winter, H. de la R. (1964a). The geology of the northern section of the Orange Free State Goldfield, *In:* Haughton, S.H., Ed., *The Geology of Some Ore Deposits in Southern Africa, Vol I.* Geol. Soc. S. Afr., 417 - 448.

Winter, H. de la R. (1986a). Cratonic Foreland Model for Witwatersrand Basin development in a Continental Back-Arc Plate-Tectonic Setting. *Ext. Abst. Geocongr. '86, Geol. Soc. S. Afr.*, Johannesburg, 75 - 80.

Winter, H. de la R. (1986b). Cratonic Foreland Model for Witwatersrand Basin development in a Continental, Back-Arc Plate-Tectonic Setting. *Inform. Circ. Econ. Geol. Res. Unit, Univ. Witwatersrand, Johannesburg*, **193**, 36 pp.

Winter, H. de la R. (1987). A Cratonic Foreland Model for Witwatersrand Basin development in a Continental Back-Arc, Plate-Tectonic Setting. *S. Afr. J. Geol.*, **90**, 409 - 427.

Zussman, J. (1977). X-ray Diffraction. *In* Zussman, J. Ed. *Physical Methods in Determinative Mineralogy*, 2nd Edn. Academic Press, London, 391 - 473.

x

ACKNOWLEDGEMENTS

The author hereby whish to acknowledge and express his appreciation towards the following persons and organizations for their valued contribution to this study:

Anglo American Prospecting Services (Pty) Limited for the research grant which made this study possible.

The South African Development Trust Corporation Limited for granting me study leave to carry out this study.

Professor N.J. Grobler, at that stage of the UOFS, the study leader of this project, for his guidance and organization.

Doctor C.S. Kingsley of AAPS, project supervisor, for guidance and practical arrangements with various organizations and mines in the Anglo American Corporation Group to facilitate this study.

Management, personnel and officials of the various mines I visited during the course of the investigation for their contribution.

Amglo American Research Laboratories for analysis of samples.

Mr A.K. Kenyon of AARL for his contribution towards the statistical manipulation and interpretation of analysis data.

The **Regional Office of AAPS in Welkom** for provision of certain plans and drafting thereof.

Professor G.J. Beukes of the Geology Department of the OFS for assistance with the XRD-analysis of samples and interpretation of the results.

Doctor H. de Bruiyn for micron probe analyses and electron microscope photographs.

Professor A.E. Schoch and **Mrs D. Elsmere** of the Fluid Inclusion Unit of the Geology Department of the OFS for the fluid inclusion study.

My valued friend **Gert Meintjes** who was always willing to help me to solve my computer problems.

Mr A. Felix for drafting of maps and figures.

All my colleagues and personnel of the **Geology Department of the OFS** for constructive comments and help in whatever way.

Friends and family for encouragement and moral support.

XI

LIST OF FIGURES

II

LIST OF TABLES

XIII

LIST OF PLATES

XIV

LIST OF APPENDICES

XV

APPENDICES

APPENDIX 1.

REPORT ON FLUID INCLUSION STUDY

REPORT ON MICROTHERMOMETRIC STUDY OF SAMPLES SUBMITTED BY PROF N.J. GROBLER AND MR J.M.A. STEENEKAMP

BY

A.E. SCHOCH, D. ELSMERE &
J. DU BOIS

OCTOBER 1989

TRANSLATED BY: J.M.A. STEENEKAMP

REPORT ON MICROTHERMOMETRIC STUDY OF SAMPLES SUBMITTED BY PROF N.J. GROBLER AND MR J.M.A. STEENEKAMP

INTRODUCTION

Four samples of quartz pebbles from conglomerates in the Witwatersrand Supergroup were submitted during August 1989. The samples represent dark-coloured quartz (samples FWS 16/2 and FWS 79) and light-coloured quartz (samples 27/2 and FWS 78). The aim of the study was to determine the composition and probable genesis of the fluid inclusions in the quartz and, especially, the distinctive microthermometric properties of the colour varieties.

Doubly polished thick sections of all the samples were prepared. The microthermometric study was done with the aid of two calibrated Chaixmeca instruments. All measurements were duplicated and only readings which corresponded within acceptable margins, were accepted (± 0,2°C for the range -185°C to 30°C in cooling mode, and ± 8°C for the range 30°C to 400°C in heating mode).

COMPOSITIONAL VARIATION

Application of the recently developed direct microanalytical methods (Raman microprobe: Dhamelincourt 1979, van den Kerkhof 1988; XRF induced by microfocused synchrotron radiation: Frantz *et al.* 1988), is expensive and can only be applied to comparatively large fluid inclusions which may not be typical of prevalent fluid populations. Because most fluid inclusions are too small for direct analysis and because the high-energy apparatuses are not generally available, the compositions are deduced from physical properties. The most useful physical property for compositional modelling is melting temperature (Tm). Only one-component systems have singular melting temperatures; complex (natural) systems are characterized by melting ranges. In ideal circumstances the entire melting range can be determined, starting with the eutectic melting temperature (Tm_e or Te) which identify the applicable model system. A melting range ends with the final melting temperature (Tm_f), which reflects the composition (suppression owing to solutes).

Variation in composition was determined by recording Tm of individual fluid inclusions. Although discrete carbon dioxide inclusions are present in one sample (FWS 79) only, evidence of ice which melts at comparative high temperatures

(> 0°C) was found in the aqueous inclusions of all the samples. This phenomenon is interpreted as clathrate ice, $CO_2.5,75H_2O$, indicating the presence of carbon dioxide. This interpretation is also confirmed by the presence of fluid inclusions containing visible immiscible fluid couplettes. The amount of carbon dioxide is appreciably less than the co-existing water, however.

The most abundant solute in natural fluids is NaCl. The composition of fluid inclusions is normally, as a first approximation, interpreted in terms of the system H_2O-NaCl. The values are given as weight percent eNaCl (NaCl-equivalent). In ideal circumstances the total melting range can be observed and the appropriate phase system can be derived from the eutectic melting temperature. For H_2O-NaCl, Te = -20,6°C and for H_2O-NaCl-KCl, Te = -22,8°C. The composition (% eNaCl) is then reflected in the final melting temperature (Tm_f). However, when a significant amount of carbon dioxide is present, in the system H_2O-NaCl-CO_2, two discrete final melting temperatures have to be considered. The formation of clathrate ice causes an inordinate rise in the salinity of the corresponding water ice. As a result, the Tm_f of the water ice will not be a reliable indicator of the solute percentage. The melting temperature of the clathrate ice is, however, a sensitive indicator of total salinity (Collins, 1979).

Accumulative melting temperature data for all the samples are summarized in Fig. 1. The principal peak at -1°C represents pure water for which discussion will be momentarily deferred. The accumulative clathrate peak is at +2,5±0,5°C, but exhibits a broad spread of ±3°C. According to the data of Collins (1979), it represents 13,5±0,5% eNaCl with a spread of ±4,5% eNaCl. Following the data of Crawford (1981), the co-existing aqueous brine peak should be at a maximum of -10,0±0,5°C, with a spread of ±4,5°C. The observed peak (Fig. 1) is, however, at -7,0±0,5°C with a possible spread from -11°C to approximately -3°C. Contrary to expectation, the water ice must therefore be <u>less</u> saline than the corresponding clathrate ice. This anomalous behaviour may, however, also be ascribed to inter-sample variation (*i.e.* the accumulative peak may not adequately represent sample variability). Before any conclusions can be drawn, the data from each sample must be evaluated individually.

The melting temperature peaks for each of the samples are given in Fig. 2. From this it is now obvious that the evidence for clathrate ice mainly originate in one sample (FWS 27/2). This is also the only sample with a well developed aqueous brine peak. The broad clathrate peak can

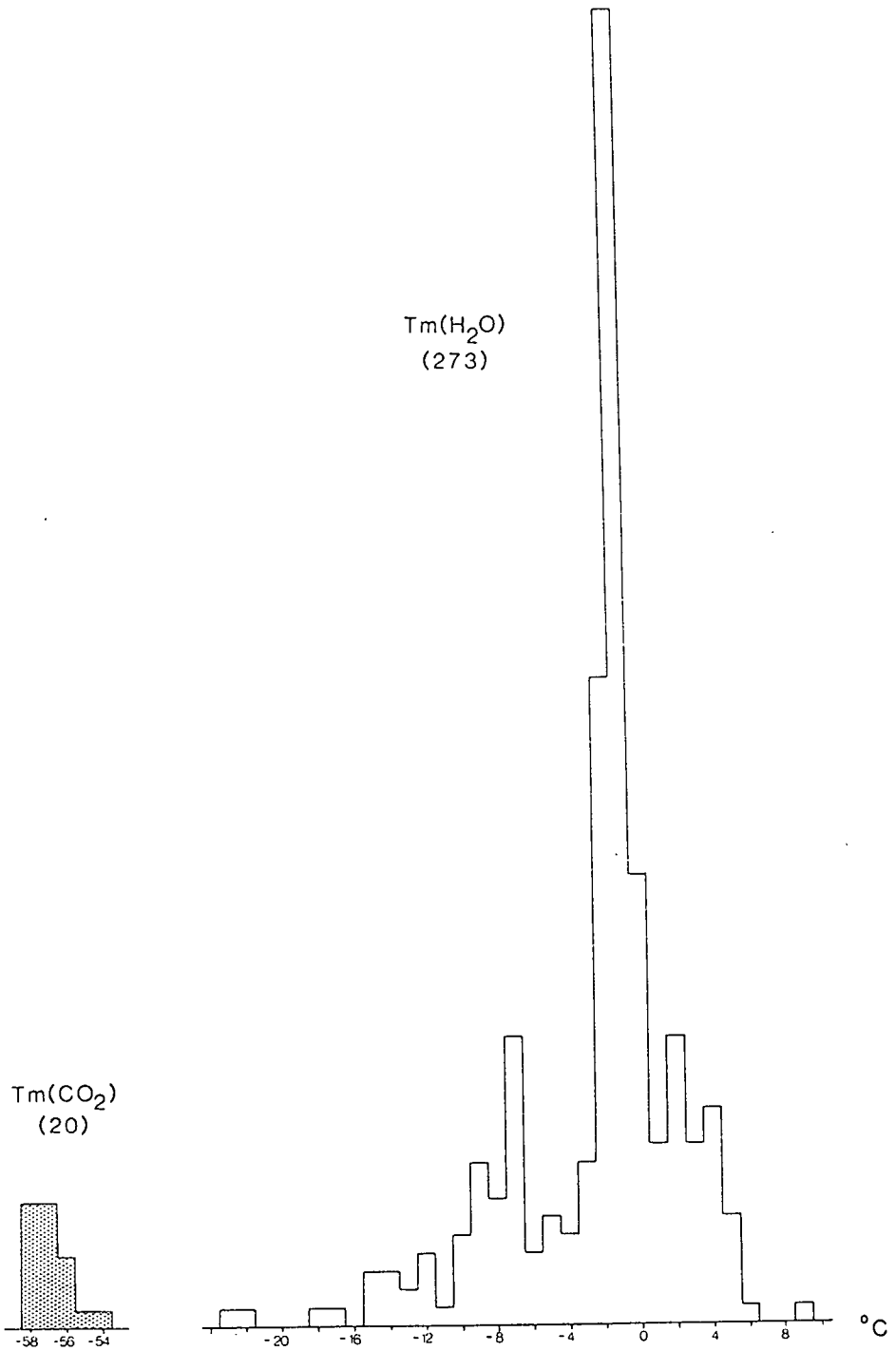

Fig. 1. Accumulative histogram of melting temperatures for samples FWS 16/2, FWS 79, FWS 27/2 and FWS 78. The number in parentheses indicates the number of duplicated readings.

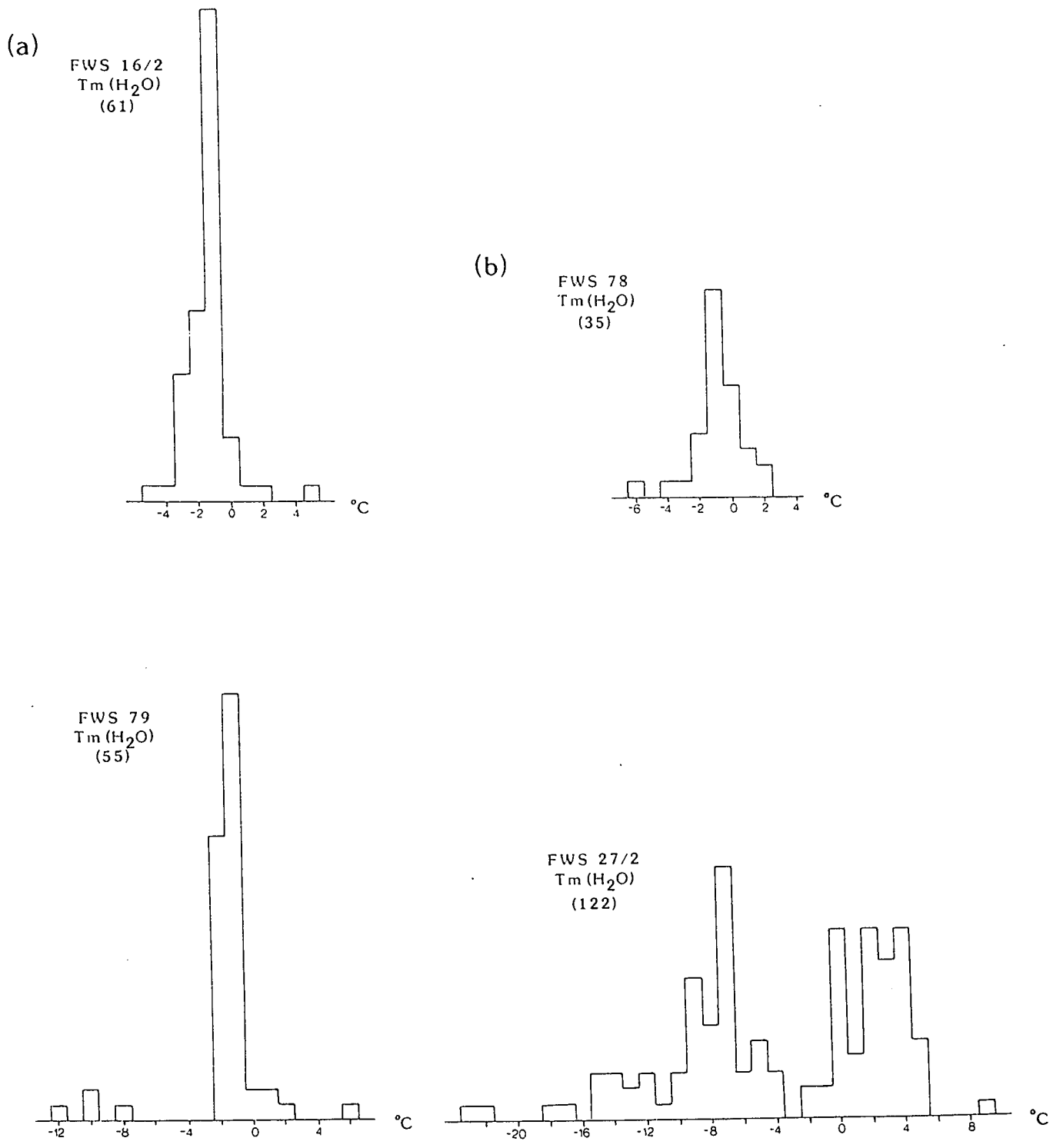

Fig. 2. Histograms of melting temperatures for the different samples. The numbers in parentheses indicate the numbers of duplicated readings.
a.) Dark coloured quartz. b.) Light coloured quartz.

be taken at any place between +2°C and +4°C, corresponding with 13,0% to 11,0% eNaCl (Collins, 1979). The predicted maximum value for the corresponding water-ice peak (Crawford, 1981) is between -7,0°C and -9,8°C, which correlates well with the observed values (Fig. 2).

It is therefore concluded that brine with 11 - 13% eNaCl is present in all samples. This H_2O-NaCl-CO_2 brine is, however, prominent in sample FWS 27/2 only (a light-coloured quartz), though definitely present in sample FWS 79 also (a dark-coloured quartz).

The dominant fluid in three of the samples, but present in all, is fairly pure water with Tm_f = -1 to 0°C (Fig. 1 and 2). This fluid contains a maximum of 1,5% eNaCl. Thus two aqueous fluid populations occur:

(i) pure water, in all the samples (dominant in FWS 16/2, FWS 79 and FWS 78) and

(ii) brine in the system H_2O-NaCl-(CO_2) with 11 - 13% eNaCl (dominant in FWS 27/2, and low in FWS 79). The melting temperature of the carbon dioxide in FWS 79 (Fig. 1), is so close to the value for pure CO_2, -56,6°C, that very few other mobile components such as CH_4 and N_2 can be present. The applicable model system is therefore H_2O-NaCl-CO_2 indeed.

In terms of composition of the fluid inclusions, there is little difference between dark- and light-coloured quartz. There is nevertheless a certain degree of correspondence between samples FWS 27/2 and FWS 79, while sample FWS 16/2 and FWS 78 correlate well. It is likely that the entrapped fluids under discussion played major roles during the diagenetic and metamorphic processes, rather than representing paleo-fluids inherited from the provenance region(s) of the quartz, in which case the microthermometric properties of different quartz types should have been very dissimilar. Remnants of provenance fluids can on occasion be recognized in the homogenization temperature spectra, even though it is not reflected in the melting temperature data. The homogenization temperatures (T_h) must therefore be studied as well, before deciding whether it is possible to distinguish between dark- and light-coloured quartz by means of microthermometry,

CONDITIONS OF ENTRAPMENT

The homogenization temperature (T_h) of a fluid inclusion is primarily controlled by the density prevailing at the time of formation (d, in g/cm^3). The variation in PT-conditions at constant density can be represented as a characteristic curve (isochore) on the PT projection plane. If a fluid

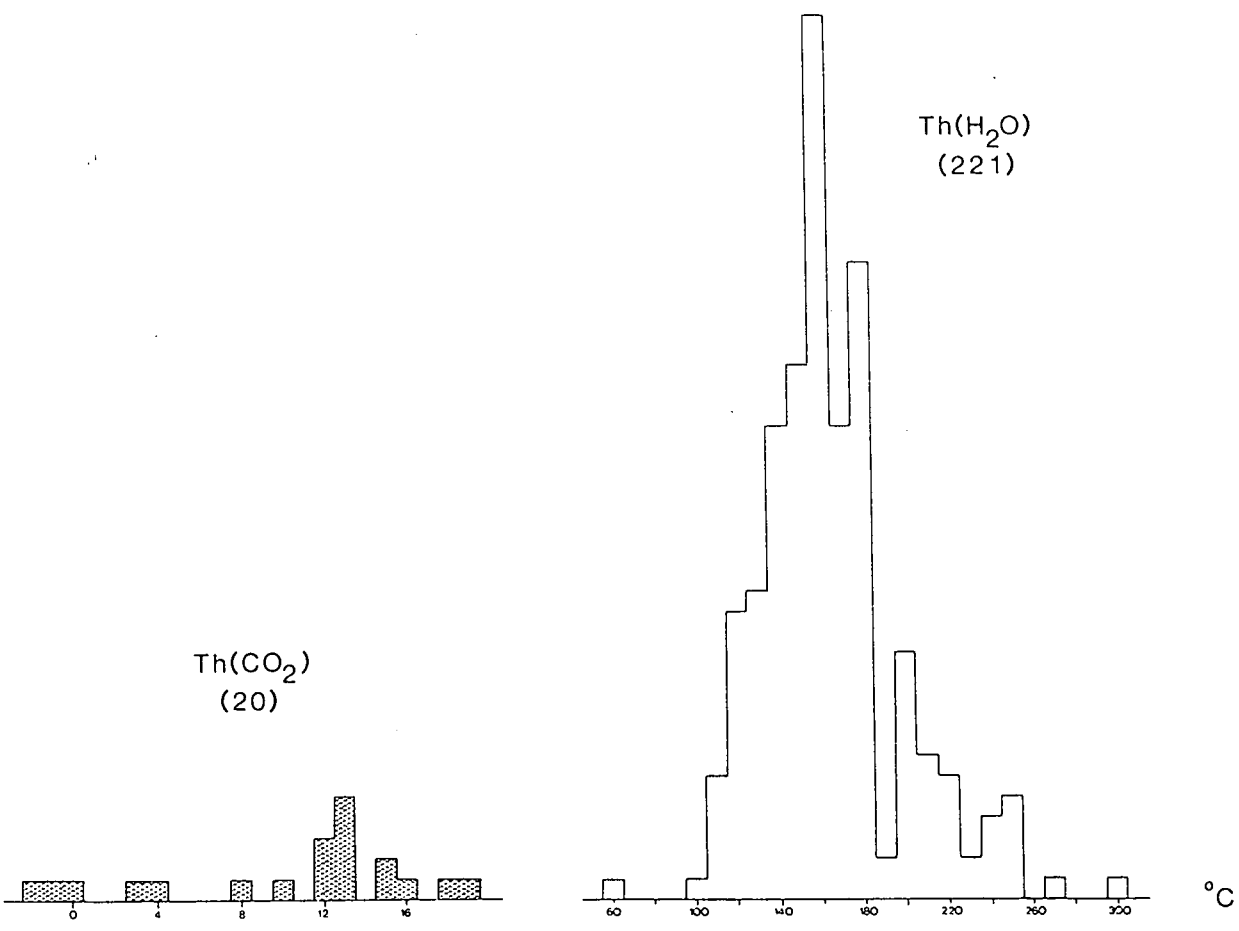

Fig. 3. Cumulative histograms for homogenization temperatures. The data for carbon dioxide was obtained exclusively from sample FWS 79. The numbers in parentheses indicate the number of readings.

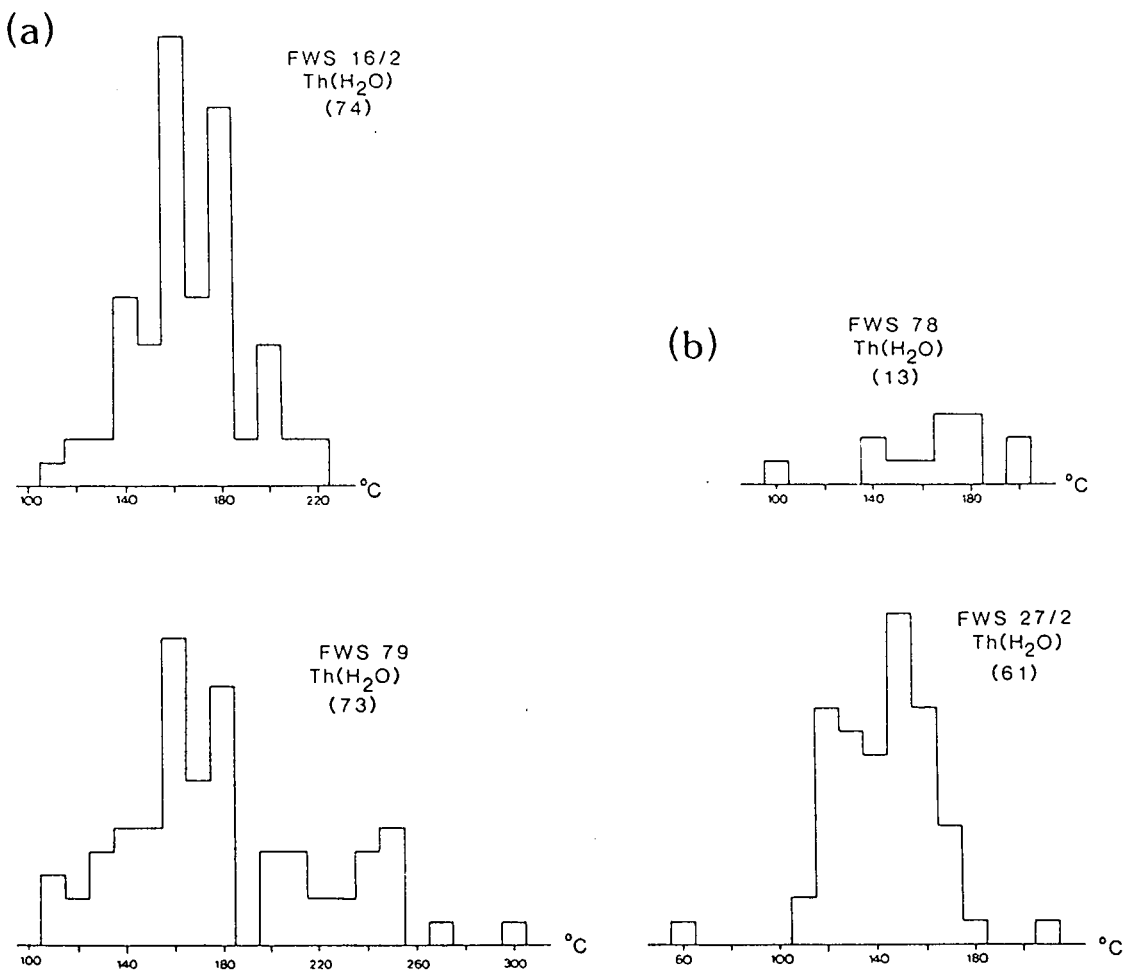

Fig. 4. Homogenization temperatures for each of the samples. Numbers in parentheses indicate the number of duplicated readings.
a.) Dark coloured quartz. b.) Light coloured quartz.

inclusion homogenizes into the fluid (i.e. the vapour bubble decreases in size until it disappears with increase in temperature), it holds a rather dense fluid with a steep isochore, while a fluid which homogenizes into the vapour phase is indicative of low density with a low angle slope isochore. All the studied inclusions homogenized into the fluid phase. The measured homogenization temperatures can therefore be used to derive the characteristic isochores (densities). The densities are not entirely independent of composition; it is necessary to ascertain which homogenization peak corresponds with which fluid composition. The isochores are then derived from isochore maps emanating from experimental results (eg. Hall *et al.* 1988) or calculated (eg. with the aid of the modified Redlich-Kwong equations, Redlich & Kwong 1949, Saxena & Fei 1987).

The accumulative homogenization temperatures of all the samples are summed up in Fig. 3. The aqueous inclusions exhibit a complex spectrum with a broad peak zone between 160°C and 180°C, and an asymmetric spread towards lower temperatures right down to 110°C. Subsidiary peaks occur at 200°C and 250°C. Because only one of the samples (FWS 27/2) produced a dominant brine peak, it should be easy to decide which homogenization peak is associated with which isochore in the system H_2O-NaCl-(CO_2). The data of this sample (Fig. 4) display two peaks at T_h = 120±10°C and T_h = 150±5°C. The other samples (Fig. 4) exhibit homogenization peaks that correspond (or nearly correspond) to the homogenization peak of the above-mentioned sample, but none display a peak comparable to that of sample FWS 27/2 (although sample FWS 79, which has already been identified as a sample which may contain a small quantity of the same brine, yields a few T_h-values at approximately 120°C). It is concluded that the T_h-value of the brine population is 120±10°C and that this is responsible for the asymmetry of the main peak in the accumulative histogram (Fig. 3). According to Roedder and Bodnar (1980), a brine with these characteristics, will have a density of 0,95g/cm^3. The presence of significant carbon dioxide implies that 0,95g/cm^3 must be regarded as a minimum value (Bowers and Helgeson, 1983; H_2O- NaCl-CO_2 in a ratio of 80:10:10 with a comparable T_h, can have a value for d of >1,0g/cm^3).

The remaining more pure water population probably represents an entire range of densities (Fig. 4). Samples FWS 79 and FWS 16/2 display a well defined peak at T_h = 160±5°C and FWS 27/2 exhibits a comparable value at T_h = 150±5°C. According to the data of Fisher (1976) this correlates with isochores of d = 0,91g/cm^3 and d = 0,92g/cm^3 respectively. A peculiar bimodality occurs in the data of samples FWS 79 and

FWS 16/2 due to the appearance of another peak at T_h = 180±5°C, representing d = 0,88g/cm³ (also discernible in sample FWS 78). Less dense fluids (T_h = 210±10°C, d = 0,85g/cm³ and T_h = 250±10°C, d = 0,80g/cm³) occur in sample FWS 79 only.

The discrete carbon dioxide inclusions which occur in sample FWS 79, have a rather high density (Fig. 3). The homogenization peak is at +13,0±0,7°C, but exhibit a wide spread between -3°C and +19°C. Because the carbon dioxide is nearly pure, the data of Angus *et al.* (1976) and Roedder (1984) can be used to derive a density (d) of 0,87g/cm³. Unfortunately sufficient data is not available to ascertain which of the peaks for water are associated with which of the carbon dioxide peaks (Fig. 4), but it is conceivable that the wide spread of $T_h(CO_2)$ correlates with the wide spread of $T_h(H_2O)$.

Due to the close association of carbon dioxide with water (clathrate ice, Figs. 1 and 2), it can be assumed that a genetic relationship exists between the discrete CO_2 and the H_2O. It is therefore appropriate, in this case, to apply the intersecting isochore method of Kalyushnyi and Koltun for an estimation of PT-conditions of entrapment. Due to the width of the complete spread of relevant T_h-values, $T_h(H_2O)$ = 120°C to 250°C and $T_h(CO_2)$ = -3°C to +19°C, the region of intersection is large; T = 170°C to 500°C and P = 0,8kb to 3,8kb. If the intersection is taken for the primary peak isochores only, values of T = 250°C and P = 1,6kb are obtained. The bulk of the carbon dioxide in the samples under discussion do not occur as discrete inclusions, but in combination with the water.

The co-existence of carbon dioxide with water in the majority of the fluid inclusions (clathrate ices, Figs. 1 and 2), indicates that the fluid was entrapped at conditions above the solvus (immiscibility curve). The H_2O-CO_2 solvus is well known (Takenouchi and Kennedy, 1964; Tödheide and Franck, 1963)(Fig. 5). It is also known that solvus conditions rise dramatically with an increase in NaCl content (Bowers and Helgeson 1983). The CO_2:H_2O ratio in the aqueous fluid inclusions must be somewhere between 30:70 and 10:90. If the carbon dioxide concentration exceeded 30%, two fluid phases ("double bubbles") would have been much more prominent, and if it was less than 10%, clathrate ice would not have formed as readily as it did, in fluid inclusions in which double bubbles are absent (Figs. 1 and 2). For the pure H_2O-CO_2 model system, the fluid inclusions must have been entrapped at temperatures in excess of 200-270°C (Fig. 5), but in the case of the brine this minimum temperature rises to 300-440°C (at 2kb). The discrete carbon dioxide

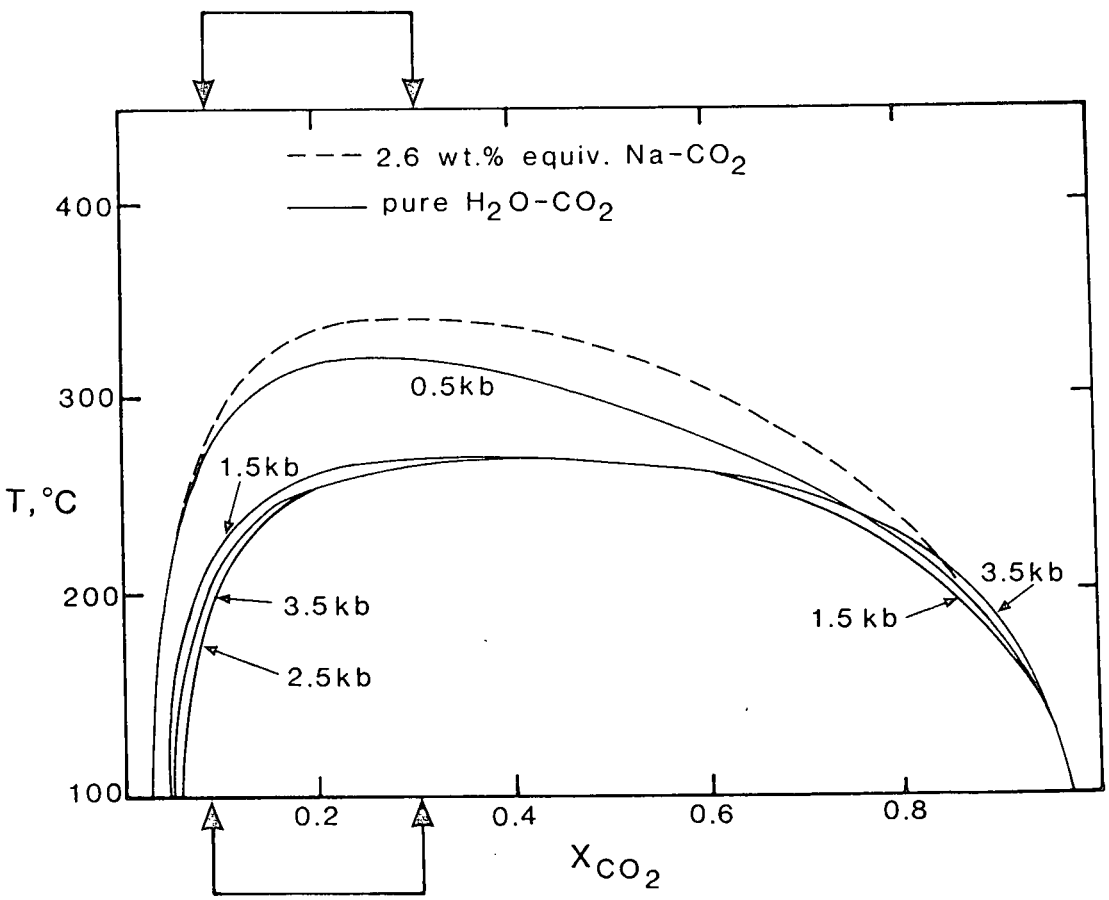

Fig. 5. The H_2O-CO_2 solvus according to experimental evidence, as summarized by Crawford, 1981. At conditions above the curve, commonly prevailing in nature, water and carbon dioxide mix in all ratios, to form a single fluid phase. At conditions below the curve, carbon dioxide and water form two immiscible fluids. The x-axis represents the $CO_2/(H_2O+CO_2)$ ratio.

inclusions in sample FWS 79 must already have been at conditions below the solvus before entrapment (a temperature of below 200-270°C for a NaCl- deficient fluids, and below 300-440°C for 12% NaCl, at 2kb). These observations correlate reasonably well with the values derived above by means of intersecting isochores.

CONCLUSIONS

All the samples contain rather pure water, with auxiliary carbon dioxide, and densities of 0,92g/cm^3 to 0,95g/cm^3. Brine, which is probably of high density (>1g/cm^3), is prominent in one sample (FWS 27/2) only. The conditions of entrapment is in the vicinity of 250±100°C and 2,0±1,5kb.

It is not possible, in terms of fluid composition, to distinguish between dark- and light- coloured quartz. The presence of auxiliary low density fluids (T_h = 200-210°C and 250°C) in the dark-coloured quartz, may portray provenance conditions. If this is the case, microthermometric discrimination between the two types of quartz can be done easily (the sample is heated only once to 200°C and inspected for the presence of a large number of as yet unhomogenized fluid inclusions, i.e. vapour bubbles still visible). However, the 13 duplicated homogenization readings for sample FWS 78, are not sufficient to ensure that the light-coloured quartz does not contain low density fluids as well.

A.E. SCHOCH

D. ELSMERE

BLOEMFONTEIN
OCTOBER 1989

REFERENCES

Angus, S., Armstrong, B., de Reuck, K.M., Altunin, V.V., Gadetskii, O.G. Chapela, G.A., & Rowlinson, J.S. (1976). *International Thermodynamic Tables of the Fluid State, Vol. 3, Carbon Dioxide.* Pergamon Press, 385 pp.

Bowers, T.S. & Helgeson, H.C. (1983). Calculation of the thermodynamic and geochemical consequences of nonideal mixing in the system H_2O-CO_2-NaCl on phase relations in geologic systems: Equation of state for H_2O-CO_2-NaCl fluids at high pressures and temperatures. *Geochim. Cosmochim. Acta*, **47**, 1247 - 1275.

Collins, P.L.F. (1979). Gas hydrates in CO_2-bearing fluid inclusions and the use of freezing data for estimating salinity. *Econ. Geol.*, **74**, 1435 - 1444.

Crawford, M.L. (1981). Phase equilibria in aqueous fluid inclusions. *In*: Hollister, L.S. & Crawford, M.L., Eds., *Short Course in Fluid Inclusions: Applications to Petrology*. Mineralog. Ass. Can., **6**, 75 - 100.

Dhamelincourt, P. (1979). *étude et réalisation d'une microsonde moléculaire à effet Raman. Quelques domaines d'application.* Thèse l'Univ. des Sciences et Techniques de Lille.

Fisher, J.R. (1976). The volumetric properties of H_2O - a graphical portayal. *J. Res. U.S. Geol. Surv.*, **4**, 189 - 193.

Frantz, J.D., Mao, H.K., Zhang, Y., Wu, Y., Thompson, A.C., Underwood, J.H., Giauque, R.D. Jones, K.W. & Rivers, M.L. (1988). Analysis of fluid inclusions by X-ray fluorescence using synchrotron radiation. *Chem. Geol.*, **69**, 235 - 244.

Hall, D.L., Sterner, M.S. & Bodnar, R.J. (1988). Freezing point depression of NaCl-KCl-H_2O solutions. *Econ. Geol.*, **83**, 197 - 202.

Redlich, O. & Kwong, J.N.S. (1949). On the thermodynamics of solutions, V: An equation of state. Fugacities of gaseous solutions. *Chem. Rev.*, **44**, 233 - 244.

Roeder, E. (1984). *Fluid Inclusions. Reviews in mineralogy, 12.* Mineralog. Soc. Am., 643 pp.

Roeder, E. & Bodnar, R.J. (1980). Geologic pressure determinations from fluid inclusion studies. *Ann. Rev. Earth Planet Sci.*, **8**, 263 - 301.

Saxena, S.K. & Fei, Y. (1987). Fluids at crustal pressures and temperatures. I. Pure species. *Contrib. Miner. Petrol.*, **95**, 370 - 375.

Takenouchi, S. & Kennedy, G.C. (1964). The binary system H_2O-CO_2 at high temperatures and pressures. *Am. J. Sci.*, 262, 1055 - 1074.

Tödheide, K. & Franck, E.U. (1963). Das Zweiphasengebied und die Kritische Kurve im System Kohlendioxid-Wasser bis zu Drucken von 3500 bar. *Zeits. Phys. Chem. Neue Folge*, **37**, 387 -401.

Van den Kerkhof, A.M. (1988). *The system CO_2-CH_4-N_2 in fluid inclusions: theoretical modeling and geological applications.* Ph.D. thesis, Vrije Univ. te Amsterdam. Free University Press, 206 pp.

APPENDIX 2.

SAS PROGRAMME

CLUSTER ANALYSES

SPEARMAN CORRELATIONS

EXAMPLE OF *SAS* PROGRAMME

LEGEND TO THE SYMBOLS USED FOR THE DIFFERENT ROCK TYPES

A	DARK QUARTZITE RDM
B	LIGHT QUARTZITE RDM
C	WHITE QUARTZ RDM
D	DARK QUARTZ RDM
E	DARK CHERT RDM
F	LIGHT CHERT RDM
G	BANDED CHERT RDM
H	IGNEOUS RDM
I	YELLOW-1 RDM
J	YELLOW-2 RDM
K	YELLOW-3 RDM
L	YELLOW-4 RDM
M	GREY-1 RDM
N	GREY-2 RDM
O	GREY-3 RDM
P	GREY-4 RDM
Q	BLACK RDM
R	DARK SILTSTONE RDM
S	YELLOW-1 BPM
T	DARK QUARTZITE BPM
U	LIGHT QUARTZITE BPM
V	WHITE QUARTZ BPM
W	DARK QUARTZ BPM
X	DARK CHERT BPM
Y	LIGHT CHERT BPM
Z	BANDED CHERT BPM
1	IGNEOUS BPM
2	DARK SILTSTONE BPM
3	YELLOW-2 BPM

```
1          SAS(R) LOG  CMS SAS 5.18       VM/CMS CMS USER AKK

NOTE: COPYRIGHT (C) 1984,1986 SAS INSTITUTE INC., CARY, N.C.  27512, U.S.A.
NOTE: CMS SAS RELEASE 5.18 AT ANGLO AMERICAN CORPORATION OF SOUTH AFRICA LIMITED (020620001).

NOTE: CPUID    VERSION = FF  SERIAL = 202252  MODEL = 3083 .

NOTE: NO OPTIONS SPECIFIED.

We have installed release 5.18 of sas which you are currently using.      SAS00010
Please contact me if you experience any problems.                         SAS00020
                                                                          SAS00030
Karen Duff (011) 638-2922 or machine KLD.                                 SAS00040

  1   * PROGRAM TO READ IN XRFME DATA FOR UPPER WITWATERSRAND STUDY:
  2           CMS FI DATAIN DISK SSCLAST1 XRFDATA A :
  3                 DATA CLASTBA1.SASET;
  4                      INFILE DATAIN LENGTH=L;
  5                      INPUT SAMPNO $
  6                            BOREHOLE $
  7                            HOLECODE $
  8                            DEPTHFM
  9                            DEPTHTO
 10                            AU
 11                            AG
 12                            FORMTION $
 13                            ROCKTYPE $
 14                            LOCATION $
 15                            DEFL $
 16                            INTSECT $
 17           U TH BI PB U TA BA TE SB SN MO NB ZR Y SR RB SE AS
 18           ZN CU NI CO FE MN CR V TI CA K S P SI AL MG NA F;
 19          IF ROCKTYPE ='A' THEN DELETE;
 20          IF ROCKTYPE ='B' THEN DELETE;
 21     *    IF ROCKTYPE ='C' THEN DELETE;
 22     *    IF ROCKTYPE ='D' THEN DELETE;
 23          IF ROCKTYPE ='E' THEN DELETE;
 24          IF ROCKTYPE ='F' THEN DELETE;
 25          IF ROCKTYPE ='G' THEN DELETE;
 26          IF ROCKTYPE ='H' THEN DELETE;
 27          IF ROCKTYPE ='I' THEN DELETE;
 28          IF ROCKTYPE ='J' THEN DELETE;
 29          IF ROCKTYPE ='K' THEN DELETE;
 30          IF ROCKTYPE ='L' THEN DELETE;
 31          IF ROCKTYPE ='M' THEN DELETE;
 32          IF ROCKTYPE ='N' THEN DELETE;
 33          IF ROCKTYPE ='O' THEN DELETE;
 34          IF ROCKTYPE ='P' THEN DELETE;
 35          IF ROCKTYPE ='Q' THEN DELETE;
 36          IF ROCKTYPE ='R' THEN DELETE;
 37          IF ROCKTYPE ='S' THEN DELETE;
 38          IF ROCKTYPE ='T' THEN DELETE;
 39          IF ROCKTYPE ='U' THEN DELETE;
 40     *    IF ROCKTYPE ='V' THEN DELETE;
 41     *    IF ROCKTYPE ='W' THEN DELETE;
 42          IF ROCKTYPE ='X' THEN DELETE;
 43          IF ROCKTYPE ='Y' THEN DELETE;
 44          IF ROCKTYPE ='Z' THEN DELETE;
 45          IF ROCKTYPE ='1' THEN DELETE;
 46          IF ROCKTYPE ='2' THEN DELETE;
 47          IF ROCKTYPE ='3' THEN DELETE;
 48          IF ROCKTYPE ='4' THEN DELETE;
 49       *  OPTIONS PAGESIZE=500 LINESIZE=250;
 50       *  OPTIONS PAGESIZE=500 LINESIZE=132;
 51       *  OPTIONS NOCENTER;
 52          LABEL SAMPNO='SAMPLE NUMBER';LABEL BOREHOLE='BOREHOLE NUMBER';
 53          LABEL DEPTHFM='DEPTH FROM';LABEL DEPTHTO='DEPTH TO';
 54          LABEL FORMTION='FORMATION';LABEL DEFL='DEFLECTION';
 55          LABEL INTSECT='INTERSECTION';
 56         *WIDTH =DEPTHTO-DEPTHFM;
 57 TITLE1 'CLAST STUDY ################## 36 ELEMENT XRF DATA';
 58

NOTE: INFILE DATAIN IS FILE SSCLAST1 XRFDATA A1
NOTE: SAS WENT TO A NEW LINE WHEN INPUT STATEMENT
      REACHED PAST THE END OF A LINE.
NOTE: 556 LINES WERE READ FROM INFILE DATAIN.
      THE MINIMUM LINE LENGTH IS 45.
      THE MAXIMUM LINE LENGTH IS 72.
NOTE: DATA SET CLASTBA1.SASET HAS 14 OBSERVATIONS AND 48 VARIABLES.
NOTE: THE DATA STATEMENT USED 0.39 SECONDS AND 212K.

 58  PROC SORT;BY FORMTION ROCKTYPE;
 59
```

```
NOTE: DATA SET CLASTBA1.SASET HAS 14 OBSERVATIONS AND 49 VARIABLES.
NOTE: THE PROCEDURE SORT USED 0.11 SECONDS AND 1556K.

 59  PROC CLUSTER METHOD=WARD OUTTREE=TREE NOPRINT;
 60 VAR   CU NI CO MN CA K NA;
 61   ID SAMPNO ;
 62 COPY FORMTION ROCKTYPE;
 63
NOTE: THE DATA SET WORK.TREE HAS 27 OBSERVATIONS AND 26 VARIABLES.
NOTE: THE PROCEDURE CLUSTER USED 0.12 SECONDS AND 532K.

 63  PROC TREE HEIGHT=NCL  OUT=PART.CLUSTER NCLUSTERS=3 NOPRINT;
 64  HEIGHT  NCL ;ID SAMPNO ;
 65 COPY  CU NI CO MN CA K NA FORMTION ROCKTYPE;
 66  TITLE3 ' C.A. NO: 0000000001 FOR CU NI CO MN CA K NA';
 67
NOTE: THE DATA SET PART.CLUSTER HAS 14 OBSERVATIONS AND 12 VARIABLES.
NOTE: THE PROCEDURE TREE USED 0.09 SECONDS AND 340K.

 67  PROC SORT;BY CLUSTER ROCKTYPE;
 68

NOTE: DATA SET PART.CLUSTER HAS 14 OBSERVATIONS AND 12 VARIABLES.
NOTE: THE PROCEDURE SORT USED 0.06 SECONDS AND 1556K.

 68  PROC PRINT LABEL N;
 69  VAR SAMPNO ROCKTYPE FORMTION
 70  CU NI CO MN CA K NA CLUSNAME;
 71  BY CLUSTER;
 72  ID SAMPNO;
 73  FOOTNOTE2 'WARD METHOD ** OUTLIERS EXCLUDED ARE =0000';
 74  PROC MEANS MAXDEC=1; BY CLUSTER;
 75
NOTE: THE PROCEDURE MEANS USED 0.08 SECONDS AND 276K AND PRINTED PAGE 2.

 75  PROC CORR SPEARMAN NOSIMPLE RANK BEST=10;
 76  VAR CU NI CO MN CA K NA;
 77  BY CLUSTER;
 78  RUN;
NOTE: NOT ENOUGH OBSERVATIONS. MUST HAVE NOBS>1.
NOTE: ABOVE MESSAGE IS FOR BY-GROUP:
      CLUSTER=2
NOTE: NOT ENOUGH OBSERVATIONS. MUST HAVE NOBS>1.
NOTE: ABOVE MESSAGE IS FOR BY-GROUP:
      CLUSTER=3
NOTE: THE PROCEDURE CORR USED 0.09 SECONDS AND 276K AND PRINTED PAGE 3.


NOTE: SAS INSTITUTE INC.
      SAS CIRCLE
      PO BOX 8000
      CARY, N.C. 27512-8000
```

CLUSTER ANALYSIS 1

(C1-01)

CLAST STUDY ########################## 36 ELEMENT XRF DATA

C.A. NO: 0000000001 FOR CU NI CO MN CA K NA

CLUSTER=1

SAMPLE NUMBER	SAMPLE NUMBER	ROCKTYPE	FORMATION	CU	NI	CO	MN	CA	K	NA	CLUSNAME
GI0096	GI0096	C	RDM	-21	-4	-5	0.2	0.3	0.2	0.0	CL3
GI0036	GI0036	C	RDM	-12	-2	-6	0.2	0.3	0.2	0.0	CL3
GI0044	GI0044	C	RDM	-12	-1	-6	0.2	0.3	0.2	0.0	CL3
GI0113	GI0113	C	RDM	-12	8	-5	0.3	0.4	0.2	0.0	CL3
GI0044	GI0044	C	RDM	-3	5	-4	0.2	0.4	0.2	0.0	CL3
GI0093	GI0093	D	RDM	-17	-1	-5	0.2	0.3	0.2	0.0	CL3
GI0064	GI0064	V	BPM	-20	1	-6	0.2	0.3	0.2	0.0	CL3
GI0085	GI0085	V	BPM	-17	-7	-5	0.2	0.3	0.2	0.0	CL3
GI0023	GI0023	V	BPM	-24	1	-6	0.2	0.3	0.2	0.3	CL3
GI0019	GI0019	W	BPM	-20	-1	-5	0.2	0.3	0.2	0.3	CL3
GI0065	GI0065	W	BPM	-22	-3	-7	0.2	0.3	0.2	0.0	CL3
GI0120	GI0120	W	BPM	-11	5	-2	0.2	0.3	0.2	0.0	CL3

N= 12

CLUSTER=2

SAMPLE NUMBER	SAMPLE NUMBER	ROCKTYPE	FORMATION	CU	NI	CO	MN	CA	K	NA	CLUSNAME
GI0054	GI0054	V	BPM	15	86	12	0.3	0.3	0.2	0	GI0054

N= 1

CLUSTER=3

SAMPLE NUMBER	SAMPLE NUMBER	ROCKTYPE	FORMATION	CU	NI	CO	MN	CA	K	NA	CLUSNAME
GI0100	GI0100	W	BPM	-8	46	5	0.2	0.3	0.3	0	GI0100

N= 1

WARD METHOD ** OUTLIERS EXCLUDED ARE =0000

VARIABLE	N	MEAN	STANDARD DEVIATION	MINIMUM VALUE	MAXIMUM VALUE	STD ERROR OF MEAN	SUM	VARIANCE	C.V.
CLUSTER=1									
CU	12	-15.9	6.0	-24.0	-3.0	1.7	-191.0	36.4	-37.9
NI	12	1.5	3.9	-4.0	8.0	1.1	19.0	15.2	246.0
CO	12	-4.9	1.4	-7.0	-2.0	0.4	-59.0	1.9	-28.0
MN	12	0.2	0.0	0.2	0.3	0.0	2.5	0.0	13.9
CA	12	0.3	0.0	0.3	0.4	0.0	3.8	0.0	12.3
K	12	0.2	0.0	0.2	0.2	0.0	2.4	0.0	0.0
NA	12	0.0	0.1	0.0	0.3	0.0	0.6	0.0	233.5
CLUSTER=2									
CU	1	15.0	.	15.0	15.0	.	15.0	.	.
NI	1	86.0	.	86.0	86.0	.	86.0	.	.
CO	1	12.0	.	12.0	12.0	.	12.0	.	.
MN	1	0.3	.	0.3	0.3	.	0.3	.	.
CA	1	0.3	.	0.3	0.3	.	0.3	.	.
K	1	0.2	.	0.2	0.2	.	0.2	.	.
NA	1	0.0	.	0.0	0.0	.	0.0	.	.
CLUSTER=3									
CU	1	-8.0	.	-8.0	-8.0	.	-8.0	.	.
NI	1	46.0	.	46.0	46.0	.	46.0	.	.
CO	1	5.0	.	5.0	5.0	.	5.0	.	.
MN	1	0.2	.	0.2	0.2	.	0.2	.	.
CA	1	0.3	.	0.3	0.3	.	0.3	.	.
K	1	0.3	.	0.3	0.3	.	0.3	.	.
NA	1	0.0	.	0.0	0.0	.	0.0	.	.

WARD METHOD ** OUTLIERS EXCLUDED ARE =0000

CLUSTER=1

SPEARMAN CORRELATION COEFFICIENTS / PROB > |R| UNDER H0:RHO=0 / N = 12

CU

CU	NI	CA	NA	CO	MN	K
1.00000	0.61250	0.52372	-0.49099	0.23629	0.22068	.
0.0000	0.0342	0.0805	0.1050	0.4597	0.4907	

NI

NI	CU	CA	MN	CO	NA	K
1.00000	0.61250	0.55646	0.48550	0.40613	-0.16366	.
0.0000	0.0342	0.0602	0.1096	0.1902	0.6113	

CO

CO	NI	NA	CA	CU	MN	K
1.00000	0.40613	0.33838	0.27071	0.23629	0.04563	.
0.0000	0.1902	0.2820	0.3948	0.4597	0.8880	

MN

MN	CA	NI	CU	NA	CO	K
1.00000	0.67420	0.48550	0.22068	-0.13484	0.04563	.
0.0000	0.0162	0.1096	0.4907	0.6761	0.8880	

CA

CA	MN	NI	CU	CO	NA	K
1.00000	0.67420	0.55646	0.52372	0.27071	-0.20000	.
0.0000	0.0162	0.0602	0.0805	0.3948	0.5331	

K

K	NI	CO	MN	CA	CU	NA
1.00000	.	.	.	.	.	.
0.0000						

NA

NA	CU	CO	CA	NI	MN	K
1.00000	-0.49099	0.33838	-0.20000	-0.16366	-0.13484	.
0.0000	0.1050	0.2820	0.5331	0.6113	0.6761	

CLUSTER ANALYSIS 2

(C1-02)

CLAST STUDY ########## 36 ELEMENT XRF DATA

C.A. NO: 0000000001 FOR CU NI CO MN CA K NA

CLUSTER=1

SAMPLE NUMBER	SAMPLE NUMBER	ROCKTYPE	FORMATION	CU	NI	CO	MN	CA	K	NA	CLUSNAME
GI0038	GI0038	E	RDM	-10	24	-4	0.4	0.3	0.3	0.0	CL3
GI0046	GI0046	E	RDM	-9	38	-2	0.4	0.3	0.3	0.0	CL3
GI0092	GI0092	E	RDM	-15	18	-2	0.2	0.3	0.2	0.0	CL3
GI0077	GI0077	E	RDM	-9	136	8	0.5	0.3	0.3	0.0	CL3
GI0095	GI0095	E	RDM	-15	134	22	0.2	0.3	0.2	0.0	CL3
GI0114	GI0114	E	RDM	-13	152	7	0.7	0.3	0.3	0.0	CL3
GI0033	GI0033	F	RDM	-9	20	-6	0.5	0.3	0.2	0.0	CL3
GI0071	GI0071	F	RDM	-10	53	-0	0.4	0.3	0.6	0.0	CL3
GI0051	GI0051	F	RDM	22	18	-7	0.2	0.3	0.4	0.0	CL3
GI0045	GI0045	G	RDM	-7	84	3	0.3	0.3	0.2	0.0	CL3
GI0119	GI0119	X	BPM	-6	16	-0	0.2	0.3	0.3	0.0	CL3
GI0119	GI0119	X	BPM	-5	16	-2	0.2	0.3	0.3	0.0	CL3
GI0056	GI0056	X	BPM	-5	18	-4	0.2	0.3	0.2	0.0	CL3
GI0089	GI0089	X	BPM	-8	59	5	0.2	0.3	0.2	0.0	CL3
GI0107	GI0107	X	BPM	-11	58	-9	0.2	0.3	0.2	0.0	CL3
GI0018	GI0018	X	BPM	14	35	14	0.2	0.3	0.3	0.3	CL3
GI0089	GI0089	X	BPM	-15	49	4	0.2	0.3	0.2	0.0	CL3
GI0017	GI0017	X	BPM	-22	65	-3	0.3	0.5	0.2	0.6	CL3
GI0083	GI0083	X	BPM	89	17	-9	0.2	0.3	0.2	0.0	CL3
GI0084	GI0084	Y	BPM	-13	8	-5	0.2	0.3	1.0	0.0	CL3
GI0024	GI0024	Y	BPM	-16	73	-9	0.2	0.3	0.2	0.3	CL3
GI0102	GI0102	Y	BPM	38	14	-3	0.2	0.3	0.6	0.0	CL3
GI0058	GI0058	Z	BPM	-3	37	-7	0.2	0.3	0.1	0.0	CL3
GI0108	GI0108	Z	BPM	-21	5	-4	0.2	0.3	0.2	0.0	CL3
GI0021	GI0021	Z	BPM	-2	23	-2	0.4	0.2	0.9	0.3	CL3
GI0060	GI0060	Z	BPM	9	32	6	0.3	0.3	0.2	0.0	CL3
GI0086	GI0086	Z	BPM	4	159	19	0.3	0.4	0.2	0.0	CL3

N= 27

CLUSTER=2

SAMPLE NUMBER	SAMPLE NUMBER	ROCKTYPE	FORMATION	CU	NI	CO	MN	CA	K	NA	CLUSNAME
GI0066	GI0066	X	BPM	47	944	451	0.6	0.2	0.1	0.0	CL4
GI0020	GI0020	Z	BPM	58	1085	305	0.7	0.2	0.2	0.4	CL4

N= 2

CLUSTER=3

SAMPLE NUMBER	SAMPLE NUMBER	ROCKTYPE	FORMATION	CU	NI	CO	MN	CA	K	NA	CLUSNAME
GI0057		X	BPM	67	378	139	0,5	0,3	0,1	0	

N= 1

WARD METHOD ** OUTLIERS EXCLUDED ARE =0000

VARIABLE	N	MEAN	STANDARD DEVIATION	MINIMUM VALUE	MAXIMUM VALUE	STD ERROR OF MEAN	SUM	VARIANCE	C.V.
CLUSTER=1									
CU	27	-1.8	22.4	-22.0	89.0	4.3	-48.0	501.0	-1259.1
NI	27	50.8	45.4	5.0	159.0	8.7	1371.0	2064.3	89.5
CO	27	3.0	7.5	-7.0	22.0	1.4	82.0	56.7	248.0
MN	27	0.3	0.1	0.2	0.7	0.0	7.7	0.0	45.3
CA	27	0.3	0.0	0.2	0.5	0.0	8.3	0.0	15.4
K	27	0.3	0.2	0.1	1.0	0.0	8.5	0.0	68.6
NA	27	0.1	0.1	0.0	0.6	0.0	1.5	0.0	261.0
CLUSTER=2									
CU	2	52.5	7.8	47.0	58.0	5.5	105.0	60.5	14.8
NI	2	1014.5	99.7	944.0	1085.0	70.5	2029.0	9940.5	9.8
CO	2	378.0	103.2	305.0	451.0	73.0	756.0	10658.0	27.3
MN	2	0.6	0.1	0.6	0.7	0.1	1.3	0.0	10.9
CA	2	0.2	0.0	0.2	0.2	0.0	0.4	0.0	0.0
K	2	0.1	0.1	0.1	0.2	0.1	0.3	0.0	47.1
NA	2	0.2	0.3	0.0	0.4	0.2	0.4	0.1	141.4
CLUSTER=3									
CU	1	67.0	.	67.0	67.0	.	67.0	.	.
NI	1	378.0	.	378.0	378.0	.	378.0	.	.
CO	1	139.0	.	139.0	139.0	.	139.0	.	.
MN	1	0.5	.	0.5	0.5	.	0.5	.	.
CA	1	0.3	.	0.3	0.3	.	0.3	.	.
K	1	0.1	.	0.1	0.1	.	0.1	.	.
NA	1	0.0	.	0.0	0.0	.	0.0	.	.

WARD METHOD ** OUTLIERS EXCLUDED ARE =0000

CLUSTER=1

SPEARMAN CORRELATION COEFFICIENTS / PROB > |R| UNDER H0:RHO=0 / N = 27

CU

CU	NI	K	CA	NA	MN	CO
1.00000	-0.26086	0.20672	-0.18262	-0.11592	-0.07467	0.06865
0.0000	0.1888	0.3009	0.3619	0.5648	0.7113	0.7337

NI

NI	CO	MN	CA	K	CU	NA
1.00000	0.64222	0.45689	0.32965	-0.27072	-0.26086	0.16828
0.0000	0.0003	0.0166	0.0931	0.1720	0.1888	0.4014

CO

CO	NI	K	CA	NA	CU	MN
1.00000	0.64222	-0.35757	0.12584	0.10955	0.06865	-0.05608
0.0000	0.0003	0.0671	0.5317	0.5865	0.7337	0.7812

MN

MN	NI	K	CU	CO	NA	CA
1.00000	0.45689	0.23915	-0.07467	-0.05608	0.03905	0.01356
0.0000	0.0166	0.2296	0.7113	0.7812	0.8467	0.9465

CA

CA	K	NI	CU	CO	NA	MN
1.00000	-0.35678	0.32965	-0.18262	0.12584	0.02356	0.01356
0.0000	0.0677	0.0931	0.3619	0.5317	0.9071	0.9465

K

K	CO	CA	NI	MN	CU	NA
1.00000	-0.35757	-0.35678	-0.27072	0.23915	0.20672	0.07215
0.0000	0.0671	0.0677	0.1720	0.2296	0.3009	0.7206

NA

NA	NI	CU	CO	K	MN	CA
1.00000	0.16828	-0.11592	0.10955	0.07215	0.03905	0.02356
0.0000	0.4014	0.5648	0.5865	0.7206	0.8467	0.9071

CLUSTER ANALYSIS 3

(C1-03)

CLAST STUDY ********** 36 ELEMENT XRF DATA

C.A. NO: 0000000001 FOR CA K AL MG NA

CLUSTER=1

SAMPLE NUMBER	SAMPLE NUMBER	ROCKTYPE	FORMATION	CA	K	AL	MG	NA	CLUSNAME
GI0029	GI0029	H	RDM	0.3	0.6	4.9	0.2	0.0	CL4
GI0029	GI0029	H	RDM	0.4	0.6	4.9	0.2	0.0	CL4
GI0115	GI0115	H	RDM	0.6	0.4	4.3	0.4	0.0	CL4
GI0116	GI0116	H	RDM	0.6	0.4	4.4	0.4	0.0	CL4
GI0078	GI0078	H	RDM	0.4	0.7	4.3	0.6	0.0	CL4
GI0098	GI0098	H	RDM	0.3	1.0	4.4	0.6	0.0	CL4
GI0012	GI0012	H	RDM	0.3	0.3	4.9	0.2	0.3	CL4
GI0062	GI0062	1	BPM	0.3	0.2	4.2	0.0	0.0	CL4

N= 8

CLUSTER=2

SAMPLE NUMBER	SAMPLE NUMBER	ROCKTYPE	FORMATION	CA	K	AL	MG	NA	CLUSNAME
GI0050	GI0050	H	RDM	0.3	0.8	5.5	0.3	0.0	CL3
GI0013	GI0013	H	RDM	0.3	1.2	5.0	0.2	0.4	CL3
GI0014	GI0014	H	RDM	0.3	1.2	5.3	0.2	0.5	CL3
GI0106	GI0106	1	BPM	0.3	1.0	5.5	0.1	0.0	CL3
GI0055	GI0055	1	BPM	0.3	0.7	5.3	0.1	0.0	CL3
GI0103	GI0103	1	BPM	0.3	1.5	5.8	0.0	0.0	CL3
GI0026	GI0026	1	BPM	0.3	0.2	7.2	0.0	0.3	CL3

N= 7

CLUSTER=3

SAMPLE NUMBER	SAMPLE NUMBER	ROCKTYPE	FORMATION	CA	K	AL	MG	NA	CLUSNAME
GI0087	GI0087	1	BPM	0.3	0.2	1.8	0	0	GI0087

N= 1

WARD METHOD ** OUTLIERS EXCLUDED ARE =0000

VARIABLE	N	MEAN	STANDARD DEVIATION	MINIMUM VALUE	MAXIMUM VALUE	STD ERROR OF MEAN	SUM	VARIANCE	C.V.
CLUSTER=1									
CA	9	0.4	0.1	0.3	0.6	0.0	3.2	0.0	32.7
K	9	0.5	0.3	0.2	1.0	0.1	4.2	0.1	48.6
AL	9	4.5	0.3	4.2	4.9	0.1	36.3	0.1	6.8
MG	9	0.3	0.2	0.0	0.6	0.1	2.6	0.0	65.3
NA	9	0.0	0.1	0.0	0.3	0.0	0.3	0.0	282.8
CLUSTER=2									
CA	7	0.3	0.0	0.3	0.3	0.0	2.1	0.0	0.0
K	7	0.9	0.4	0.2	1.5	0.2	6.6	0.2	44.9
AL	7	5.7	0.7	5.0	7.2	0.3	39.6	0.5	12.9
MG	7	0.1	0.1	0.0	0.3	0.0	0.9	0.0	86.5
NA	7	0.2	0.2	0.0	0.5	0.1	1.2	0.0	129.2
CLUSTER=3									
CA	1	0.3	.	0.3	0.3	.	0.3	.	.
K	1	0.2	.	0.2	0.2	.	0.2	.	.
AL	1	1.8	.	1.8	1.8	.	1.8	.	.
MG	1	0.0	.	0.0	0.0	.	0.0	.	.
NA	1	0.0	.	0.0	0.0	.	0.0	.	.

WARD METHOD ** OUTLIERS EXCLUDED ARE =0000

CLUSTER=1

SPEARMAN CORRELATION COEFFICIENTS / PROB > |R| UNDER H0:RHO=0 / N = 9

CA

CA	MG	NA	AL	K
1.00000	0.38498	-0.35635	-0.22685	0.01301
0.0000	0.3436	0.3863	0.5890	0.9756

K

K	MG	NA	AL	CA
1.00000	0.72523	-0.41739	0.20006	0.01301
0.0000	0.0418	0.3035	0.6348	0.9756

AL

AL	NA	CA	K	MG
1.00000	0.42796	-0.22685	0.20006	-0.17949
0.0000	0.2902	0.5890	0.6348	0.6706

MG

MG	K	CA	NA	AL
1.00000	0.72523	0.38498	-0.25678	-0.17949
0.0000	0.0418	0.3436	0.5393	0.6706

NA

NA	AL	K	CA	MG
1.00000	0.42796	-0.41739	-0.35635	-0.25678
0.0000	0.2902	0.3035	0.3863	0.5393

CLUSTER=2

SPEARMAN CORRELATION COEFFICIENTS / PROB > |R| UNDER H0:RHO=0 / N = 7

CA

CA	K	AL	MG	NA
1.00000	.	.	.	.
0.0000				

K

K	AL	NA	MG	CA
1.00000	-0.26607	0.17893	0.09261	.
0.0000	0.5641	0.7011	0.8435	

AL

AL	MG	NA	K	CA
1.00000	-0.64489	-0.39125	-0.26607	.
0.0000	0.1178	0.3854	0.5641	

MG

MG	AL	NA	K	CA
1.00000	-0.64489	0.23291	0.09261	.
0.0000	0.1178	0.6152	0.8435	

NA

NA	AL	MG	K	CA
1.00000	-0.39125	0.23291	0.17893	.
0.0000	0.3854	0.6152	0.7011	

CLUSTER ANALYSIS 4

(C1-04)

CLAST STUDY ################ 36 ELEMENT XRF DATA

C.A. NO: 0000000001 FOR CA K AL MG NA

CLUSTER=1

SAMPLE NUMBER	SAMPLE NUMBER	ROCKTYPE	FORMATION	CA	K	AL	MG	NA	CLUSNAME
GI0003	GI0003	K	RDM	0.2	0.5	5.1	0.3	0.3	CL7
GI0007	GI0007	M	RDM	0.3	0.2	5.4	0.3	0.3	CL7
GI0042	GI0042	M	RDM	0.2	0.6	4.9	0.2	0.0	CL7
GI0032	GI0032	M	RDM	0.3	0.6	4.6	0.5	0.0	CL7
GI0070	GI0070	M	RDM	0.3	0.9	4.4	0.3	0.0	CL7
GI0001	GI0001	O	RDM	0.3	0.2	5.3	0.2	0.3	CL7
GI0001	GI0001	O	RDM	0.3	0.2	5.0	0.2	0.2	CL7
GI0040	GI0040	O	RDM	0.3	0.4	5.0	0.5	0.0	CL7
GI0109	GI0109	O	RDM	0.3	0.6	5.3	0.3	0.0	CL7

N= 9

CLUSTER=2

SAMPLE NUMBER	SAMPLE NUMBER	ROCKTYPE	FORMATION	CA	K	AL	MG	NA	CLUSNAME
GI0030	GI0030	I	RDM	0.4	1.0	5.3	0.6	0.0	CL9
GI0073	GI0073	I	RDM	0.3	1.1	5.6	0.8	0.0	CL9
GI0006	GI0006	I	RDM	0.4	1.3	5.1	0.2	0.4	CL9
GI0067	GI0067	K	RDM	0.3	1.1	5.7	0.5	0.0	CL9
GI0035	GI0035	L	RDM	0.4	1.2	5.3	0.4	0.0	CL9
GI0110	GI0110	N	RDM	0.4	1.1	6.0	0.7	0.0	CL9
GI0111	GI0111	P	RDM	0.4	1.1	6.2	0.7	0.0	CL9
GI0059	GI0059	S	BPM	0.3	1.3	6.1	0.1	0.0	CL9
GI0059	GI0059	S	BPM	0.3	1.3	5.9	0.0	0.0	CL9

N= 9

CLUSTER=3

SAMPLE NUMBER	SAMPLE NUMBER	ROCKTYPE	FORMATION	CA	K	AL	MG	NA	CLUSNAME
GI0043	GI0043	I	RDM	0.3	0.7	6.1	0.2	0.0	CL6
GI0041	GI0041	J	RDM	0.3	0.8	6.7	0.2	0.0	CL6
GI0010	GI0010	L	RDM	0.3	0.5	6.8	0.2	0.3	CL6
GI0005	GI0005	N	RDM	0.3	0.6	5.7	0.1	0.3	CL6
GI0002	GI0002	P	RDM	0.2	0.5	6.2	0.2	0.3	CL6
GI0031	GI0031	P	RDM	0.3	0.7	7.1	0.7	0.0	CL6
GI0027	GI0027	S	BPM	0.3	0.3	6.7	0.0	0.3	CL6
GI0082	GI0082	S	BPM	0.4	0.2	5.9	0.1	0.0	CL6

N= 8

CLUSTER=4

SAMPLE NUMBER	SAMPLE NUMBER	ROCKTYPE	FORMATION	CA	K	AL	MG	NA	CLUSNAME
GI0004	GI0004	J	RDM	0.3	0.8	8.4	0.1	0.4	CL5
GI0069	GI0069	P	RDM	0.3	1.5	7.8	0.6	0.0	CL5
GI0028	GI0028	3	BPM	0.3	1.2	8.5	0.1	0.5	CL5
GI0081	GI0081	3	BPM	0.3	0.4	9.8	0.1	0.0	CL5
GI0052	GI0052	3	BPM	0.3	0.3	10.5	0.1	0.0	CL5

N= 5

CLUSTER=5

SAMPLE NUMBER	SAMPLE NUMBER	ROCKTYPE	FORMATION	CA	K	AL	MG	NA	CLUSNAME
GI0068	GI0068	J	RDM	0.3	4.1	9.4	-0.1	0	CL20
GI0076	GI0076	N	RDM	0.3	3.7	9.2	0.0	0	CL20

N= 2

WARD METHOD ** OUTLIERS EXCLUDED ARE =0000

VARIABLE	N	MEAN	STANDARD DEVIATION	MINIMUM VALUE	MAXIMUM VALUE	STD ERROR OF MEAN	SUM	VARIANCE	C.V.
CLUSTER=1									
CA	9	0.3	0.0	0.2	0.3	0.0	2.5	0.0	15.9
K	9	0.5	0.2	0.2	0.9	0.1	4.2	0.1	51.4
AL	9	5.0	0.3	4.4	5.4	0.1	45.0	0.1	6.6
MG	9	0.4	0.2	0.2	0.8	0.1	3.4	0.0	55.8
NA	9	0.1	0.1	0.0	0.3	0.0	1.1	0.0	121.2
CLUSTER=2									
CA	9	0.4	0.1	0.3	0.4	0.0	3.2	0.0	14.8
K	9	1.2	0.1	1.0	1.3	0.0	10.5	0.0	9.6
AL	9	5.7	0.4	5.1	6.2	0.1	51.2	0.2	6.9
MG	9	0.4	0.3	0.0	0.8	0.1	4.0	0.1	64.7
NA	9	0.0	0.1	0.0	0.4	0.0	0.4	0.0	300.0
CLUSTER=3									
CA	8	0.3	0.1	0.2	0.4	0.0	2.4	0.0	17.8
K	8	0.5	0.2	0.2	0.8	0.1	4.3	0.0	39.4
AL	8	6.4	0.5	5.7	7.1	0.2	51.2	0.2	7.7
MG	8	0.2	0.2	0.0	0.7	0.1	1.7	0.0	99.8
NA	8	0.1	0.2	0.0	0.3	0.1	1.2	0.0	106.9
CLUSTER=4									
CA	5	0.3	0.0	0.3	0.3	0.0	1.5	0.0	0.0
K	5	0.8	0.5	0.3	1.5	0.2	4.2	0.3	61.1
AL	5	8.8	1.0	7.8	10.5	0.5	44.0	1.0	11.6
MG	5	0.2	0.2	0.1	0.6	0.1	1.0	0.0	111.8
NA	5	0.2	0.2	0.0	0.5	0.1	0.9	0.1	138.3
CLUSTER=5									
CA	2	0.3	0.0	0.3	0.3	0.0	0.6	0.0	0.0
K	2	3.9	0.3	3.7	4.1	0.2	7.8	0.1	7.3
AL	2	9.3	0.1	9.2	9.4	0.1	18.6	0.0	1.5
MG	2	-0.0	0.1	-0.1	0.0	0.0	-0.1	0.0	-141.4
NA	2	0.0	0.0	0.0	0.0	0.0	0.0	0.0	.

WARD METHOD ** OUTLIERS EXCLUDED ARE =0000

CLUSTER=1

SPEARMAN CORRELATION COEFFICIENTS / PROB > |R| UNDER H0:RHO=0 / N = 9

CA

	CA	MG	K	NA	AL
CA	1.00000	0.32143	-0.21429	-0.11573	0.10438
	0.0000	0.3990	0.5798	0.7669	0.7893

K

	K	NA	AL	MG	CA
K	1.00000	-0.75223	-0.66979	0.57143	-0.21429
	0.0000	0.0194	0.0484	0.1080	0.5798

AL

	AL	NA	K	MG	CA
AL	1.00000	0.67648	-0.66979	-0.45233	0.10438
	0.0000	0.0454	0.0484	0.2215	0.7893

MG

	MG	K	NA	AL	CA
MG	1.00000	0.57143	-0.46291	-0.45233	0.32143
	0.0000	0.1080	0.2096	0.2215	0.3990

NA

	NA	K	AL	MG	CA
NA	1.00000	-0.75223	0.67648	-0.46291	-0.11573
	0.0000	0.0194	0.0454	0.2096	0.7669

CLUSTER=2

SPEARMAN CORRELATION COEFFICIENTS / PROB > |R| UNDER H0:RHO=0 / N = 9

CA

	CA	NA	K	MG	AL
CA	1.00000	0.31623	-0.27643	0.26090	-0.26090
	0.0000	0.4071	0.4715	0.4977	0.4977

K

	K	MG	NA	CA	AL
K	1.00000	-0.81024	0.43708	-0.27643	0.00000
	0.0000	0.0081	0.2394	0.4715	1.0000

AL

	AL	NA	CA	MG	K
AL	1.00000	-0.55002	-0.26090	0.10084	0.00000
	0.0000	0.1250	0.4977	0.7963	1.0000

MG

	MG	K	NA	CA	AL
MG	1.00000	-0.81024	-0.27501	0.26090	0.10084
	0.0000	0.0081	0.4739	0.4977	0.7963

NA

	NA	AL	K	CA	MG
NA	1.00000	-0.55002	0.43708	0.31623	-0.27501
	0.0000	0.1250	0.2394	0.4071	0.4739

CLUSTER=3

SPEARMAN CORRELATION COEFFICIENTS / PROB > |R| UNDER H0:RHO=0 / N = 8

CA

	CA	NA	MG	K	AL
CA	1.00000	-0.50000	-0.35112	-0.27608	-0.21953
	0.0000	0.2070	0.3938	0.5081	0.6014

K

	K	MG	NA	CA	AL
K	1.00000	0.65271	-0.44173	-0.27608	0.24243
	0.0000	0.0793	0.2732	0.5081	0.5629

AL

	AL	MG	K	CA	NA
AL	1.00000	0.57169	0.24243	-0.21953	-0.05488
	0.0000	0.1387	0.5629	0.6014	0.8973

MG

	MG	K	AL	NA	CA
MG	1.00000	0.65271	0.57169	-0.40964	-0.35112
	0.0000	0.0793	0.1387	0.3135	0.3938

NA

	NA	CA	K	MG	AL
NA	1.00000	-0.50000	-0.44173	-0.40964	-0.05488
	0.0000	0.2070	0.2732	0.3135	0.8973

CLUSTER=4

SPEARMAN CORRELATION COEFFICIENTS / PROB > |R| UNDER H0:RHO=0 / N = 5

CA

	CA	K	AL	MG	NA
CA	1.00000	.	.	.	.
	0.0000				

K

	K	AL	MG	NA	CA
K	1.00000	-0.90000	0.70711	0.33541	.
	0.0000	0.0374	0.1817	0.5811	

AL

	AL	K	MG	NA	CA
AL	1.00000	-0.90000	-0.70711	-0.22361	.
	0.0000	0.0374	0.1817	0.7177	

MG

	MG	AL	K	NA	CA
MG	1.00000	-0.70711	0.70711	-0.39528	.
	0.0000	0.1817	0.1817	0.5101	

NA

	NA	MG	K	AL	CA
NA	1.00000	-0.39528	0.33541	-0.22361	.
	0.0000	0.5101	0.5811	0.7177	

CLUSTER ANALYSIS 5

(C1-05)

CLAST STUDY ################## 36 ELEMENT XRF DATA

C.A. NO: 0000000001 FOR CA K AL MG NA

CLUSTER=1

SAMPLE NUMBER	SAMPLE NUMBER	ROCKTYPE	FORMATION	CA	K	AL	MG	NA	CLUSNAME
GI0029	GI0029	H	RDM	0.3	0.6	4.9	0.2	0.0	CL7
GI0115	GI0115	H	RDM	0.6	0.4	4.3	0.4	0.0	CL7
GI0116	GI0116	H	RDM	0.6	0.4	4.4	0.4	0.0	CL7
GI0029	GI0029	H	RDM	0.4	0.6	4.9	0.2	0.0	CL7
GI0012	GI0012	H	RDM	0.3	0.3	4.9	0.2	0.3	CL7
GI0098	GI0098	H	RDM	0.3	1.0	4.4	0.6	0.0	CL7
GI0078	GI0078	H	RDM	0.4	0.7	4.3	0.6	0.0	CL7
GI0003	GI0003	K	RDM	0.2	0.5	5.1	0.3	0.3	CL7
GI0042	GI0042	M	RDM	0.2	0.6	4.9	0.2	0.0	CL7
GI0007	GI0007	M	RDM	0.3	0.2	5.4	0.3	0.3	CL7
GI0070	GI0070	M	RDM	0.3	0.9	4.4	0.8	0.0	CL7
GI0032	GI0032	M	RDM	0.3	0.6	4.6	0.6	0.0	CL7
GI0001	GI0001	O	RDM	0.3	0.2	5.3	0.2	0.3	CL7
GI0001	GI0001	O	RDM	0.3	0.2	5.0	0.2	0.2	CL7
GI0040	GI0040	O	RDM	0.3	0.4	5.0	0.5	0.0	CL7
GI0062	GI0062	1	BPM	0.3	0.2	4.2	0.0	0.0	CL7

N= 16

CLUSTER=2

SAMPLE NUMBER	SAMPLE NUMBER	ROCKTYPE	FORMATION	CA	K	AL	MG	NA	CLUSNAME
GI0013	GI0013	H	RDM	0.3	1.2	5.0	0.2	0.4	CL5
GI0050	GI0050	H	RDM	0.3	0.8	5.5	0.3	0.0	CL5
GI0014	GI0014	H	RDM	0.3	1.2	5.3	0.2	0.5	CL5
GI0006	GI0006	I	RDM	0.4	1.3	5.1	0.2	0.4	CL5
GI0030	GI0030	I	RDM	0.4	1.0	5.3	0.6	0.0	CL5
GI0073	GI0073	I	RDM	0.3	1.1	5.6	0.8	0.0	CL5
GI0043	GI0043	I	RDM	0.3	0.7	6.1	0.2	0.0	CL5
GI0041	GI0041	J	RDM	0.3	0.8	6.7	0.2	0.0	CL5
GI0067	GI0067	K	RDM	0.3	1.1	5.7	0.5	0.0	CL5
GI0035	GI0035	L	RDM	0.4	1.2	5.3	0.4	0.0	CL5
GI0010	GI0010	L	RDM	0.3	0.5	6.8	0.2	0.3	CL5
GI0110	GI0110	N	RDM	0.4	1.1	6.9	0.7	0.0	CL5
GI0005	GI0005	N	RDM	0.3	0.6	5.7	0.1	0.3	CL5
GI0109	GI0109	O	RDM	0.3	0.6	5.3	0.3	0.0	CL5
GI0111	GI0111	P	RDM	0.4	1.1	6.2	0.7	0.0	CL5
GI0002	GI0002	P	RDM	0.2	0.5	6.2	0.2	0.3	CL5
GI0031	GI0031	P	RDM	0.3	0.7	7.1	0.7	0.0	CL5
GI0059	GI0059	S	BPM	0.3	1.3	6.1	0.1	0.0	CL5
GI0059	GI0059	S	BPM	0.3	1.3	5.9	0.0	0.0	CL5
GI0027	GI0027	S	BPM	0.3	0.3	6.7	0.0	0.3	CL5
GI0082	GI0082	S	BPM	0.4	0.2	5.9	0.1	0.0	CL5
GI0055	GI0055	1	BPM	0.3	0.7	5.3	0.1	0.0	CL5
GI0106	GI0106	1	BPM	0.3	1.0	5.5	0.1	0.0	CL5
GI0103	GI0103	1	BPM	0.3	1.5	5.8	0.0	0.0	CL5
GI0026	GI0026	1	BPM	0.3	0.2	7.2	0.0	0.3	CL5

N= 25

CLUSTER=3

SAMPLE NUMBER	SAMPLE NUMBER	ROCKTYPE	FORMATION	CA	K	AL	MG	NA	CLUSNAME
GI0004	GI0004	J	RDM	0.3	0.8	8.4	0.1	0.4	CL6
GI0069	GI0069	P	RDM	0.3	1.5	7.8	0.6	0.0	CL6
GI0028	GI0028	3	BPM	0.3	1.2	8.5	0.1	0.5	CL6
GI0081	GI0081	3	BPM	0.3	0.4	8.8	0.1	0.0	CL6
GI0052	GI0052	3	BPM	0.3	0.3	10.5	0.1	0.0	CL6

N= 5

CLUSTER=4

SAMPLE NUMBER	SAMPLE NUMBER	ROCKTYPE	FORMATION	CA	K	AL	MG	NA	CLUSNAME
GI0068	GI0068	J	RDM	0.3	4.1	9.4	-0.1	0	CL27
GI0076	GI0076	N	RDM	0.3	3.7	9.2	0.0	0	CL27

N= 2

CLUSTER=5

SAMPLE NUMBER	SAMPLE NUMBER	ROCKTYPE	FORMATION	CA	K	AL	MG	NA	CLUSNAME
GI0087	GI0087	1	BPM	0.3	0.2	1.8	0	0	GI0087

N= 1

WARD METHOD ** OUTLIERS EXCLUDED ARE =0000

VARIABLE	N	MEAN	STANDARD DEVIATION	MINIMUM VALUE	MAXIMUM VALUE	STD ERROR OF MEAN	SUM	VARIANCE	C.V.
CLUSTER=1									
CA	16	0.3	0.1	0.2	0.6	0.0	5.4	0.0	34.0
K	16	0.5	0.2	0.2	1.0	0.1	7.8	0.1	50.7
AL	16	4.7	0.4	4.2	5.4	0.1	76.0	0.1	8.9
MG	16	0.4	0.2	0.0	0.8	0.1	5.7	0.0	59.7
NA	16	0.1	0.1	0.0	0.3	0.0	1.4	0.0	155.4
CLUSTER=2									
CA	25	0.3	0.0	0.2	0.4	0.0	8.0	0.0	15.6
K	25	0.9	0.4	0.2	1.5	0.1	22.0	0.1	41.9
AL	25	5.9	0.6	5.0	7.2	0.1	147.3	0.4	10.5
MG	25	0.3	0.2	0.0	0.8	0.0	6.9	0.1	90.1
NA	25	0.1	0.2	0.0	0.5	0.0	2.8	0.0	153.2
CLUSTER=3									
CA	5	0.3	0.0	0.3	0.3	0.0	1.5	0.0	0.0
K	5	0.8	0.5	0.3	1.5	0.2	4.2	0.3	61.1
AL	5	8.8	1.0	7.8	10.5	0.5	44.0	1.0	11.6
MG	5	0.2	0.2	0.1	0.6	0.1	1.0	0.0	111.8
NA	5	0.2	0.2	0.0	0.5	0.1	0.9	0.1	138.3
CLUSTER=4									
CA	2	0.3	0.0	0.3	0.3	0.0	0.6	0.0	0.0
K	2	3.9	0.3	3.7	4.1	0.2	7.8	0.1	7.3
AL	2	9.3	0.1	9.2	9.4	0.1	18.6	0.0	1.5
MG	2	-0.0	0.1	-0.1	0.0	0.0	-0.1	0.0	-141.4
NA	2	0.0	0.0	0.0	0.0	0.0	0.0	0.0	.
CLUSTER=5									
CA	1	0.3	.	0.3	0.3	.	0.3	.	.
K	1	0.2	.	0.2	0.2	.	0.2	.	.
AL	1	1.8	.	1.8	1.8	.	1.8	.	.
MG	1	0.0	.	0.0	0.0	.	0.0	.	.
NA	1	0.0	.	0.0	0.0	.	0.0	.	.

WARD METHOD ** OUTLIERS EXCLUDED ARE =0000

CLUSTER=1

SPEARMAN CORRELATION COEFFICIENTS / PROB > |R| UNDER H0:RHO=0 / N = 16

CA

	CA	AL	NA	MG	K
	1.00000	-0.49737	-0.37917	0.22728	0.02071
	0.0000	0.0500	0.1475	0.3973	0.9393

K

	K	MG	NA	AL	CA
	1.00000	0.60700	-0.60185	-0.40304	0.02071
	0.0000	0.0127	0.0136	0.1216	0.9393

AL

	AL	NA	CA	K	MG
	1.00000	0.72536	-0.49737	-0.40304	-0.28708
	0.0000	0.0015	0.0500	0.1216	0.2810

MG

	MG	K	NA	AL	CA
	1.00000	0.60700	-0.34313	-0.28708	0.22728
	0.0000	0.0127	0.1932	0.2810	0.3973

NA

	NA	AL	K	CA	MG
	1.00000	0.72536	-0.60185	-0.37917	-0.34313
	0.0000	0.0015	0.0136	0.1475	0.1932

CLUSTER=2

SPEARMAN CORRELATION COEFFICIENTS / PROB > |R| UNDER H0:RHO=0 / N = 25

CA

	CA	MG	AL	K	NA
	1.00000	0.33582	-0.25039	0.23366	-0.21521
	0.0000	0.1008	0.2274	0.2610	0.3015

K

	K	AL	CA	MG	NA
	1.00000	-0.45813	0.23366	0.13401	-0.12818
	0.0000	0.0213	0.2610	0.5230	0.5415

AL

	AL	K	CA	MG	NA
	1.00000	-0.45813	-0.25039	-0.15169	-0.06666
	0.0000	0.0213	0.2274	0.4692	0.7516

MG

	MG	CA	NA	AL	K
	1.00000	0.33582	-0.28243	-0.15169	0.13401
	0.0000	0.1008	0.1713	0.4692	0.5230

NA

	NA	MG	CA	K	AL
	1.00000	-0.28243	-0.21521	-0.12818	-0.06666
	0.0000	0.1713	0.3015	0.5415	0.7516

CLUSTER=3

SPEARMAN CORRELATION COEFFICIENTS / PROB > |R| UNDER H0:RHO=0 / N = 5

CA

	CA	K	AL	MG	NA
	1.00000	.	.	.	.
	0.0000				

K

	K	AL	MG	NA	CA
	1.00000	-0.90000	0.70711	0.33541	.
	0.0000	0.0374	0.1817	0.5811	

AL

	AL	K	MG	NA	CA
	1.00000	-0.90000	-0.70711	-0.22361	.
	0.0000	0.0374	0.1817	0.7177	

MG

	MG	AL	K	NA	CA
	1.00000	-0.70711	0.70711	-0.39528	.
	0.0000	0.1817	0.1817	0.5101	

NA

	NA	MG	K	AL	CA
	1.00000	-0.39528	0.33541	-0.22361	.
	0.0000	0.5101	0.5811	0.7177	